Ca^{2+} CHANNEL INDEPENDENT FUNCTIONS OF AN ALTERNATIVELY SPLICED β4 SUBUNIT

A Dissertation

Presented to the Faculty of the Graduate School

of Cornell University

In Partial Fulfillment of the Requirements for the Degree of

Doctor of Philosophy

by

Yoon Jung Lee

August 2014

Ca^{2+} CHANNEL INDEPENDENT FUNCTIONS OF AN ALTERNATIVELY SPLICED β4 SUBUNIT

Yoon Jung Lee, Ph. D.

Cornell University 2014

The β subunits of voltage-gated Ca^{2+} channels are multifunctional proteins, which act primarily as a Ca^{2+} channel regulatory subunit to regulate trafficking and gating properties of pore-forming Ca^{2+} channel α1 subunits. Recent studies have revealed, however, that β4 subunits also play crucial roles in a variety of Ca^{2+} channel independent functions. These processes involve translocation of β subunits to the nucleus where they associate with and regulate expression of proteins involved in gene transcription**.** The latter emerging role of the Ca^{2+} channel β4 subunit began with the cloning of various alternatively spliced isoforms of the β4 subunit. Here we cloned the mammalian form of an alternatively spliced, truncated β4 subunit (β4c-207aa) from human brain, and showed that it interacts with heterochromatin protein 1γ (HP1γ) through a PXVXL consensus motif. We also showed that β4c is highly expressed in vestibular, and deep cerebellar nuclei of mouse brain.

In our subsequent study, we found that β4c nuclear transport is independent of its PXVXL motif interaction with HP1γ. Instead, we found that the nuclear targeting of heterologously expressed β4c in Neuro2a cells is under the control of two sequence motifs that are separated by 63 amino acids. The first is identical to a classical monopartite nuclear localization sequence (cNLS), K(K/R)X(K/R), located in the HOOK domain, and the second is a previously unidentified C-terminal sequence that is generated by alternative splicing. Both sequences are required for optimal targeting of β4c to the nucleus. Next we determined the

functional consequences of β4c nuclear targeting by performing a whole genome expression study. We determined that β4c regulates the transcription of a number of genes that include components of the cytoskeleton assembly machinery and other ion channel genes. Notably, β4c did not regulate expression of Ca^{2+} channel genes. The β4c splice variant was not capable of modulating Ca^{2+} channel trafficking or gating properties. Therefore, the overall conclusion of this thesis is that β4c does not affect the expression or function of Ca^{2+} channel subunits, rather it acts independently of Ca^{2+} channels to regulate genes that are involved in neurite outgrowth.

BIOGRAPHICAL SKETCH

Yoon Jung was born and grew up in Seoul, South Korea. When she attended Chung-Ang Elementary School, several teachers encouraged Yoon's curiosity of the natural world with activities that ranged from observing microbes in soil to a variety of different science projects. In high school, she achieved the goal of graduating at the top of her class, as well as working in the editorial club for the school newspaper.

After she graduated from high school, Yoon started her undergraduate study at the College of Pharmacy, Seoul National University. In pharmacy school, she had opportunities to experience various areas including an internship at a hospital, and working at a pharmacy and pharmaceutical company. She was also exposed to scientific research. Under the guidance of Professor Hun Huh and Young-Jung Kim, Yoon investigated the hepatoprotective effect of *Lycium chinense*. After getting her Bachelor's degree, she continued her research in the same lab, and then got her Master's degree. Since she wanted to put her scientific knowledge to practical use, she turned her career to the pharmaceutical industry.

Three years later, she moved to Ithaca and started a new round of life in a new environment. Even though Yoon spent valuable time with her husband and kids, she always had hoped to continue her study. Fortunately, she was admitted to the field of Molecular and Integrative Physiology at Cornell University and joined Dr. William Horne's laboratory for her graduate study. In Dr. Horne's lab, Yoon focused on the Ca^{2+} channel biology, specifically the function of the Ca^{2+} channel β4 subunit. During her six years at Cornell, Yoon had a great experience in the Horne lab, and enjoyed the challenging and wonderful time of exploration.

To my mother, 공보임

ACKNOWLEDGMENTS

During the last several years at Cornell, I have learned a tremendous amount both on a scientific and personal level, and I am indebted to many people.

First and foremost, I thank my advisor and committee chair, Dr. William Horne, for his exceptional mentoring and the example he sets. Thank you for taking me as your student, and for your patience and full support.

I want to thank my committee members. Dr. Robert Oswald provided me a nesting place and great emotional support. Dr. Robert Weiss gave me an opportunity to work his lab before I started my graduate study and provided me with lots of encouragement. Dr. David Lin always gave wonderful advice on my project.

During my time in the laboratory, I had the opportunity to work with many very special people, and I wish to express my gratitude to the following individuals:

Dr. Xingfu Xu for his enormous help in every step of my study; Johanna Holm for teaching me the electrophysiology technique; Dr. Christropher Ptak for his helpful recommendations; Madeline Martinez for her words of comfort; and Carol Merkur for her invaluable administrative support. Thanks to all my dear friends, especially Yoon-young for being an outstanding listener.

I would also like to thank my parents, Jae-Ho Lee and Bo-Im Kong, for bringing me up to be an optimistic and determined person. Their endless support and love always encouraged me and helped me to overcome difficulties. Thanks to my brothers, Byung-Hee and Byung-Guk, for cheering me up even though we were separated by an ocean.

Finally, I would like to thank my kids, Andrew and Grace, for giving me the joy of life and the energy to make a step forward.

TABLE OF CONTENTS

LIST OF FIGURES

LIST OF TABLES

LIST OF ABBREVIATIONS

ABP: α-binding pocket

AID: α-interaction domain

ARM: armadillo

BID: β interaction domain

Best1: bestrophin-1

CAF1: chromatin assembly factor 1

CaMKII : $Ca^{2+/}$calmodulin-dependent protein kinase II

CASK: calcium/calmodulin-dependent serine protein kinase

CAT: chloramphenicol acetyltransferase

CD: chromo domain

CGC: cerebellar granule cell

CNS: central nervous system

CSD: chromo shadow domain

DAPI: 4',6-diamidino-2-phenylindole

DHPR: dihydropyridine receptor

DIV: days in vitro

EC: excitation-contraction

ER: endoplasmic reticulum

FDR: false discovery rate

FI: fluorescence intensity

GFP: green fluorescence protein

GK: guanylate kinase

GPCR: G protein-coupled receptors

H3K9me3: methylated lysine 9 of histone H3

HP1: heterochromatin protein 1

HVA: high-voltage-activated

IBB: importin β binding

Impα: importin α

ITC: isothermal titration calorimetry

LVA: low-voltage-activated

MAGUK: membrane-associated guanylated kinase

MVN: medial vestibular nucleus

NLS: nuclear localization sequence

NMR: nuclear magnetic resonance

PCA: Principal component analysis

PCR: polymerase chain reaction

PI3K: Phosphoinositide 3-kinase

PIP_2: phosphatidylinositol 4,5-biphosphate

PIP3: phosphatidylinositol 3,4,5-triphosphate

PKA: protein kinase A

PKB: protein kinase B

PP2A: phosphatase 2A

PSD95: post synaptic density protein 95

RGK: Rad, Rem, Rem2, Gem/Kir

RIM1: RAB3-interacting molecule 1

RPE: retinal pigment epithelium

RyR1: ryanodine receptor type 1

SAP97: synapse-associated protein 97

SAPE: streptavidin-phycoerythrin

SH3: Sar homology 3

SR: sarcoplasmic reticulum

TH: tyrosine hydroxylase

TIF1: transcriptional intermediate factor 1

VGCC: voltage-gated Ca^{2+} channel

VOR: vestibular-ocular reflex

YSL: yolk syncytial layer

CHAPTER 1

Overview

Introduction

The Ca^{2+} channel β subunit is a multifunctional protein that acts primarily as a Ca^{2+} channel regulatory subunit but also performs Ca^{2+} channel independent functions. In the former role, the β subunit is responsible for trafficking the channel to the plasma membrane and modulating voltage dependence of channel gating. The latter emerging roles were discovered with the cloning of various alternatively spliced isoforms of the β subunits. Subcellular localization of β subunit splice variants, particularly to the nucleus, is closely related to its channel independent functions. In this thesis, I present the molecular determinants of subcellular localization of the newly cloned mammalian β4c, a splice variant of the β4 subunit, and the functional consequences of its nuclear targeting in neuronal cells.

The purpose of this chapter is to provide an overview of the β subunit, including the structural features that are important for its Ca^{2+} channel dependent and independent functions. I will begin with the brief introduction of general features of the voltage-gated Ca^{2+} channel complexes (VGCCs), which included the β subunit as one of the main auxiliary subunits. Next, I will provide an overview of the Ca^{2+} channel regulatory functions of the β subunit, its various interactions with other proteins, and the recent findings about the Ca^{2+} channel independent functions, which provide the background information for my study.

Voltage-gated Ca^{2+} channels

Voltage-gated Ca^{2+} channels (VGCCs) are large protein complexes composed of a α1 pore forming subunit and ancillary α2δ, β, and γ subunits depending on their tissue distribution. As the principal entryway of Ca^{2+} into cells, VGCCs play a crucial role in Ca^{2+} signaling. They are involved in a variety of physiological functions, including neurotransmitter and hormone release, muscle excitation-contraction coupling, and gene transcription (1-4). They are classified broadly into high-voltage-activated (HVA) and low-voltage-activated (LVA) Ca^{2+} channels based upon the membrane potential at which they are activated (5-8). Ca^{2+} currents are further sub-classified into L-, N-, P/Q-, R, and T-type according to unique biophysical and pharmacological characteristics (9-17). Among these VGCCs, the HVA channels (L-, N-, P/Q-, and R-type) require an auxiliary β subunit for their proper membrane expression and gating (18). Mammalian α1 subunits are encoded by 10 distinct genes. Based on amino acid sequence similarity, channels are divided into three subfamilies: Ca_v1, Ca_v2, and Ca_v3. The Ca_v1 subfamily includes channels that conduct L-type Ca^{2+} currents; the Ca_v2 subfamily includes channels that conduct N-, P/Q-, and R-type Ca^{2+} currents; and the Ca_v3 subfamily includes channels that conduct T-type Ca^{2+} currents (Figure 1.1) (2,19-22). All of these subtypes are present in neuronal tissue, but N-, P/Q-, R-type Ca^{2+} currents are the most prominent in neurons. The α1 subunit defines the key characteristics of the channels such as ion selectivity, voltage-dependent gating, and ion permeation. The α1 subunit has four domains, each containing six transmembrane α helices that form a ~200-kD transmembrane protein that is able to respond to changes in membrane potentials to open the Ca^{2+} permeable pore (Figure 1.2) (21,23-26).

Figure 1.1 A family tree of mammalian voltage-gated Ca^{2+} channels.

Voltage-gated Ca^{2+} channels (VGCC) can be categorized based on the amino acid identity of the α1 subunit. Phylogenetic representation of the primary sequences of the α1 subunits are shown in bold lines. Only the membrane-spanning segments and pore loops (~350 amino acids) are compared. First, all sequence pairs were compared, which clearly defines three subfamilies with intra family sequence identities above 80% (Cav1, Ca_v2, and Ca_v3). Then a consensus sequence was defined for each subfamily, and these three sequences were compared to one another, with inter subfamily sequence identities of ~52% (Ca_{v1} vs. Ca_v2) and 28% (Ca_v3 vs. Ca_v1 or Ca_v2). The Ca_v1 and Ca_v2 types are high-voltage-activated (HVA) channels. The Ca_v3 types are low-voltage-activated (LVA) channels. The molecular nomenclature is shown; new nomenclature is in bold, and old nomenclature is in the parenthesis. The physiological classification based on kinetic and pharmacological properties is shown in red (L, P/Q, N, R, and T type).

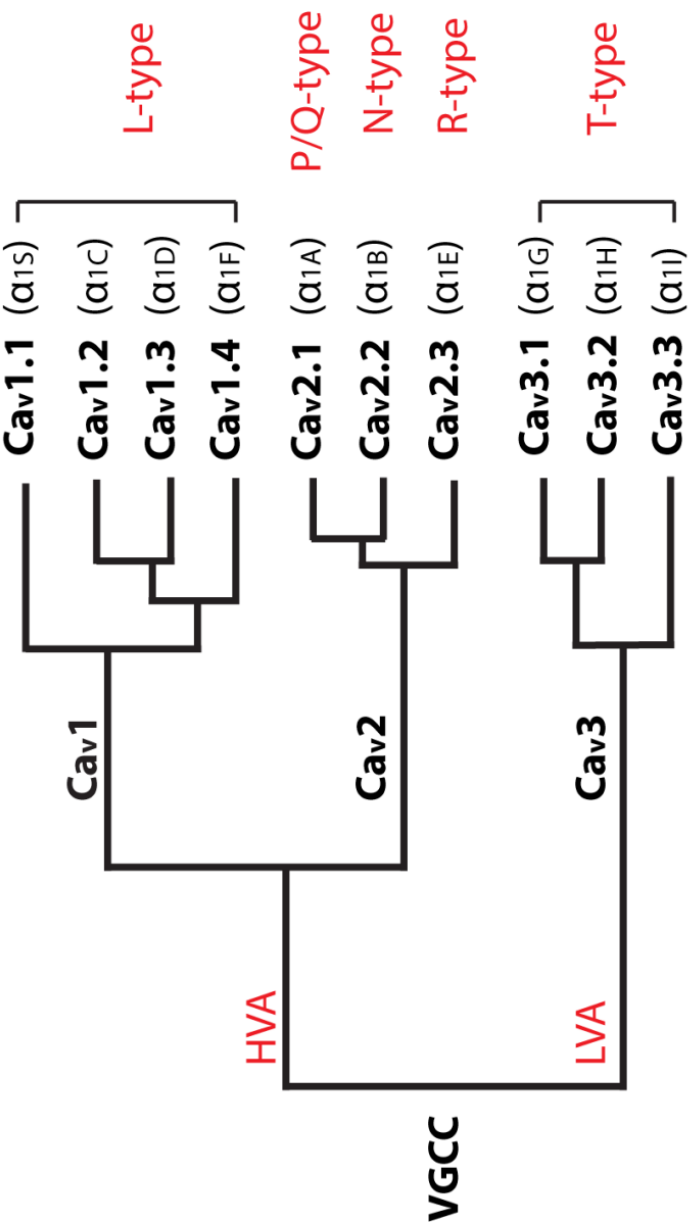
VGCC
HVA
LVA
Cav1
Cav2
Cav3
Cav1.1 (α1S)
Cav1.2 (α1C)
Cav1.3 (α1D)
Cav1.4 (α1F)
Cav2.1 (α1A)
Cav2.2 (α1B)
Cav2.3 (α1E)
Cav3.1 (α1G)
Cav3.2 (α1H)
Cav3.3 (α1I)
L-type
P/Q-type
N-type
R-type
T-type

Figure 1.2 Molecular composition of voltage-gated Ca^{2+} channel.

(A) Simplified representation of the HVA Ca^{2+} channel composed of five subunits: α1 (blue), α2 and δ (yellow), γ (green) and β subunit (red).

(B) A predicted topology of the α1 subunit of the VGCC, which has 24 transmembrane α-helices grouped into four homologous repeats (I-IV). '+' signs in the fourth segments of the each repeat indicate the charged amino acids acting as a voltage sensor. The AID shown in red is located on the I-II loop. [Modified from Buraei el al. (27)]

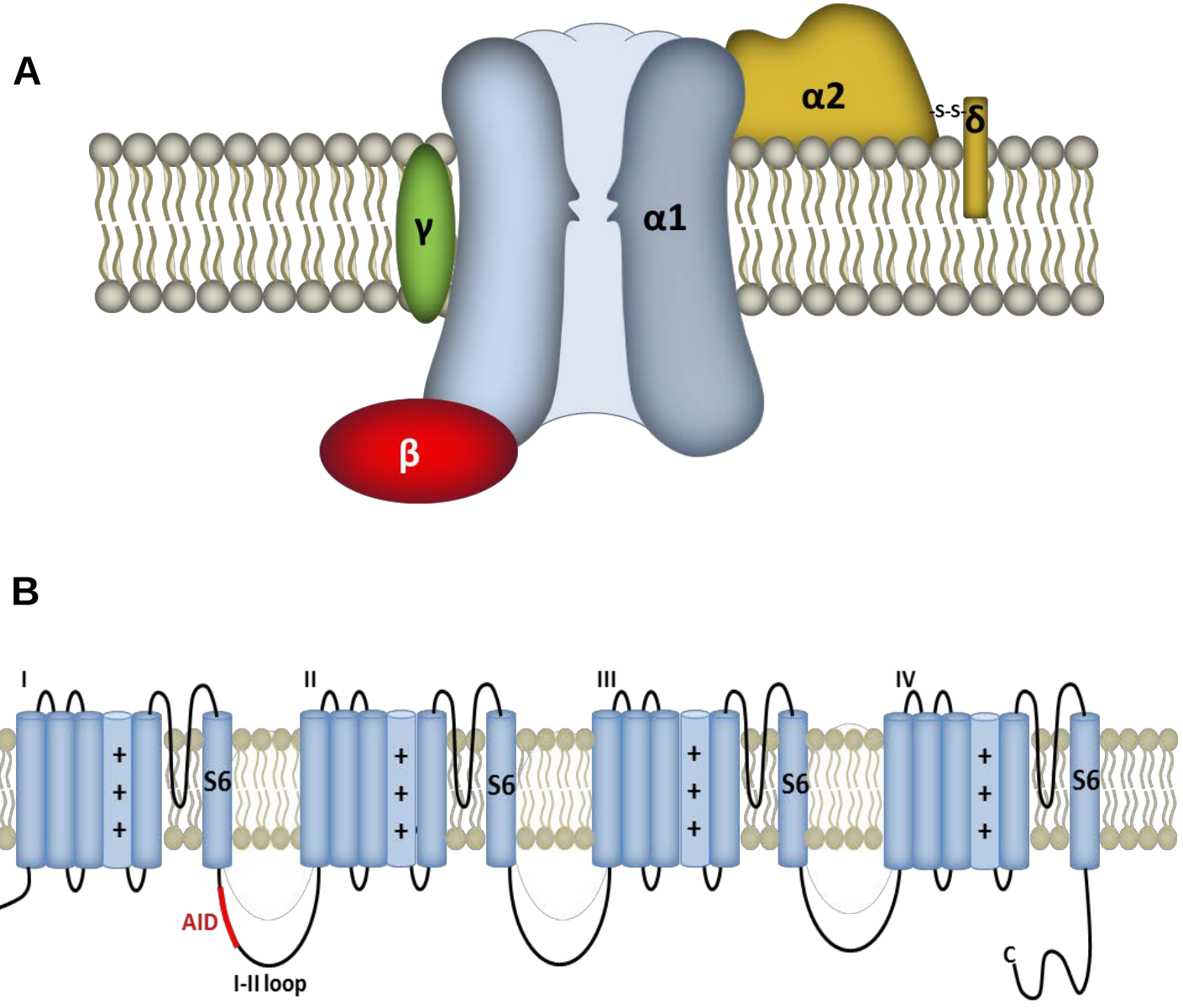
A
α2
δ
-s-s-
γ
α1
β
B
I
II
III
IV
S6
S6
S6
S6
+
+
+
N
AID
I-II loop
C

In the electrophysiology studies of this thesis, I used the α1 subunit of $Ca_v2.1$ (P/Q type) channel, which is highly expressed in the presynaptic terminal, and thus has a fundamental role in mediating fast synaptic transmission at central and peripheral nerve terminals.

Structure of β subunits

A putative β subunit structure consisting of five distinct domains was first predicted by several different studies including amino acid sequence alignments, modeling, and biochemical and functional studies (28-30). All β subunits are composed of two highly conserved Src homology 3 (SH3) and guanylate kinase (GK) domains, and three variable regions, the N terminus, HOOK, and C terminal domains (Figure 1.3). The middle three domains of the β subunit form the β subunit core. This SH3-HOOK-GK core has been shown to recapitulate the many functions of the β subunit through the interaction with α1 subunit (28,31-37); however, it is still controversial whether only the core is sufficient for all β subunit functions. Other regions may also be important to both Ca^{2+} channel dependent and independent functions.

In 2004, the three dimensional structure of the β subunit was determined by X-ray crystallography. Three groups reported the crystal structures of the three isoforms of β subunit core regions: β2a, β3 and β4, alone or in complex with the α-interaction domain (AID) (31,38,39). The structures verified that the core contains an SH3 domain and a GK domain, which are connected by a non-structured HOOK region. This modular organization places the β subunit into the membrane-associated guanylated kinase (MAGUK) protein family (Figure 1.3).

Figure 1.3 Structure of the β subunit.

(A) A schematic representation of the five domains of the β subunit. It is composed of the two highly conserved SH3 and GK domains and three variable regions, the N-terminus, C-terminus, and Hook domain.

(B) Crystal structure of the β3 core. The following regions are indicated: N-terminus (light blue, residues 38-59), SH3 domain (yellow, residues 60-120 and 170-175), HOOK region (purple, residues 121-169), GK domain (green, residues 176-300). [Modified from Chen et al. (31)]

A


N
SH3
HOOK
GK
C

B

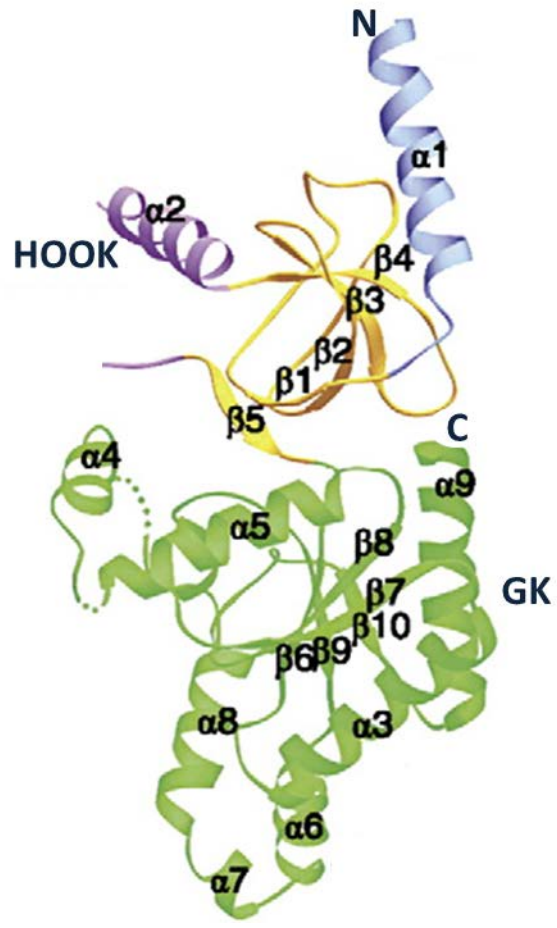
N
α1
α2
HOOK
β4
β3
β2
β1
β5
C
α4
α9
α5
β8
β7
GK
β10
β6
β9
α8
α3
α6
α7

MAGUKs are scaffolding proteins, examples of which include post synaptic density protein 95 (PSD95), synapse-associated protein 97 (SAP97), calcium/calmodulin-dependent serine protein kinase (CASK), and Shank, all of which use their various domains to create a web of protein-protein interactions at or near the cell membrane (40-42). However, the β subunit structure has evolved differentially from most MAGUKs; it does not contain a well-defined PDZ domain in its N-terminal region. As a result the functions of the β subunits are quite different from the "classical" MAGUKs (43).

The crystal structures revealed that the previously known AID, an 18 amino acid consensus binding motif (QQXEXXLXGYXXWIXXXE) located in the I-II loop of the α1 subunit (Figure 1.2 (B)), is critical for binding to the cytoplasmic β subunits (31,38,39,44-46). The structure showed that β subunit interacts with AID through a deep hydrophobic groove on the GK domain, referred to now as the α-binding pocket (ABP) (31,39,47), not through a previously mutagenically identified interaction motif, referred to as the β interaction domain (BID). Mutations of the key residues in the AID or the ABP abolish both β subunit-mediated Ca^{2+} channel surface expression and gating modulation (34,35,45,48,49). Therefore, this AID-ABP interaction is necessary for proper β subunit regulation of Ca^{2+} channels. The BID is crucial for their structural integrity as it participates in the intramolecular association of the SH3 and GK domains (28,50). Interestingly, a recent study suggests that $Ca_v\beta$ fragments can associate to form GK–GK (51,52) or SH3–SH3 domain dimers (53).

β subunits splice variants

There are four mammalian Ca^{2+} channel β subunit genes, *Cacnb 1-4* (27). The genes are composed of 14 exons (except for *Cacnb3* which has 13), and each gene has the potential to create a number of splice variants (29,54). Based on the sequence similarities, the SH3 and GK

regions show variability, and these are where the most of the alternative splicing occurs. The four different *Cacnb* genes utilize different alternative splicing sites and are expressed in specific tissues at different stages of development (27). All β subunits that contain a GK domain can bind to the different high-voltage activated α1 subunits. The end result is that alternative splicing of β subunits markedly expands the molecular diversity and functionality of HVA Ca^{2+} channels.

Among the four β subunits, our lab has studied the β4 subunit encoded by *Cacnb4*. The β4 subunit is the most prevalent partner to Ca_v 2.1 (P/Q type), and is expressed abundantly in cerebellum and spinal cord. The expression level and distribution of the β4 subunit change significantly at different stages of development. During morphogenesis of the mouse central nervous system (CNS), β4 is initially expressed in the mantle zone throughout the entire brain and spinal cord at E13–E15. Postnatally, β4 expression quickly attenuates in the brain with the exception of the cerebellum and olfactory bulb (55). In adults, β4 is again expressed broadly throughout the brain, but the expression in the cerebellum is the most prominent (56). In the transition from newborn to adult, β4 subunit protein levels in the brain increase 10-fold, which represents the most dramatic increase in expression of any β subunit during this period (57).

In 2002, our lab reported a novel alternatively spliced β4 subunit (β4a) containing a short form of the N-terminal domain that is highly homologous to the N termini of *Xenopus* and rat β3 subunits. The expression study in *Xenopus* oocytes revealed that the two different β4 splice variants, β4a and β4b, differentially affect Ca^{2+} channel activation and inactivation depending on the α1 subtypes (58,59). In addition, the β4a and β4b show different pattern of distribution in the human CNS: β4a is the dominantly expressed isoform in the spinal cord, and it is distributed throughout evolutionarily older regions of the CNS, including cerebrum, temporal lobe and

occipital lobe. On the contrary, β4b is expressed abundantly in the forebrain (58). These findings about β4a and β4b manifest that the alternative splice variants have functional significance by uniquely modulating and fine-tuning the neuronal Ca^{2+} currents.

Several truncated isoforms of β subunits have also been identified (51,60-63). These appear to arise as a result of exon skipping in the region that codes for the HOOK or GK domain. These splicing events cause a frame-shift and premature stop codon. In case of the truncated β3 found in heart, the skipped exon is the 20 bp of exon 6 (51), and a similar truncated β3 was observed in mouse brain (63). This truncation results in a short protein lacking the GK domain, which cannot interact with the α1 subunit.

In 2003 Hibino et al. identified a truncated β4 subunit splice variant, termed cβ4c, that resulted from skipping of exon 9 and creation of a premature stop codon. This short splice form was the exclusive isoform in the chicken cochlea, and it lacked most of the GK domain (61). The cloning of this short isoform that cannot interact with AID in the α1 subunit prompted a research quest to identify β subunit Ca^{2+} channel independent functions.

The physiological importance of the β4 subunits

As a predominant partner of the neuronal P/Q and N-type Ca^{2+} channels in the brain (64), aberrant β4 function shows mostly neurological defects. A naturally-occurring null mutation of β4 was first reported in *lethargic(lh)* mice(65). This null mutation is caused by a four nucleotide insertion in *Cacnb4*, making a translational frame shift and a premature stop codon. The *lethargic* mice show complex abnormal neurological disorders, including absence epilepsy, ataxia, seizures, and paroxysmal dyskinesia (65-67). It is not yet established why the remaining β subunits fail to compensate for the lack of β4 and result in these severe phenotypes; however,

one very recent study suggests that in *lethargic* mice, the excitation-transcription pathway mediated by β4 might not function normally (68). There are cases where mutations in β4 cause epilepsy and ataxia in humans. In severe infant myoclonic epilepsy, a missense mutation (R468Q) of the *CACNB4* gene increases $Ca_v2.1$ current and somehow causes febrile seizures (69). In a juvenile myoclonic epilepsy patient, a truncated β4 (R482x) was identified and found to have a minor effect on Ca^{2+} channel properties (70). The missense mutation C104F in SH3 domain was identified both in a family with generalized epilepsy and praxis-induced seizures and in another family with episodic ataxia (70).

β subunit Ca^{2+} channel regulatory function

Traditionally, the β subunits are considered cytosolic proteins based both on primary sequence analyses (71,72) and subcellular localization when the β subunit is expressed, in the absence of the α1 subunit (33,73). In the presence of the α1 subunit, the β protein switches its localization from cytosolic to membrane-bound through the AID–ABP interaction. Single point mutations in the AID of $Ca_v1.2$ that disrupt binding with the β subunit abolish both membrane localization and dendritic clustering of the β subunits in hippocampal neurons (74). The membrane targeting of the β subunits coincide with their functional effects on Ca^{2+} channels. In addition, as a scaffolding protein, the β subunit is important for targeting of HVA Ca^{2+} channels to specific locations. For example, β4 is implicated in the synaptic localization of P/Q-type channels in cultured hippocampal neurons (75).

The β subunits have two well-characterized cellular functions involving the HVA Ca^{2+} channel. They chaperone the pore-forming α1 subunit to the cell membrane for Ca^{2+} channel assembly, and they set voltage parameters for channel opening and closing (gating) (Figure 1.4 (A) (B)).

Figure 1.4 Main functions of the β subunit

(A) Enhance membrane expression of Ca^{2+} channels.

(B) Regulate gating properties of Ca^{2+} channels.

(C) Interact with ryanodine receptor (RYR) in the sarcoplasmic reticulum (SR) of muscle cells.

(D) Translocate into the nucleus where it can regulate transcription.

(E) Interact with a variety of proteins that regulate VGCC function such as RGK proteins, ion channels, synaptic proteins, and signaling proteins. [Modified from Buraei et al. (1)]

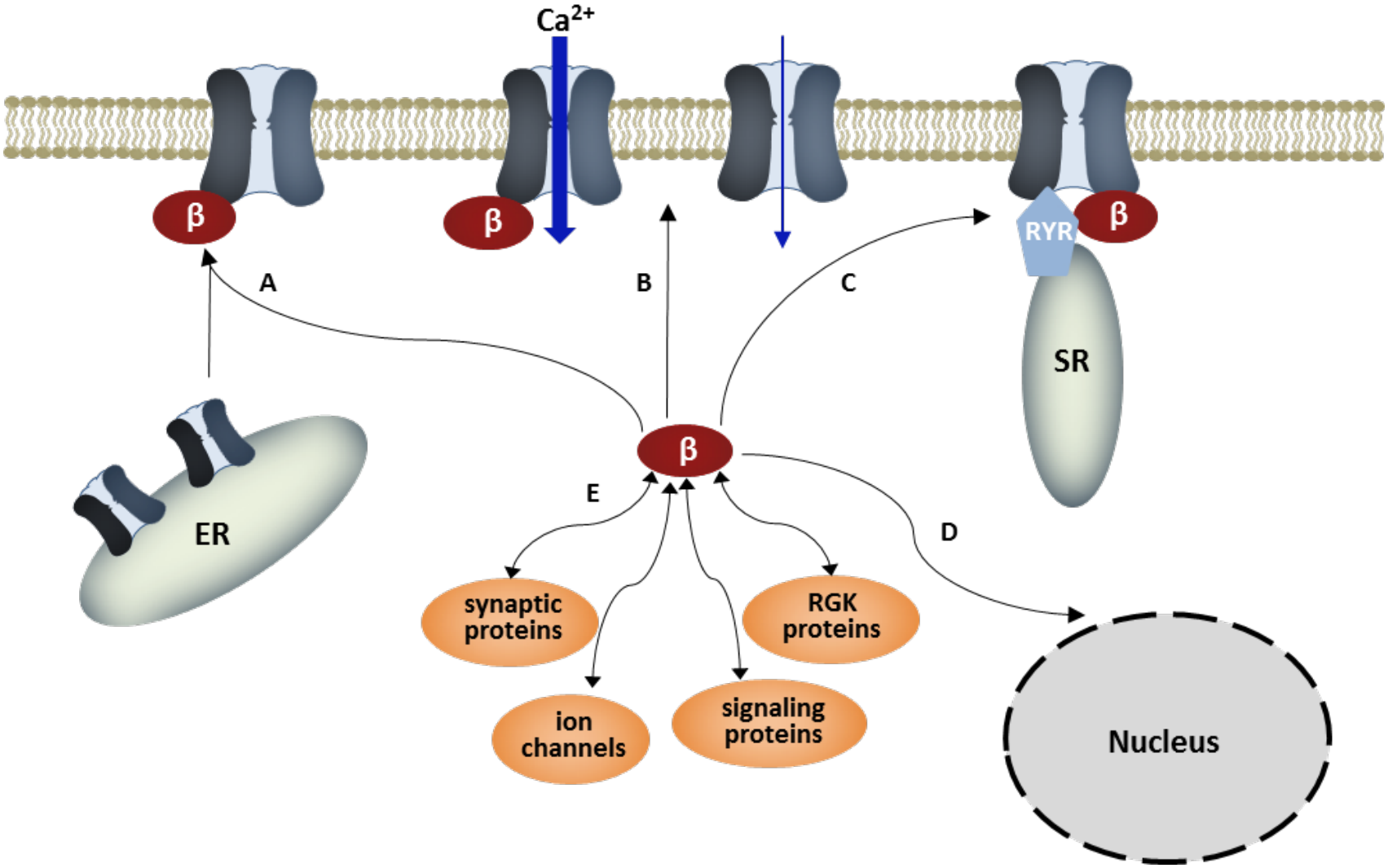
Ca2+
β
β
β
β
RYR
A
B
C
D
E
ER
SR
synaptic proteins
RGK proteins
ion channels
signaling proteins
Nucleus

When β subunits are expressed together with α1 subunits, they result in increased current size. The β subunits generally hyperpolarize the voltage-dependence of activation, and also increase maximum open probability of the channel, which will increase current through individual channels (76-78). Moreover, β subunits increase the number of channels that are targeted to the plasma membrane (79-81). More specifically, β subunits:

1) regulate membrane expression of voltage gated Ca^{2+} channels.

The β subunits promote the expression of the α1 subunits on the plasma membrane. The increase in surface expression of all Ca_v1 and Ca_v2 α1 subunits has been observed both in native cells (82-84) and in various heterologous expression systems (19,29,54,85). We confirmed that β4a coexpression with α1A and α2δ1 in *Xenopus laevis* oocytes increased Ca^{2+} current expression. In addition to this, $Ca_v2.1$ expression rate is highly dependent on the concentration of β subunits (86,87). As shown in Figure 1.5 (A), the expression rate of $Ca_v2.1$ increased significantly in the β4a coexpression group compared to that of the group without β4a (Figure 1.5 (A)). The small Ca^{2+} current in the group without β4a subunit can be explained that the endogenous β subunits in the *Xenopus laevis* oocytes transport part of the exogenously expressed α1A to the plasma membrane (88,89).

1-1) How does the β subunit enhance Ca^{2+} channel surface expression?

Several recent studies have examined the mechanisms by which the β subunits increase Ca^{2+} channel surface expression. One study using $Ca_v1.2$ channel found that both ER export and ER retention signals existed in the α1 subunit. The intracellular regions of α1 form a complex that yields a prevailing ER retention signal. When the β subunit binds to the I–II linker, it modifies the complex such that the ER export signal becomes dominant and α1 surface expression is enhanced (90).

Figure 1.5 Regulation of Ca^{2+} channels by β subunits.

(A) Modulation of Ca^{2+} channel expression. $Ca_v2.1$ current expression rate as a function of β4a-subunit concentration. The averaged peak currents indicated as squares or triangles are plotted against average time (hour) of recording after cRNA injection into the *Xenopus* oocytes.

(B) Modulation of Ca^{2+}channel gating: Enhancement of the voltage-dependent activation.

The current-voltage (I-V) curves resulting from increasing concentrations of β4a. Data represent averaged, normalized peak currents elicited by incremental depolarizing steps of 5 mV for 300 ms each from a holding potential of -80 mV.

(C) Modulation of Ca^{2+}channel gating: Enhancement of the voltage-dependent inactivation.

The current-voltage (I-V) curves resulting from increasing concentrations of β4a. Data represent averaged, normalized peak currents resulting from 300-ms depolarizations to -5, 0, or +5 mV from the range of indicated potentials held for 20 s.

* α1A:α2δ-1:β4a cRNA molar ratio: 1:1:0 ■, 1:1:1 ●, 1:1:10 ▲

* These are summary of several data sets performed in our lab.

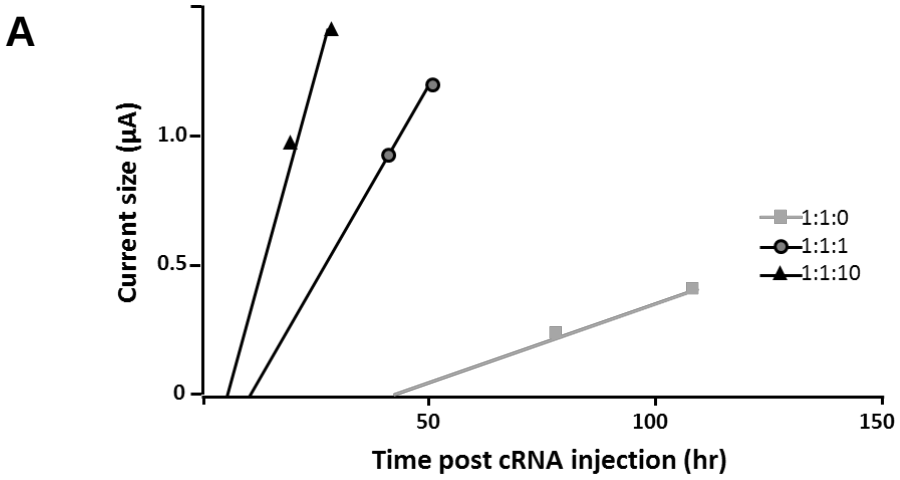
A
Current size (μA)
1.0
0.5
0
50
100
150
Time post cRNA injection (hr)
1:1:0
1:1:1
1:1:10

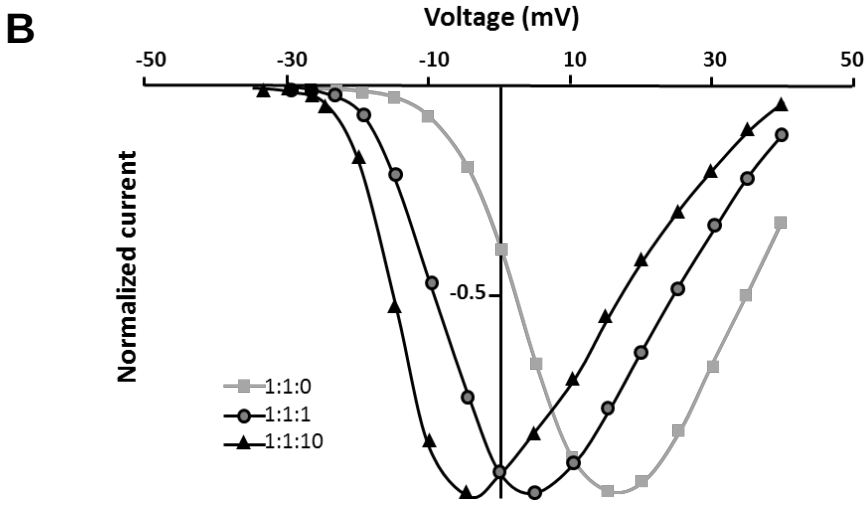
B
Voltage (mV)
-50
-30
-10
10
30
50
Normalized current
-0.5
1:1:0
1:1:1
1:1:10

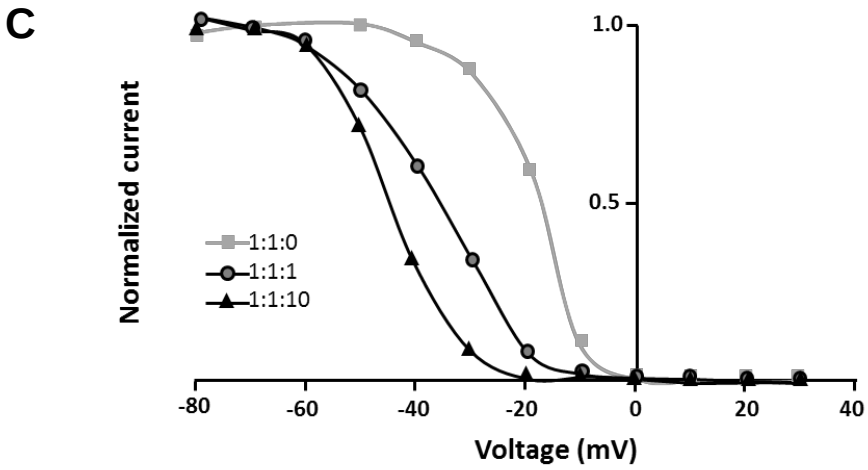
C
Normalized current
1.0
0.5
1:1:0
1:1:1
1:1:10
-80
-60
-40
-20
0
20
40
Voltage (mV)

A few studies proposed that the molecular interaction between the β subunits and the I-II linker of Ca_v1 and Ca_v2 channels results in protection from proteasomal degradation, thus promoting retention at the cell surface (79,91,92). This mechanism was proposed for $Ca_v2.2$ channels (92). However, $Ca_v2.1$ channels do not appear to be subject to this type of regulation (79), indicating that there might be different mechanism for different types of Ca^{2+} channels (93).

2) regulate gating properties of voltage gated Ca^{2+} channels

The β subunits modulate voltage-dependent activation and voltage-dependent inactivation of HVA Ca^{2+} channels. First, the β subunits assist channel opening by shifting the voltage dependence of channel activation by ~10-15 mV to more hyperpolarized voltages (94-96). At the single channel level the β subunit increases the channel open probability (97,98), and also accelerates channel activation (18,99), which is observed as a shortened latency to first channel opening in single channel recordings (51,100). Voltage-dependent inactivation lowers the amount of Ca^{2+} current following depolarization and reduces the number of channels responsive to subsequent depolarization. The β subunits (except β2a) also shift the voltage-dependent inactivation to more hyperpolarized voltages (by ~10-20 mV), decreasing the number of channels available to open at a given membrane potential. (28,34,58,59,101,102). In addition, the β subunits promote 'closed state' inactivation of the Ca_v2 channels (103,104) and affect inactivation kinetics (34,59). As shown in Figure 1.5 (B) and (C), coexpression of β4a with α1A and α2δ1 in *Xenopus* oocytes causes a hyperpolarizing shift both in voltage-dependent activation and voltage-dependent inactivation. This effect is dependent on the concentration of β4a. Therefore, β4a makes it easier for the channel to open (requiring less depolarization), but at

the same time, decreases the number of $Ca_v2.1$ channels available to open (Figure 1.5 (B) (C)).

2-1) How does the β subunit regulate gating properties?

The molecular determinants of voltage-dependent activation include (i) the external pore and the ion selectivity filter formed by the pore loop between the S5 and S6 transmembrane segments of α1 subunit (23-26), (ii) the inner pore formed by all four S6 segments of α1 subunit (105) , and (iii) the activation gate, located at the cytoplasmic end of the S6 segments (106). For the voltage-dependent inactivation, the cytosolic ends of the S6 segments, the I–II linker, and the N- and C-termini of α1 subunit are considered to be involved (102,107). Even though the precise mechanism is still unclear, the most probable hypothesis is that the S6 segments of the α1 subunits play critical role for regulation of the gating parameters of HVA Ca^{2+} channels. When β subunit is bound to the AID, the entire region starting with IS6 to the end of the AID becomes a continuous α-helix (38,102,108,109). This rigid structure allows the β subunit to regulate both activation and inactivation, most likely by affecting the energetics of voltage-dependent movement of both IS6 and the inactivation gate. When this rigid α-helix formation is disrupted by the insertion of glycine residues, the ability of β subunit to regulate gating properties is severely compromised, while Ca^{2+} channel surface expression remains unaffected (35,102,110). In addition to this structural change, several studies indicate that the orientation of the β subunit relative to α1 subunit is also essential for the regulation of gating (35,110). Insertions or deletions in the IS6-AID linker, which are expected to maintain the α-helical structure of the linker but induce a 180° rotation of the β subunit with respect to α1, diminish or abolish the β subunit regulation of activation and inactivation (35,110). Another important aspect of this model is that the anchoring of β subunit to α1 through the AID-GK interaction enables the formation of intrinsically low-affinity interactions between the β subunit and other parts of the

α1 subunit that fully normalize channel gating (27). For example, β subunit SH3 domain interacts with the I-II loop via different region from the AID (111). Other regions of α1 subunit including N- and C-termini and the III-IV loop have also been shown to interact directly with β subunit (112,113). These additional α1 and β subunit interactions do not produce significant gating regulation on their own. Some studies have shown that many of β subunits' effects can be reconstituted by the core region and in some cases the GK domain alone (114). Our preliminary studies indicate that the GK domain alone cannot act like the full-length β subunit (unpublished).

Role of the β subunit in Gβγ inhibition of Ca_v2 channels

Calcium currents of Ca_v2 channel family (i.e., N-, P/Q-, and R-type channels) can be inhibited by activation of G protein-coupled receptors (GPCRs) that are linked to $G_{i/o}$ (115,116). Direct binding of Gβγ demonstrates opposing effects on the channel compared to β subunit binding (115). When Gβγ binds to the Ca_v2 channels, the effects are: (i) inhibition of the current amplitude (ranging from 15% to 80% depending on the Ca_V channel and GPCR combination); (ii) a slowing of the kinetics of current activation ; (iii) a depolarizing shift of the voltage-dependence of channel activation; and (iv) a shift to hyperpolarized potentials of the steady-state inactivation curve (117). This inhibition can be reversed by a strong depolarizing pre-pulse, which expedites Gβγ dissociation from the α1 subunit (117,118). The β subunit is required for this voltage-dependent inhibition of Gβγ. Initially it was thought that the β subunit competed with Gβγ binding to the I–II linker of the α1 subunit (119,120). Absence of the β subunit does not prevent G-protein modulation of calcium channels; however it does abolish the voltage dependence of the process. That is, the G-protein modulation of Ca.2 channels cannot be relieved by depolarizing voltage steps (77). Furthermore, the Trp391Ala mutant in AID of Ca.2.2 that

cannot bind to β subunits does not exhibit voltage-dependent G-protein modulation. This confirms the essential role of β subunits in voltage-dependent Gβγ inhibition of the channel (81). A recent allosteric model explains the opposing actions of Gβγ and the β subunit on channel function (35). Although the Gβγ-binding pocket in the channel is still unknown, it is likely formed by several regions including the I–II linker, the N-terminus, and the C-terminus of α1. As discussed above binding of the β subunit transforms IS6 and a large portion of the I–II linker, including the AID, into a α-helix. Upon depolarization, the rigid α-helix structure allows movements in IS6 and conformational change of the Gβγ binding pocket, causing Gβγ dissociation. In the absence of β subunit, the AID is a random coil and IS6 movements cannot be efficiently transmitted to the I–II linker. Thus, Gβγ stays on the channel, inhibiting it with no voltage dependence. This model concluded that β subunit binding is essential for the voltage dependence of Gβγ inhibition (35,121).

Role of the β subunit in RGK protein inhibition of HVA Ca^{2+} channels

The RGK (Rad, Rem, Rem2, Gem/Kir) family of small GTP-binding proteins has been shown to inhibit HVA calcium channels, although the underlying molecular mechanism and physiological relevance of this inhibition is still unclear (122,123). All four RGKs bind β subunits and it has been widely assumed that the RGK/β interaction is essential for Ca_V1/Ca_V2 channel inhibition (122-124) (Figure 1.4 (E)). This notion has been challenged by a recent finding that β binding is not necessary for Gem inhibition of neuronal P/Q-type ($Ca_v2.1$) channels (125). This study suggests that Gem interacts directly with $Ca_v2.1$ through an anchoring site with or without the β subunit being present. They concluded that the role of the β subunit in Gem inhibition is to produce a conformational change that results in the formation of an

inhibitory site on $Ca_v2.1$ where Gem can then bind to produce inhibition (125). Another recent report shows that Rem uses both β-binding-dependent and β-binding-independent mechanisms to inhibit recombinant $Ca_v1.2$ channels (126). This study identifies a novel Rem binding region on the N-terminus of the pore-forming $Ca_V1.2$ α1C subunit that mediates β-binding-independent inhibition. The N-type ($Ca_v2.2$) channel α1B subunit lacks the Rem binding site in the N-terminus and displays only β-binding-dependent inhibition. They conclude that distinct RGK GTPases differ in their use of the two determinants for $Ca_v1.2$ channel suppression— Rem and Rad use both β-binding-dependent and independent mechanisms, whereas Gem and Rem2 use only the a β-binding-dependent mode of inhibition (126).

Role of β subunit in phospho- and lipid regulation of HVA Ca^{2+} channels

VGCC β subunits are also important targets for phosphorylation by a variety of protein kinases and phosphatases. Ca^{2+}/calmodulin-dependent protein kinase II (CaMKII) interacts with α1 of HVA Ca^{2+} channels and regulates their activities. In cardiomyocytes, CaMKII binds directly to the C terminus of β2a, phosphorylates it, and thereby causes facilitation of $Ca_v1.2$ currents (127). Moreover, the phosphorylation of β2a promotes the dissociation of CaMKII from β2a, in a manner that suggest a negative-feedback mechanism. The β1b, β3, β4 subunits have also been shown to be phosphorylated by CaMKII, but the physiological significance of this remains to be elucidated (128).

Cyclic AMP-dependent protein kinase A (PKA) mediates up-regulation of cardiac L-type Ca^{2+} currents. Even though the target of PKA phosphorylation still remains obscure, the extent of PKA modulation is influenced by the association of β subunit (129). A recent study demonstrates that channel complexes containing β1b show the strongest up-regulation, followed by those containing β3 and β4; channel complexes containing β2a show the least modulation (130).

Ca^{2+} channels are opened upon membrane depolarization; however, the amplitude of Ca^{2+} influx is also controlled by extracellular signals binding to membrane receptors and relayed by transduction effectors including G-proteins and phosphatidylinositol 3-kinases (PI3Ks) (131,132).

In cerebellar granule neurons, insulin-like growth factor (IGF-1), which binds to tyrosine kinase–associated receptors(TKRs) and PI3K up-regulate native L- and N-type Ca^{2+} channels currents (133). Phosphatidylinositol 3-kinases (PI3Ks) are lipid kinases that phosphorylate phosphoinositides on position 3 of their inositol head group. The two main phosphoinositide products created in response to extracellular stimuli are phosphatidylinositol 4,5-biphosphate (PIP_2) and phosphatidylinositol 3,4,5-triphosphate (PIP_3), known regulators of HVA Ca^{2+} channels (131,132). One study demonstrates that elevated PIP_3 levels recruit protein kinase B (PKB), which phosphorylates β2a subunit on a serine residue. This causes increased $Ca_v1.2$ channel expression on the plasma membrane (134). The mechanism underlying this PIP_3/PKB effect was found to involve a reduction in $Ca_v1.2$ degradation (135). β2a phosphorylation by active PKB masks the degradation sequences on $Ca_v1.2$ α1 subunit and thus leads to the increased expression of the channel complex (135).

Interaction of β subunit with variety of proteins

The β subunit interacts not only with the Ca^{2+} channel α1 subunit but also with a variety of proteins, and thus regulates diverse cellular functions.

1) Ryanodine receptors

Excitation-contraction (EC) coupling in skeletal muscle is thought to depend on a physical interaction between the dihydropyridine receptor (DHPR) voltage sensor and ryanodine receptor (136). The entire complex is made up of plasma membrane bound $Ca_v1.1$, β1a, α2δ1, and γ1 subunits, and sarcoplasmic reticulum (SR) ryanodine receptor type 1 (RyR1) Ca^{2+} release channels. The β1a subunits are essential for skeletal EC coupling not only for the trafficking of α1s subunit but also for tetrad formation: DHPRs are arranged in groups of four to properly interact with RyRs (137,138). It has been suggested that the C-terminal tail of the β1a subunit may contribute to voltage-activated Ca^{2+} release in skeletal muscle by interacting with the ryanodine receptor (RyR1)(137) (Figure 1.4 (C)). Recently, it was reported that the C-terminal 35 residues of β1a subunit directly interact with RyR1 in vitro (139). Also, the C-terminal 35 residues of the β1a subunit adopt a nascent α-helix in which 3 hydrophobic residues align to form a hydrophobic surface that binds to RyR1 isolated from rabbit skeletal muscle (140).

2) Dynamin

It has been reported that the SH3 domain of β2a downregulates $Ca_v1.2$ channel surface expression by interacting with the endocytic protein dynamin (141). Dynamin belongs to a family of large GTPases that promote membrane fission during endocytosis, and it contains a proline-rich region with several P*XX*P consensus motifs that serve as a docking site for SH3 domains. The SH3/proline-rich region-mediated interactions appear to recruit dynamin to areas of endocytosis (141). Recently, the same group showed that the SH3 domain of β2a homodimerizes through a single disulfide bond (53). Substitution of the only cysteine residue abolishes dimerization and impairs internalization of $Ca_V1.2$ channels expressed in *Xenopus*

oocytes while preserving dynamin binding. Covalent linkage of the β-SH3 dimerization-deficient mutant yields a concatamer that binds to dynamin and restores endocytosis. Association of the β subunit with a polypeptide encoding the binding motif in $Ca_V1.2$ α1 subunit inhibited endocytosis. Together, these findings reveal that SH3 dimerization is crucial for endocytosis and suggest that channel activation and internalization are two mutually exclusive functions of β subunit (53).

3) Synaptic proteins: Synaptotagmin I and RIMI

The α1 subunit of the Ca_v2 family interacts with presynaptic proteins involved in synaptic vesicle transmission, including synaptotagmin I, syntaxin, and SNAP-25(142). Apart from the α1 interaction, our lab found that the β subunit can also interact with synaptic proteins. Yeast two-hybrid and pull-down results show that the N-terminus of β4a, and perhaps β3 interact with synaptotagmin I in the absence of Ca^{2+}. However, addition of Ca^{2+} prevents this interaction. How this interaction affects neurotransmitter release remains to be determined (87).

The presynaptic active zone protein RIM1 (RAB3-interacting molecule 1) binds, through its C terminus, to the SH3-HOOK-GK core domain of β subunits (143). RIM1 suppresses inactivation of both the Ca_V1 and Ca_V2 channels, and thus enhances neurotransmitter release, both by augmenting flux through presynaptic calcium channels and by anchoring the channels close to release sites (143,144). RIM1 also interacts with RIM-binding protein, which was found to bind directly to α1 subunits (145). RIM-binding protein is essential for vesicular release of neurotransmitters, and surrounds a central core of calcium channels in *D. melanogaster* neuromuscular junction active zones (146). Thus, β subunits may participate in targeting calcium channels to the presynaptic active zones.

4) Ahnak

Ahnak, originally identified as a giant, tumor-related phosphoprotein has been implicated in the beta-adrenergic regulation of the cardiac L-type Ca^{2+} channel current by its binding to the regulatory β2a subunit (147). β2 subunit interaction with Ahnak has been identified by co-immunoprecipitation with several cardiac preparations derived from a variety of species, including rodents and humans. Subsequent in vitro binding studies disclosed that multiple sites in the C terminus of Ahnak can bind to β2a. The Ahnak interaction region on β2a is still unknown; however, the conserved β subunit modules, SH3 and/or GK, are important for Ahnak interaction since Ahnak coimmunoprecipitates with β1b, β3, and β2a (147). It is suggested that Ahnak plays an auto-inhibitory role on cardiac L-type Ca^{2+} channel current through β2a sequestration that can be relieved by PKA phosphorylation of Ahnak1 and/or β2a (148).

5) Bestrophin

Bestrophin-1 (Best1) is a chloride channel expressed in the retinal pigment epithelium (RPE) that can function as both Cl^- channel and Ca^{2+} channel regulator (149). Bestrophin-1 modulates currents through voltage-dependent L-type Ca^{2+} channels by physically interacting with β subunits (150). Bestrophin -1 showed co-immunoprecipitation with either β3 or β4 subunits when heterologously expressed in CHO cells. Recently it was determined that a highly conserved cluster of proline-rich motifs on the Best1 C-terminus is required for the binding to SH3-domains of β subunits (151). A Best1 that lacks these proline-rich motifs showed reduced efficiency to co-immunoprecipitate with β3 and β4 subunits. Currents from $Ca_V1.3$ subunits were modified in the presence of the β4 subunit and wild-type Best1: accelerated time-dependent activation and reduced current density (151).

Ca^{2+} channel independent functions

Besides the Ca^{2+} channel-related functions of β subunits, a host of recent studies show that the β subunits may have functions independent of their association with VGCCs. The question of Ca^{2+} channel independent functions started with the cloning of various short isoforms of β subunits, some of which lacked the GK domain, which meant they were not able to interact with the AID of the Ca^{2+} channel α1 subunit. (51,60,61,152,153). This line of study started from the finding of a truncated splice variant of β4 in chicken cochlea and brain, termed cβ4c. The cβ4c lacks 90% of the GK domain and the entire COOH terminus (Figure 1.6 (A)). It interacts with heterochromatin protein 1 (HP1), a nuclear protein involved in gene silencing and transcriptional regulation. When the cβ4c was co-expressed with HP1 in tsA201 cells, it translocated to the nucleus. In addition, cβ4c was shown to attenuate the repressor function of HP1 in a dose-dependent manner in chloramphenicol acetyltransferase (CAT) assays using Cos-1 cells. These findings suggest that cβ4c may function as a transcription regulator (61). The possible VGCC independent role of the short β4 isoform prompted us to ask several interesting research questions. Does this type of isoform exist in mammalian brain, and if it does, what is the subcellular localization? Does it function as a transcriptional regulator? To examine these questions, first we worked to clone the mammalian β4c protein from human brain . We then went on to figure out the specific subcellular localization of hβ4c in the neuronal Neuro2a cells. These are topics of the remaining chapters of my thesis (Figure 1.6).

Figure 1.6 Short splice variant of the β4 subunit

(A) Upper exon diagram: Fourteen β4a exons are color-coded based on the regions they give rise to: N-terminus (blue), SH3 domain (yellow), HOOK region (purple), GK domain (green), and C-terminus (white). Red arrow points to exon 9 splicing, which results in translational frame shift and subsequent stop codon.

Lower exon diagram: Nine chicken β4c exons are color-coded based on the regions they code for: N-terminus (blue), SH3 domain (yellow), HOOK region (purple), truncated GK domain (green), and newly formed exon 9 (orange).

(B) Transcriptional regulation by chicken β4c: the cβ4c interacts with heterochromatin protein 1 (HP1), and then translocates into the nucleus.

A

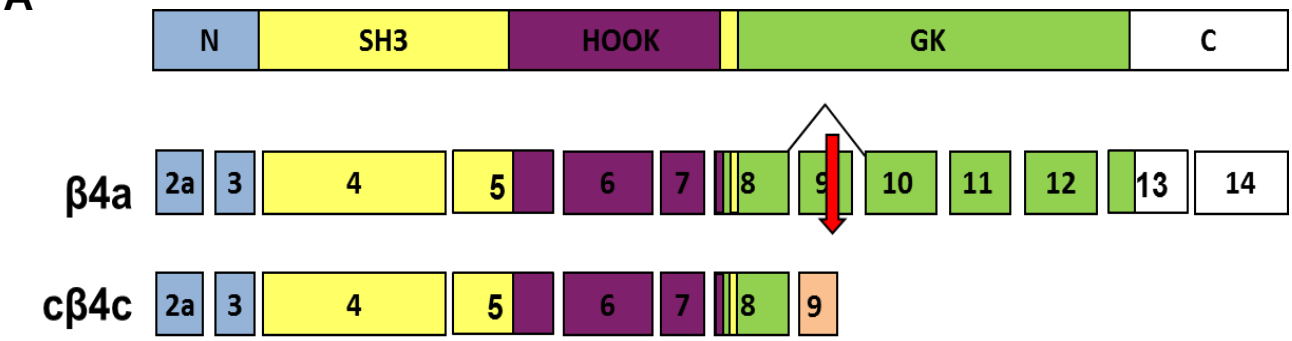
N
SH3
HOOK
GK
C
β4a
2a
3
4
5
6
7
8
9
10
11
12
13
14
cβ4c
2a
3
4
5
6
7
8
9

B

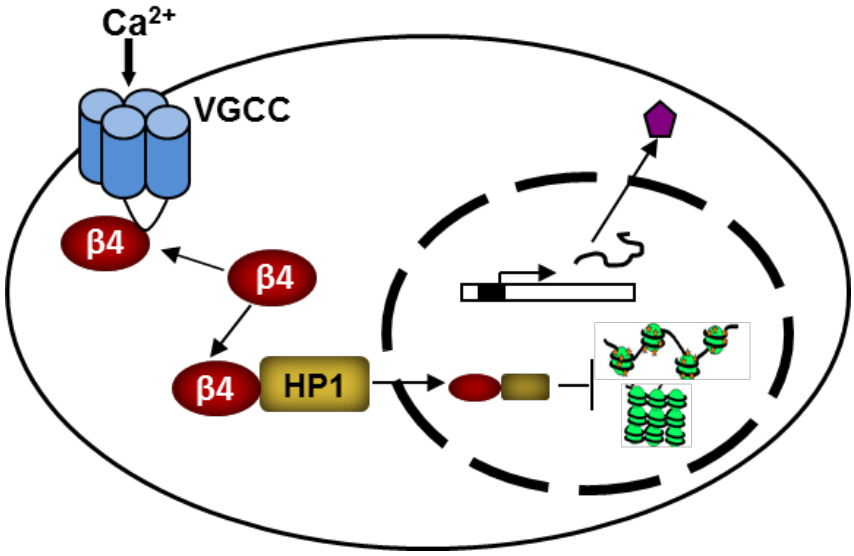
Ca2+
VGCC
β4
β4
β4
HP1

Previously, our lab reported another possible VGCC independent function of β4 in zebra fish (*Danio rerio*) (154), which expresses two copies of all four β subunit subtypes (155). To assess the functional roles of β4.1 and β4.2 genes during embryogenesis, a loss of function study was performed by injection of subtype-specific morpholinos. Surprisingly, the knockdown of β4 inhibited the initiation of epiboly, the first morphogenetic movement of teleost embryos. Reduced β4 function in the yolk syncytial layer (YSL) resulted in abnormal division and dispersal of yolk syncytial nuclei, blastoderm retraction, and death. This phenotype is similar to that seen with microtubule disruption by nocodazole. Epiboly could be rescued by coinjection of human β4a or β4b cRNA, even when containing a triple mutation (M204A/L208A/L350A) that rendered it incapable of binding to α1 subunits. This provides strong evidence that β4 functions in epiboly are independent of Ca^{2+} channel activity. The specific role of the β4 subunits in epiboly and its mechanism of actions have not yet been determined, but we believe that it involves nuclear translocation of β4.

Before Hibino et al. demonstrated the role of the short isoform of β subunit as a transcriptional regulator in the nucleus, Colecraft et al. showed that full-length β subunits can target to the nucleus in native cells (97). They reported that β4, and to a lesser extent, β1b and β3, can be found in the nucleus when they are exogenously expressed in adult rat heart cells (97). They reported that β4, and to a lesser extent, β1b and β3, can be found in the nucleus when they are exogenously expressed in adult rat heart cells (97). In accordance with this study, a recent study demonstrates that the endogenous β4 is located in the nuclei of granule cells and Purkinje cells in the cerebellar cortex (156). The β4b is targeted to the nucleus, when it is heterologously expressed in skeletal myotubes or cultured hippocampal neurons (156). Other β subunits, including the β4a isoform do not show nuclear localization. The N terminus of the β4b,

specifically the Arg-Arg-Ser motif is necessary and sufficient for its nuclear targeting, since mutation of these residues significantly reduces nuclear localization. In addition, fusing this motif to β4a increases nuclear targeting. Moreover, they show that the β4b nuclear targeting is negatively regulated by increased electrical activity and Ca^{2+} influx through L-type Ca^{2+} channels. These results indicate that β4b may possess specific functions in communicating Ca^{2+} channel activity to the nucleus (156).

Regarding the nuclear localization of the β subunits, one study demonstrates the nuclear relocalization of β3 and thus sequestration in the nucleus might be one of the regulation mechanisms of the Rad and Rem activity on the VGCC (124). Rad and Rem, which are members of the RGK family of Ras-related small G proteins, are known to interact with the β subunits and negatively regulate the surface expression of the Ca^{2+} channels (124).

A recent study shows that full-length β subunit may function as a transcriptional regulator (157). In this study, Zhang et al. showed that full-length β3 interacts with a new splicing isoform of Pax6, a transcription factor playing an important role in development of the eye and the nervous system. The new splicing isoform of Pax6, named Pax6(S) shows almost the same in vitro transcriptional activity as Pax6. In vitro luciferase assays show that the β3 suppresses transcriptional activity of the Pax6(S), whereas coexpression of Pax6(S) with $Ca_v2.1$ channels containing β3 in *Xenopus* oocytes does not affect the biophysical properties of the channels. In addition, heterologously expressed β3 is translocated into the nucleus of the HEK 293T cells when it is co-expressed with Pax6(S). This nuclear targeting in combination with the repressor effect upon the transcription activity of Pax6(S) suggests that full-length β3 may act directly as a transcriptional regulator independent of its role as a Ca^{2+} channel regulator (157).

The newly emerging role of the β subunit as a transcriptional regulator in relation to HP1

was examined by two very recent studies (68,158). The first study shows that full-length β4 targets to the nucleus upon neuronal differentiation in primary cultures of hippocampal neurons and NG108-15 cells (68). Yeast two-hybrid assays reveal that β4 interacts with B56δ, one of the two regulatory subunits of phosphatase 2A (PP2A), known to target PP2A to the nucleus. Upon binding with B56δ, the β4/B56δ/PP2A complex relocates to the nucleus, where it associates with nucleosomes and regulates the dephosphorylation of histones, a key mechanism in transcriptional regulation. The C-terminus of the β4 is critical for its nuclear targeting since a mutant β4 lacking the last 38 C-terminal residues corresponds to the human juvenile myoclonic epilepsy mutation can neither associate with B56δ nor translocate to the nucleus (70). Another important factor for the nuclear localization of β4 is that an intact intramolecular SH3-GK domain interaction is required to form the β4/B56δ complex. Interestingly, the membrane depolarization of HEK 293 cells enhances interaction of β4 with B56δ, indicating that plasma membrane depolarization triggers β4/B56δ interaction to cause a signaling cascade into the nucleus (68). This finding is contrary to the previous study by Subramnyam et al. showing that depolarization promotes nuclear export of β4 (156). We can assume that there might be different pathways of β4 nuclear localization in different cells under different conditions. The authors further report that β4 represses tyrosine hydroxylase (TH) gene expression, which is aberrantly up-regulated in *lh* mouse brain that lacks β4 expression, by interacting with the thyroid hormone receptor α *in vitro*. In addition, an immunoprecipitation experiment shows that β4 associates with HP1γ in the presence of B56δ. This suggests that the β4 subunit acts as a platform to recruit the nuclear receptor and HP1γ, and then this complex binds to the TH gene promoter and induces gene repression (68). Along with this gene regulation pathway, a relevant microarray study reinforces the notion that β4 functions as a gene transcriptional regulator (158). Ronjat et al.

demonstrate that expression of β4 in HEK 293 cells regulate expression of several genes compared with expression of a C-terminus truncated mutant β4, which cannot target to the nucleus. They also confirm that neuronal differentiation causes nuclear translocation of β4, and that β4 in the nucleus regulates gene expression in NG108-15 cells. However, the type of genes and the up- or down-regulation direction in HEK 293 cells and NG108-15 cells do not exactly match (158). This result indicates that a gene may be differently regulated by expression of β4 in different cells, and that β4 might interact with specific transcription factors depending on the cell type.

There is a new report about β4 nuclear targeting and gene regulation in cultured cerebellar granule cells (CGCs) from lethargic mice individually reconstituted with three different β4 isotypes: β4a, β4b, and β4e (159). Etemad et al. identified an alternatively spliced β4 subunit (β4e) lacking the variable N-terminus that can modulate Ca^{2+} channel function but cannot target to the nucleus. Microarray studies show that the number of genes regulated by each β4 splice variant correlated with the rank order of their nuclear targeting properties (β4b> β4a> β4e). There is substantial gene regulation in CGCs reconstituted with β4b, which can target to the nucleus, and there is no gene regulation in β4e-reconsititued CGCs. Therefore, the gene regulation activities of β4 subunits are closely related to their nuclear targeting properties (159).

The newly emerging roles of the β subunits beyond its Ca^{2+} channel dependent functions, underlie the functional complexity of the various isoforms of the β subunits. It is highly likely that additional functions along with additional binding partners will be elucidated in the near future. My thesis work adds to our understanding of the role of β4c in the nucleus. We cloned a mammalian short splice variant of β4 subunit (hβ4c) from human brain, and showed that hβ4c interacts with HP1γ via a consensus PXVXL motif. When β4c is ectopically expressed in

Neuro2a cells, it is translocated into the nucleus. The β4c nuclear targeting is independent of its interaction with HP1γ, instead two sequence motifs are required for the proper nuclear targeting: a putative classical monopartite nuclear localization sequence (cNLS), K(K/R)X(K/R), located in the HOOK domain, and a newly generated C-terminal sequence by alternative splicing. Moreover, we showed that β4c regulates transcription of a number of genes including ion channel genes that are related to cell excitability, and genes that regulate cytoskeletal formation. Considering that the alternative splicing of β subunit serves a specific role in fine tuning of neuronal activities, β4c might bear specific role in the nuclei of excitable cells. Our results support the notion that the short splice variant of β4 subunit can function as a transcriptional regulator. In summary, this study set to provides insight on the newly discovered role for β4 subunits.

REFERENCES

1. Buraei, Z., and Yang, J. (2013) Structure and function of the beta subunit of voltage-gated Ca^{2+} channels. *Biochim Biophys Acta* **1828**, 1530-1540

2. Catterall, W. A. (2011) Voltage-gated calcium channels. *Cold Spring Harb Perspect Biol* **3**, a003947

3. Dolphin, A. C. (2009) Calcium channel diversity: multiple roles of calcium channel subunits. *Curr Opin Neurobiol* **19**, 237-244

4. Dolphin, A. C. (2012) Calcium channel auxiliary alpha2delta and beta subunits: trafficking and one step beyond. *Nat Rev Neurosci* **13**, 542-555

5. Carbone, E., and Lux, H. D. (1984) A low voltage-activated calcium conductance in embryonic chick sensory neurons. *Biophys J* **46**, 413-418

6. Carbone, E., and Lux, H. D. (1984) A Low voltage-activated, fully inactivating Ca^{2+} channel in vertebrate sensory neurons. *Nature* **310**, 501-502

7. Fedulova, S. A., Kostyuk, P. G., and Veselovsky, N. S. (1985) Two types of calcium channels in the somatic membrane of newborn rat dorsal-root ganglion neurons. *Journal of Physiology-London* **359**, 431-446

8. Llinas, R., and Yarom, Y. (1981) Properties and distribution of ionic conductances generating electroresponsiveness of mammalian inferior olivary neurons in vitro. *Journal of Physiology-London* **315**, 569-584

9. Zhang, J. F., Randall, A. D., Ellinor, P. T., Horne, W. A., Sather, W. A., Tanabe, T., Schwarz, T. L., and Tsien, R. W. (1993) Distinctive pharmacology and kinetics of cloned neuronal Ca^{2+} channels and their possible counterparts in mammalian CNS neurons. *Neuropharmacology* **32**, 1075-1088

10. Dolphin, A. C. (2006) A short history of voltage-gated calcium channels. *Br J Pharmacol* **147 Suppl 1**, S56-62

11. Ellinor, P. T., Zhang, J. F., Randall, A. D., Zhou, M., Schwarz, T. L., Tsien, R. W., and Horne, W. A. (1993) Functional expression of a rapidly inactivating neuronal calcium channel. *Nature* **363**, 455-458

12. Llinas, R., Sugimori, M., Lin, J. W., and Cherksey, B. (1989) Blocking and isolation of a calcium channel from neurons in mammals and cephalopods utilizing a toxin fraction (FTX) from funnel-web spider poison. *Proc Natl Acad Sci U S A* **86**, 1689-1693

13. Nowycky, M. C., Fox, A. P., and Tsien, R. W. (1985) Three types of neuronal calcium channel with different calcium agonist sensitivity. *Nature* **316**, 440-443

14. Plummer, M. R., Logothetis, D. E., and Hess, P. (1989) Elementary properties and pharmacological sensitivities of calcium channels in mammalian peripheral neurons. *Neuron* **2**, 1453-1463

15. Soong, T. W., Stea, A., Hodson, C. D., Dubel, S. J., Vincent, S. R., and Snutch, T. P. (1993) Structure and functional expression of a member of the low voltage-activated calcium channel family. *Science* **260**, 1133-1136

16. Tsien, R. W., Ellinor, P. T., and Horne, W. A. (1991) Molecular diversity of voltage-dependent Ca^{2+} channels. *Trends Pharmacol Sci* **12**, 349-354

17. Tsien, R. W., Lipscombe, D., Madison, D. V., Bley, K. R., and Fox, A. P. (1988) Multiple types of neuronal calcium channels and their selective modulation. *Trends in Neurosciences* **11**, 431-438

18. Lacerda, A. E., Kim, H. S., Ruth, P., Perez-Reyes, E., Flockerzi, V., Hofmann, F., Birnbaumer, L., and Brown, A. M. (1991) Normalization of current kinetics by interaction between the alpha 1 and beta subunits of the skeletal muscle dihydropyridine-sensitive Ca^{2+} channel. *Nature* **352**, 527-530

19. Arikkath, J., and Campbell, K. P. (2003) Auxiliary subunits: essential components of the voltage-gated calcium channel complex. *Curr Opin Neurobiol* **13**, 298-307

20. Ertel, E. A., Campbell, K. P., Harpold, M. M., Hofmann, F., Mori, Y., Perez-Reyes, E., Schwartz, A., Snutch, T. P., Tanabe, T., Birnbaumer, L., Tsien, R. W., and Catterall, W. A. (2000) Nomenclature of voltage-gated calcium channels. *Neuron* **25**, 533-535

21. Catterall, W. A. (2000) Structure and regulation of voltage-gated Ca^{2+} channels. *Annu Rev Cell Dev Biol* **16**, 521-555

22. Perez-Reyes, E. (2003) Molecular physiology of low-voltage-activated t-type calcium channels. *Physiol Rev* **83**, 117-161

23. Kim, M. S., Morii, T., Sun, L. X., Imoto, K., and Mori, Y. (1993) Structural determinants of ion selectivity in brain calcium channel. *FEBS Lett* **318**, 145-148

24. Kuo, C. C., and Hess, P. (1993) Ion permeation through the L-Type Ca^{2+} channel in rat pheochromocytoma cells - 2 sets of ion-binding sites in the pore. *Journal of Physiology-London* **466**, 629-655

25. Sather, W. A., and McCleskey, E. W. (2003) Permeation and selectivity in calcium channels. *Annu Rev Physiol* **65**, 133-159

26. Yang, J., Ellinor, P. T., Sather, W. A., Zhang, J. F., and Tsien, R. W. (1993) Molecular determinants of Ca^{2+} selectivity and ion permeation in L-type Ca^{2+} channels. *Nature* **366**, 158-161

27. Buraei, Z., and Yang, J. (2010) The β subunit of voltage-gated Ca^{2+} channels. *Physiol Rev* **90**, 1461-1506

28. De Waard, M., Pragnell, M., and Campbell, K. P. (1994) Ca^{2+} channel regulation by a conserved beta subunit domain. *Neuron* **13**, 495-503

29. Birnbaumer, L., Qin, N., Olcese, R., Tareilus, E., Platano, D., Costantin, J., and Stefani, E. (1998) Structures and functions of calcium channel beta subunits. *J Bioenerg Biomembr* **30**, 357-375

30. Hanlon, M. R., Berrow, N. S., Dolphin, A. C., and Wallace, B. A. (1999) Modelling of a voltage-dependent Ca^{2+} channel β subunit as a basis for understanding its functional properties. *FEBS Letters* **445**, 366-370

31. Chen, Y. H., Li, M. H., Zhang, Y., He, L. L., Yamada, Y., Fitzmaurice, A., Shen, Y., Zhang, H., Tong, L., and Yang, J. (2004) Structural basis of the alpha1-beta subunit interaction of voltage-gated Ca^{2+} channels. *Nature* **429**, 675-680

32. Chen, Y.-h., He, L.-l., Buchanan, D. R., Zhang, Y., Fitzmaurice, A., and Yang, J. (2009) Functional dissection of the intramolecular Src homology 3-guanylate kinase domain coupling in voltage-gated Ca^{2+} channel beta-subunits. *FEBS Letters* **583**, 1969-1975

33. Gao, T., Chien, A. J., and Hosey, M. M. (1999) Complexes of the alpha1C and beta subunits generate the necessary signal for membrane targeting of class C L-type calcium channels. *J Biol Chem* **274**, 2137-2144

34. He, L. L., Zhang, Y., Chen, Y. H., Yamada, Y., and Yang, J. (2007) Functional modularity of the beta-subunit of voltage-gated Ca^{2+} channels. *Biophys J* **93**, 834-845

35. Zhang, Y., Chen, Y. H., Bangaru, S. D., He, L., Abele, K., Tanabe, S., Kozasa, T., and Yang, J. (2008) Origin of the voltage dependence of G-protein regulation of P/Q-type Ca^{2+} channels. *J Neurosci* **28**, 14176-14188

36. McGee, A. W., Nunziato, D. A., Maltez, J. M., Prehoda, K. E., Pitt, G. S., and Bredt, D. S. (2004) Calcium channel function regulated by the SH3-GK module in beta subunits. *Neuron* **42**, 89-99

37. Opatowsky, Y., Chomsky-Hecht, O., Kang, M. G., Campbell, K. P., and Hirsch, J. A. (2003) The voltage-dependent calcium channel beta subunit contains two stable interacting domains. *J Biol Chem* **278**, 52323-52332

38. Opatowsky, Y., Chen, C. C., Campbell, K. P., and Hirsch, J. A. (2004) Structural analysis of the voltage-dependent calcium channel beta subunit functional core and its complex with the alpha 1 interaction domain. *Neuron* **42**, 387-399

39. Van Petegem, F., Clark, K. A., Chatelain, F. C., and Minor, D. L., Jr. (2004) Structure of a complex between a voltage-gated calcium channel beta-subunit and an alpha-subunit domain. *Nature* **429**, 671-675

40. Elias, G. M., and Nicoll, R. A. (2007) Synaptic trafficking of glutamate receptors by MAGUK scaffolding proteins. *Trends Cell Biol* **17**, 343-352

41. Funke, L., Dakoji, S., and Bredt, D. S. (2005) Membrane-associated guanylate kinases regulate adhesion and plasticity at cell junctions. in *Annual Review of Biochemistry*. pp 219-245

42. Takahashi, S. X., Miriyala, J., and Colecraft, H. M. (2004) Membrane-associated guanylate kinase-like properties of beta-subunits required for modulation of voltage-dependent Ca^{2+} channels. *Proc Natl Acad Sci U S A* **101**, 7193-7198

43. Vendel, A. C., Rithner, C. D., Lyons, B. A., and Horne, W. A. (2006) Solution structure of the N-terminal A domain of the human voltage-gated Ca^{2+} channel beta(4a) subunit. *Protein Science* **15**, 378-383

44. Dewaard, M., Witcher, D. R., Pragnell, M., Liu, H. Y., and Campbell, K. P. (1995) Properties of the Alpha(1)-Beta Anchoring Site in Voltage-Dependent Ca^{2+} Channels. *Journal of Biological Chemistry* **270**, 12056-12064

45. Pragnell, M., De Waard, M., Mori, Y., Tanabe, T., Snutch, T. P., and Campbell, K. P. (1994) Calcium channel beta-subunit binds to a conserved motif in the I-II cytoplasmic linker of the alpha 1-subunit. *Nature* **368**, 67-70

46. Witcher, D. R., De Waard, M., Liu, H., Pragnell, M., and Campbell, K. P. (1995) Association of native Ca^{2+} channel beta subunits with the alpha 1 subunit interaction domain. *J Biol Chem* **270**, 18088-18093

47. Van Petegem, F., Duderstadt, K. E., Clark, K. A., Wang, M., and Minor, D. L., Jr. (2008) Alanine-scanning mutagenesis defines a conserved energetic hotspot in the Ca_V alpha1 AID-Ca_V beta interaction site that is critical for channel modulation. *Structure* **16**, 280-294

48. Berrou, L., Dodier, Y., Raybaud, A., Tousignant, A., Dafi, O., Pelletier, J. N., and Parent, L. (2005) The C-terminal residues in the alpha-interacting domain (AID) helix anchor Ca_V beta subunit interaction and modulation of Ca_V2.3 channels. *J Biol Chem* **280**, 494-505

49. Gonzalez-Gutierrez, G., Miranda-Laferte, E., Naranjo, D., Hidalgo, P., and Neely, A. (2008) Mutations of nonconserved residues within the calcium channel alpha1-interaction domain inhibit beta-subunit potentiation. *J Gen Physiol* **132**, 383-395

50. DeWaard, M., Scott, V. E. S., Pragnell, M., and Campbell, K. P. (1996) Identification of critical amino acids involved in alpha(1)-beta interaction in voltage-dependent Ca^{2+} channels. *FEBS Lett* **380**, 272-276

51. Hullin, R., Khan, I. F., Wirtz, S., Mohacsi, P., Varadi, G., Schwartz, A., and Herzig, S. (2003) Cardiac L-type calcium channel beta-subunits expressed in human heart have differential effects on single channel characteristics. *J Biol Chem* **278**, 21623-21630

52. Lao, Q. Z., Kobrinsky, E., Liu, Z., and Soldatov, N. M. (2010) Oligomerization of Cav beta subunits is an essential correlate of Ca^{2+} channel activity. *FASEB J* **24**, 5013-5023

53. Miranda-Laferte, E., Gonzalez-Gutierrez, G., Schmidt, S., Zeug, A., Ponimaskin, E. G., Neely, A., and Hidalgo, P. (2011) Homodimerization of the Src homology 3 domain of the calcium channel beta-subunit drives dynamin-dependent endocytosis. *J Biol Chem* **286**, 22203-22210

54. Dolphin, A. C. (2003) Beta subunits of voltage-gated calcium channels. *J Bioenerg Biomembr* **35**, 599-620

55. Tanaka, O., Sakagami, H., and Kondo, H. (1995) Localization of mRNAs of voltage-dependent Ca^{2+} channels: four subtypes of alpha 1- and beta-subunits in developing and mature rat brain. *Brain Res Mol Brain Res* **30**, 1-16

56. Ludwig, A., Flockerzi, V., and Hofmann, F. (1997) Regional expression and cellular localization of the alpha(1) and beta subunit of high voltage-activated calcium channels in rat brain. *Journal of Neuroscience* **17**, 1339-1349

57. Vance, C. L., Begg, C. M., Lee, W. L., Haase, H., Copeland, T. D., and McEnery, M. W. (1998) Differential expression and association of calcium channel alpha(1B) and beta subunits during rat brain ontogeny. *Journal of Biological Chemistry* **273**, 14495-14502

58. Helton, T. D., Kojetin, D. J., Cavanagh, J., and Horne, W. A. (2002) Alternative splicing of a beta4 subunit proline-rich motif regulates voltage-dependent gating and toxin block of Cav2.1 Ca^{2+} channels. *J Neurosci* **22**, 9331-9339

59. Helton, T. D., and Horne, W. A. (2002) Alternative splicing of the beta4 subunit has alpha1 subunit subtype-specific effects on Ca^{2+} channel gating. *Journal of Neuroscience* **22**, 1573-1582

60. Foell, J. D., Balijepalli, R. C., Delisle, B. P., Yunker, A. M., Robia, S. L., Walker, J. W., McEnery, M. W., January, C. T., and Kamp, T. J. (2004) Molecular heterogeneity of calcium channel beta-subunits in canine and human heart: evidence for differential subcellular localization. *Physiol Genomics* **17**, 183-200

61. Hibino, H., Pironkova, R., Onwumere, O., Rousset, M., Charnet, P., Hudspeth, A. J., and Lesage, F. (2003) Direct interaction with a nuclear protein and regulation of gene

silencing by a variant of the Ca^{2+} channel beta 4 subunit. *Proc Natl Acad Sci U S A* **100**, 307-312

62. Yu, A. S., Boim, M., Hebert, S. C., Castellano, A., Perez-Reyes, E., and Lytton, J. (1995) Molecular characterization of renal calcium channel beta-subunit transcripts. *Am J Physiol* **268**, F525-531

63. Murakami, M., Wissenbach, U., and Flockerzi, V. (1996) Gene structure of the murine calcium channel beta 3 subunit, cDNA and characterization of alternative splicing and transcription products. *European Journal of Biochemistry* **236**, 138-143

64. McEnery, M. W., Vance, C. L., Begg, C. M., Lee, W. L., Choi, Y., and Dubel, S. J. (1998) Differential expression and association of calcium channel subunits in development and disease. *J Bioenerg Biomembr* **30**, 409-418

65. Burgess, D. L., Jones, J. M., Meisler, M. H., and Noebels, J. L. (1997) Mutation of the Ca^{2+} Channel β Subunit Gene Cchb4 Is Associated with Ataxia and Seizures in the Lethargic (lh) Mouse. *Cell* **88**, 385-392

66. Barclay, J., and Rees, M. (1999) Mouse models of spike-wave epilepsy. *Epilepsia* **40 Suppl 3**, 17-22

67. Hosford, D. A., Lin, F. H., Wang, Y., Caddick, S. J., Rees, M., Parkinson, N. J., Barclay, J., Cox, R. D., Gardiner, R. M., Hosford, D. A., Denton, P., Wang, Y., Seldin, M. F., and Chen, B. (1999) Studies of the lethargic (lh/lh) mouse model of absence seizures: regulatory mechanisms and identification of the lh gene. *Adv Neurol* **79**, 239-252

68. Tadmouri, A., Kiyonaka, S., Barbado, M., Rousset, M., Fablet, K., Sawamura, S., Bahembera, E., Pernet-Gallay, K., Arnoult, C., Miki, T., Sadoul, K., Gory-Faure, S., Lambrecht, C., Lesage, F., Akiyama, S., Khochbin, S., Baulande, S., Janssens, V., Andrieux, A., Dolmetsch, R., Ronjat, M., Mori, Y., and De Waard, M. (2012) Cacnb4 directly couples electrical activity to gene expression, a process defective in juvenile epilepsy. *EMBO J* **31**, 3730-3744

69. Ohmori, I., Ouchida, M., Miki, T., Mimaki, N., Kiyonaka, S., Nishiki, T., Tomizawa, K., Mori, Y., and Matsui, H. (2008) A CACNB4 mutation shows that altered Ca(v)2.1 function may be a genetic modifier of severe myoclonic epilepsy in infancy. *Neurobiol Dis* **32**, 349-354

70. Escayg, A., De Waard, M., Lee, D. D., Bichet, D., Wolf, P., Mayer, T., Johnston, J., Baloh, R., Sander, T., and Meisler, M. H. (2000) Coding and noncoding variation of the human calcium-channel beta4-subunit gene CACNB4 in patients with idiopathic generalized epilepsy and episodic ataxia. *Am J Hum Genet* **66**, 1531-1539

71. Perez-Reyes, E., Castellano, A., Kim, H. S., Bertrand, P., Baggstrom, E., Lacerda, A. E., Wei, X. Y., and Birnbaumer, L. (1992) Cloning and expression of a cardiac/brain beta subunit of the L-type calcium channel. *J Biol Chem* **267**, 1792-1797

72. Ruth, P., Rohrkasten, A., Biel, M., Bosse, E., Regulla, S., Meyer, H. E., Flockerzi, V., and Hofmann, F. (1989) Primary structure of the beta subunit of the DHP-sensitive calcium channel from skeletal muscle. *Science* **245**, 1115-1118

73. Gerster, U., Neuhuber, B., Groschner, K., Striessnig, J., and Flucher, B. E. (1999) Current modulation and membrane targeting of the calcium channel alpha1C subunit are independent functions of the beta subunit. *J Physiol* **517 (Pt 2)**, 353-368

74. Obermair, G. J., Schlick, B., Di Biase, V., Subramanyam, P., Gebhart, M., Baumgartner, S., and Flucher, B. E. (2010) Reciprocal interactions regulate targeting of calcium channel beta subunits and membrane expression of alpha1 subunits in cultured hippocampal neurons. *J Biol Chem* **285**, 5776-5791

75. Wittemann, S., Mark, M. D., Rettig, J., and Herlitze, S. (2000) Synaptic localization and presynaptic function of calcium channel beta 4-subunits in cultured hippocampal neurons. *J Biol Chem* **275**, 37807-37814

76. Matsuyama, Z., Wakamori, M., Mori, Y., Kawakami, H., Nakamura, S., and Imoto, K. (1999) Direct alteration of the P/Q-type Ca^{2+} channel property by polyglutamine expansion in spinocerebellar ataxia 6. *J Neurosci* **19**, RC14

77. Meir, A., Bell, D. C., Stephens, G. J., Page, K. M., and Dolphin, A. C. (2000) Calcium channel beta subunit promotes voltage-dependent modulation of alpha 1B by G beta gamma. *Biophysical Journal* **79**, 731-746

78. Neely, A., Garcia-Olivares, J., Voswinkel, S., Horstkott, H., and Hidalgo, P. (2004) Folding of active calcium channel beta(1b) -subunit by size-exclusion chromatography and its role on channel function. *J Biol Chem* **279**, 21689-21694

79. Altier, C., Garcia-Caballero, A., Simms, B., You, H., Chen, L., Walcher, J., Tedford, H. W., Hermosilla, T., and Zamponi, G. W. (2011) The Cavbeta subunit prevents RFP2-mediated ubiquitination and proteasomal degradation of L-type channels. *Nat Neurosci* **14**, 173-180

80. Bichet, D., Cornet, V., Geib, S., Carlier, E., Volsen, S., Hoshi, T., Mori, Y., and De Waard, M. (2000) The I-II loop of the Ca^{2+} channel alpha(1) subunit contains an endoplasmic reticulum retention signal antagonized by the beta subunit. *Neuron* **25**, 177-190

81. Leroy, J., Richards, M. W., Butcher, A. J., Nieto-Rostro, M., Pratt, W. S., Davies, A., and Dolphin, A. C. (2005) Interaction via a key tryptophan in the I-II linker of N-type calcium channels is required for beta1 but not for palmitoylated beta2, implicating an

additional binding site in the regulation of channel voltage-dependent properties. *J Neurosci* **25**, 6984-6996

82. Berrow, N. S., Campbell, V., Fitzgerald, E. M., Brickley, K., and Dolphin, A. C. (1995) Antisense depletion of beta-subunits modulates the biophysical and pharmacological properties of neuronal calcium channels. *J Physiol* **482 (Pt 3)**, 481-491

83. Leuranguer, V., Bourinet, E., Lory, P., and Nargeot, J. (1998) Antisense depletion of beta-subunits fails to affect T-type calcium channels properties in a neuroblastoma cell line. *Neuropharmacology* **37**, 701-708

84. Wei, S., Colecraft, H. M., DeMaria, C. D., Peterson, B. Z., Zhang, R., Kohout, T. A., Rogers, T. B., and Yue, D. T. (2000) Ca^{2+} channel modulation by recombinant auxiliary beta subunits expressed in young adult heart cells. *Circulation Research* **86**, 175-184

85. Jarvis, S. E., and Zamponi, G. W. (2007) Trafficking and regulation of neuronal voltage-gated calcium channels. *Curr Opin Cell Biol* **19**, 474-482

86. Mich, P. M., and Horne, W. A. (2008) Alternative splicing of the Ca^{2+} channel beta4 subunit confers specificity for gabapentin inhibition of Cav2.1 trafficking. *Mol Pharmacol* **74**, 904-912

87. Vendel, A. C., Terry, M. D., Striegel, A. R., Iverson, N. M., Leuranguer, V., Rithner, C. D., Lyons, B. A., Pickard, G. E., Tobet, S. A., and Horne, W. A. (2006) Alternative splicing of the voltage-gated Ca^{2+} channel beta4 subunit creates a uniquely folded N-terminal protein binding domain with cell-specific expression in the cerebellar cortex. *J Neurosci* **26**, 2635-2644

88. Canti, C., Davies, A., Berrow, N. S., Butcher, A. J., Page, K. M., and Dolphin, A. C. (2001) Evidence for two concentration-dependent processes for beta-subunit effects on alpha1B calcium channels. *Biophys J* **81**, 1439-1451

89. Tareilus, E., Roux, M., Qin, N., Olcese, R., Zhou, J., Stefani, E., and Birnbaumer, L. (1997) A Xenopus oocyte subunit: Evidence for a role in the assembly/expression of voltage-gated calcium channels that is separate from its role as a regulatory subunit. *Proceedings of the National Academy of Sciences* **94**, 1703-1708

90. Fang, K., and Colecraft, H. M. (2011) Mechanism of auxiliary beta-subunit-mediated membrane targeting of L-type (Ca_V)1.2) channels. *J Physiol* **589**, 4437-4455

91. Rougier, J. S., Albesa, M., Abriel, H., and Viard, P. (2011) Neuronal precursor cell-expressed developmentally down-regulated 4-1 (NEDD4-1) controls the sorting of newly synthesized Ca(V)1.2 calcium channels. *J Biol Chem* **286**, 8829-8838

92. Waithe, D., Ferron, L., Page, K. M., Chaggar, K., and Dolphin, A. C. (2011) Beta-subunits promote the expression of Ca(V)2.2 channels by reducing their proteasomal degradation. *J Biol Chem* **286**, 9598-9611

93. Simms, B. A., and Zamponi, G. W. (2012) Trafficking and stability of voltage-gated calcium channels. *Cell Mol Life Sci* **69**, 843-856

94. Gregg, R. G., Messing, A., Strube, C., Beurg, M., Moss, R., Behan, M., Sukhareva, M., Haynes, S., Powell, J. A., Coronado, R., and Powers, P. A. (1996) Absence of the beta subunit (cchb1) of the skeletal muscle dihydropyridine receptor alters expression of the alpha 1 subunit and eliminates excitation-contraction coupling. *Proc Natl Acad Sci U S A* **93**, 13961-13966

95. Murakami, M., Fleischmann, B., De Felipe, C., Freichel, M., Trost, C., Ludwig, A., Wissenbach, U., Schwegler, H., Hofmann, F., Hescheler, J., Flockerzi, V., and Cavalie, A. (2002) Pain perception in mice lacking the beta3 subunit of voltage-activated calcium channels. *J Biol Chem* **277**, 40342-40351

96. Weissgerber, P., Held, B., Bloch, W., Kaestner, L., Chien, K. R., Fleischmann, B. K., Lipp, P., Flockerzi, V., and Freichel, M. (2006) Reduced cardiac L-type Ca^{2+} current in Ca(V)beta2-/- embryos impairs cardiac development and contraction with secondary defects in vascular maturation. *Circ Res* **99**, 749-757

97. Colecraft, H. M., Alseikhan, B., Takahashi, S. X., Chaudhuri, D., Mittman, S., Yegnasubramanian, V., Alvania, R. S., Johns, D. C., Marban, E., and Yue, D. T. (2002) Novel functional properties of Ca^{2+} channel beta subunits revealed by their expression in adult rat heart cells. *Journal of Physiology-London* **541**, 435-452

98. Wakamori, M., Mikala, G., and Mori, Y. (1999) Auxiliary subunits operate as a molecular switch in determining gating behaviour of the unitary N-type Ca^{2+} channel current in Xenopus oocytes. *Journal of Physiology-London* **517**, 659-672

99. Stea, A., Dubel, S. J., Pragnell, M., Leonard, J. P., Campbell, K. P., and Snutch, T. P. (1993) A beta-subunit normalizes the electrophysiological properties of a cloned N-type Ca^{2+} channel alpha 1-subunit. *Neuropharmacology* **32**, 1103-1116

100. Luvisetto, S., Fellin, T., Spagnolo, M., Hivert, B., Brust, P. F., Harpold, M. M., Stauderman, K. A., Williams, M. E., and Pietrobon, D. (2004) Modal gating of human CaV2.1 (P/Q-type) calcium channels: I. The slow and the fast gating modes and their modulation by beta subunits. *J Gen Physiol* **124**, 445-461

101. Geib, S., Sandoz, G., Mabrouk, K., Matavel, A., Marchot, P., Hoshi, T., Villaz, M., Ronjat, M., Miquelis, R., Leveques, C., and De Waard, M. (2002) Use of a purified and functional recombinant calcium-channel beta4 subunit in surface-plasmon resonance studies. *Biochemical Journal* **364**, 285-292

102. Findeisen, F., and Minor, D. L., Jr. (2009) Disruption of the IS6-AID linker affects voltage-gated calcium channel inactivation and facilitation. *J Gen Physiol* **133**, 327-343

103. Patil, P. G., Brody, D. L., and Yue, D. T. (1998) Preferential closed-state inactivation of neuronal calcium channels. *Neuron* **20**, 1027-1038

104. Yasuda, T., Lewis, R. J., and Adams, D. J. (2004) Overexpressed Ca(v)beta3 inhibits N-type (Cav2.2) calcium channel currents through a hyperpolarizing shift of ultra-slow and closed-state inactivation. *J Gen Physiol* **123**, 401-416

105. Zhen, X. G., Xie, C., Fitzmaurice, A., Schoonover, C. E., Orenstein, E. T., and Yang, J. (2005) Functional architecture of the inner pore of a voltage-gated Ca^{2+} channel. *J Gen Physiol* **126**, 193-204

106. Xie, C., Zhen, X. G., and Yang, J. (2005) Localization of the activation gate of a voltage-gated Ca^{2+} channel. *J Gen Physiol* **126**, 205-212

107. Hering, S., Berjukow, S., Sokolov, S., Marksteiner, R., Weiss, R. G., Kraus, R., and Timin, E. N. (2000) Molecular determinants of inactivation in voltage-gated Ca^{2+} channels. *J Physiol* **528 Pt 2**, 237-249

108. Almagor, L., Chomsky-Hecht, O., Ben-Mocha, A., Hendin-Barak, D., Dascal, N., and Hirsch, J. A. (2012) The role of a voltage-dependent Ca^{2+} channel intracellular linker: a structure-function analysis. *J Neurosci* **32**, 7602-7613

109. Arias, J. M., Murbartian, J., Vitko, I., Lee, J. H., and Perez-Reyes, E. (2005) Transfer of beta subunit regulation from high to low voltage-gated Ca^{2+} channels. *FEBS Lett* **579**, 3907-3912

110. Vitko, I., Shcheglovitov, A., Baumgart, J. P., Arias, O., II, Murbartian, J., Arias, J. M., and Perez-Reyes, E. (2008) Orientation of the calcium channel beta relative to the alpha(1)2.2 subunit is critical for its regulation of channel activity. *PLoS One* **3**, e3560

111. Maltez, J. M., Nunziato, D. A., Kim, J., and Pitt, G. S. (2005) Essential Ca(V)beta modulatory properties are AID-independent. *Nat Struct Mol Biol* **12**, 372-377

112. Walker, D., Bichet, D., Campbell, K. P., and De Waard, M. (1998) A beta 4 isoform-specific interaction site in the carboxyl-terminal region of the voltage-dependent Ca^{2+} channel alpha 1A subunit. *J Biol Chem* **273**, 2361-2367

113. Walker, D., Bichet, D., Geib, S., Mori, E., Cornet, V., Snutch, T. P., Mori, Y., and De Waard, M. (1999) A new beta subtype-specific interaction in alpha1A subunit controls P/Q-type Ca^{2+} channel activation. *J Biol Chem* **274**, 12383-12390

114. Gonzalez-Gutierrez, G., Miranda-Laferte, E., Nothmann, D., Schmidt, S., Neely, A., and Hidalgo, P. (2008) The guanylate kinase domain of the beta-subunit of voltage-gated

calcium channels suffices to modulate gating. *Proc Natl Acad Sci U S A* **105**, 14198-14203

115. Dolphin, A. C. (2003) G protein modulation of voltage-gated calcium channels. *Pharmacol Rev* **55**, 607-627

116. Herlitze, S., Garcia, D. E., Mackie, K., Hille, B., Scheuer, T., and Catterall, W. A. (1996) Modulation of Ca^{2+} channels by G-protein beta gamma subunits. *Nature* **380**, 258-262

117. Bean, B. P. (1989) Neurotransmitter inhibition of neuronal calcium currents by changes in channel voltage dependence. *Nature* **340**, 153-156

118. Kasai, H., and Aosaki, T. (1989) Modulation of Ca-channel current by an adenosine analog mediated by a GTP-binding protein in chick sensory neurons. *Pflugers Archiv European Journal of Physiology* **414**, 145-149

119. Bourinet, E., Soong, T. W., Stea, A., and Snutch, T. P. (1996) Determinants of the G protein-dependent opioid modulation of neuronal calcium channels. *Proc Natl Acad Sci U S A* **93**, 1486-1491

120. Campbell, V., Berrow, N. S., Fitzgerald, E. M., Brickley, K., and Dolphin, A. C. (1995) Inhibition of the interaction of G protein G(o) with calcium channels by the calcium channel beta-subunit in rat neurones. *J Physiol* **485 (Pt 2)**, 365-372

121. Currie, K. P. (2010) Inhibition of Ca^{2+} channels and adrenal catecholamine release by G protein coupled receptors. *Cell Mol Neurobiol* **30**, 1201-1208

122. Beguin, P., Nagashima, K., Gonoi, T., Shibasaki, T., Takahashi, K., Kashima, Y., Ozaki, N., Geering, K., Iwanaga, T., and Seino, S. (2001) Regulation of Ca^{2+} channel expression at the cell surface by the small G-protein kir/Gem. *Nature* **411**, 701-706

123. Finlin, B. S., Crump, S. M., Satin, J., and Andres, D. A. (2003) Regulation of voltage-gated calcium channel activity by the Rem and Rad GTPases. *Proc Natl Acad Sci U S A* **100**, 14469-14474

124. Beguin, P., Mahalakshmi, R. N., Nagashima, K., Cher, D. H., Ikeda, H., Yamada, Y., Seino, Y., and Hunziker, W. (2006) Nuclear sequestration of beta-subunits by Rad and Rem is controlled by 14-3-3 and calmodulin and reveals a novel mechanism for Ca^{2+} channel regulation. *J Mol Biol* **355**, 34-46

125. Fan, M., Buraei, Z., Luo, H. R., Levenson-Palmer, R., and Yang, J. (2010) Direct inhibition of P/Q-type voltage-gated Ca^{2+} channels by Gem does not require a direct Gem/Cavbeta interaction. *Proc Natl Acad Sci U S A* **107**, 14887-14892

126. Yang, T., Puckerin, A., and Colecraft, H. M. (2012) Distinct RGK GTPases differentially use alpha1- and auxiliary beta-binding-dependent mechanisms to inhibit CaV1.2/CaV2.2 channels. *PLoS One* **7**, e37079

127. Grueter, C. E., Abiria, S. A., Dzhura, I., Wu, Y., Ham, A. J., Mohler, P. J., Anderson, M. E., and Colbran, R. J. (2006) L-type Ca^{2+} channel facilitation mediated by phosphorylation of the beta subunit by CaMKII. *Mol Cell* **23**, 641-650

128. Grueter, C. E., Abiria, S. A., Wu, Y., Anderson, M. E., and Colbran, R. J. (2008) Differential regulated interactions of calcium/calmodulin-dependent protein kinase II with isoforms of voltage-gated calcium channel beta subunits. *Biochemistry* **47**, 1760-1767

129. Gerhardstein, B. L., Puri, T. S., Chien, A. J., and Hosey, M. M. (1999) Identification of the sites phosphorylated by cyclic AMP-dependent protein kinase on the beta 2 subunit of L-type voltage-dependent calcium channels. *Biochemistry* **38**, 10361-10370

130. Miriyala, J., Nguyen, T., Yue, D. T., and Colecraft, H. M. (2008) Role of Cav beta subunits, and lack of functional reserve, in protein kinase A modulation of cardiac Cav1.2 channels. *Circ Res* **102**, e54-64

131. Delmas, P., Coste, B., Gamper, N., and Shapiro, M. S. (2005) Phosphoinositide lipid second messengers: new paradigms for calcium channel modulation. *Neuron* **47**, 179-182

132. Michailidis, I. E., Zhang, Y., and Yang, J. (2007) The lipid connection-regulation of voltage-gated Ca^{2+} channels by phosphoinositides. *Pflugers Arch* **455**, 147-155

133. Blair, L. A., and Marshall, J. (1997) IGF-1 modulates N and L calcium channels in a PI 3-kinase-dependent manner. *Neuron* **19**, 421-429

134. Viard, P., Butcher, A. J., Halet, G., Davies, A., Nurnberg, B., Heblich, F., and Dolphin, A. C. (2004) PI3K promotes voltage-dependent calcium channel trafficking to the plasma membrane. *Nat Neurosci* **7**, 939-946

135. Catalucci, D., Zhang, D.-H., DeSantiago, J., Aimond, F., Barbara, G., Chemin, J., Bonci, D., Picht, E., Rusconi, F., Dalton, N. D., Peterson, K. L., Richard, S., Bers, D. M., Brown, J. H., and Condorelli, G. (2009) Akt regulates L-type Ca^{2+} channel activity by modulating Cav alpha 1 protein stability. *Journal of Cell Biology* **184**, 923-933

136. Protasi, F. (2002) Structural interaction between RYRs and DHPRs in calcium release units of cardiac and skeletal muscle cells. *Frontiers in Bioscience* **7**, d650

137. Schredelseker, J., Dayal, A., Schwerte, T., Franzini-Armstrong, C., and Grabner, M. (2009) Proper restoration of excitation-contraction coupling in the dihydropyridine receptor beta1-null zebrafish relaxed is an exclusive function of the beta1a subunit. *J Biol Chem* **284**, 1242-1251

138. Schredelseker, J., Di Biase, V., Obermair, G. J., Felder, E. T., Flucher, B. E., Franzini-Armstrong, C., and Grabner, M. (2005) The beta 1a subunit is essential for the assembly of dihydropyridine-receptor arrays in skeletal muscle. *Proc Natl Acad Sci U S A* **102**, 17219-17224

139. Rebbeck, R. T., Karunasekara, Y., Gallant, E. M., Board, P. G., Beard, N. A., Casarotto, M. G., and Dulhunty, A. F. (2011) The beta(1a) subunit of the skeletal DHPR binds to skeletal RyR1 and activates the channel via its 35-residue C-terminal tail. *Biophys J* **100**, 922-930

140. Karunasekara, Y., Rebbeck, R. T., Weaver, L. M., Board, P. G., Dulhunty, A. F., and Casarotto, M. G. (2012) An alpha-helical C-terminal tail segment of the skeletal L-type Ca^{2+} channel beta1a subunit activates ryanodine receptor type 1 via a hydrophobic surface. *FASEB J* **26**, 5049-5059

141. Gonzalez-Gutierrez, G., Miranda-Laferte, E., Neely, A., and Hidalgo, P. (2007) The Src homology 3 domain of the beta-subunit of voltage-gated calcium channels promotes endocytosis via dynamin interaction. *J Biol Chem* **282**, 2156-2162

142. Catterall, W. A., Leal, K., and Nanou, E. (2013) Calcium Channels and Short-term Synaptic Plasticity. *Journal of Biological Chemistry* **288**, 10742-10749

143. Kiyonaka, S., Wakamori, M., Miki, T., Uriu, Y., Nonaka, M., Bito, H., Beedle, A. M., Mori, E., Hara, Y., De Waard, M., Kanagawa, M., Itakura, M., Takahashi, M., Campbell, K. P., and Mori, Y. (2007) RIM1 confers sustained activity and neurotransmitter vesicle anchoring to presynaptic Ca^{2+} channels. *Nat Neurosci* **10**, 691-701

144. Gandini, M. A., Sandoval, A., Gonzalez-Ramirez, R., Mori, Y., de Waard, M., and Felix, R. (2011) Functional coupling of Rab3-interacting molecule 1 (RIM1) and L-type Ca^{2+} channels in insulin release. *J Biol Chem* **286**, 15757-15765

145. Hibino, H., Pironkova, R., Onwumere, O., Vologodskaia, M., Hudspeth, A. J., and Lesage, F. (2002) RIM binding proteins (RBPs) couple Rab3-interacting molecules (RIMs) to voltage-gated Ca^{2+} channels. *Neuron* **34**, 411-423

146. Liu, K. S., Siebert, M., Mertel, S., Knoche, E., Wegener, S., Wichmann, C., Matkovic, T., Muhammad, K., Depner, H., Mettke, C., Buckers, J., Hell, S. W., Muller, M., Davis, G. W., Schmitz, D., and Sigrist, S. J. (2011) RIM-binding protein, a central part of the active zone, is essential for neurotransmitter release. *Science* **334**, 1565-1569

147. Haase, H. (2007) Ahnak, a new player in beta-adrenergic regulation of the cardiac L-type Ca^{2+} channel. *Cardiovasc Res* **73**, 19-25

148. Pankonien, I., Alvarez, J. L., Doller, A., Kohncke, C., Rotte, D., Regitz-Zagrosek, V., Morano, I., and Haase, H. (2011) Ahnak1 is a tuneable modulator of cardiac Ca(v)1.2 calcium channel activity. *J Muscle Res Cell Motil* **32**, 281-290

149. Hartzell, H. C., Qu, Z., Yu, K., Xiao, Q., and Chien, L. T. (2008) Molecular physiology of bestrophins: multifunctional membrane proteins linked to best disease and other retinopathies. *Physiol Rev* **88**, 639-672

150. Yu, K., Xiao, Q., Cui, G., Lee, A., and Hartzell, H. C. (2008) The best disease-linked Cl- channel hBest1 regulates Ca_V1 (L-type) Ca^{2+} channels via src-homology-binding domains. *J Neurosci* **28**, 5660-5670

151. Milenkovic, V. M., Krejcova, S., Reichhart, N., Wagner, A., and Strauss, O. (2011) Interaction of bestrophin-1 and Ca^{2+} channel beta-subunits: identification of new binding domains on the bestrophin-1 C-terminus. *PLoS One* **6**, e19364

152. Cohen, R. M., Foell, J. D., Balijepalli, R. C., Shah, V., Hell, J. W., and Kamp, T. J. (2005) Unique modulation of L-type Ca^{2+} channels by short auxiliary beta1d subunit present in cardiac muscle. *Am J Physiol Heart Circ Physiol* **288**, H2363-2374

153. Harry, J. B., Kobrinsky, E., Abernethy, D. R., and Soldatov, N. M. (2004) New short splice variants of the human cardiac Cav beta2 subunit: redefining the major functional motifs implemented in modulation of the Cav1.2 channel. *J Biol Chem* **279**, 46367-46372

154. Ebert, A. M., McAnelly, C. A., Srinivasan, A., Linker, J. L., Horne, W. A., and Garrity, D. M. (2008) Ca^{2+} channel-independent requirement for MAGUK family CACNB4 genes in initiation of zebrafish epiboly. *Proc Natl Acad Sci U S A* **105**, 198-203

155. Zhou, W., Horstick, E. J., Hirata, H., and Kuwada, J. Y. (2008) Identification and expression of voltage-gated calcium channel beta subunits in Zebrafish. *Dev Dyn* **237**, 3842-3852

156. Subramanyam, P., Obermair, G. J., Baumgartner, S., Gebhart, M., Striessnig, J., Kaufmann, W. A., Geley, S., and Flucher, B. E. (2009) Activity and calcium regulate nuclear targeting of the calcium channel beta4b subunit in nerve and muscle cells. *Channels* **3**, 343-355

157. Zhang, Y., Yamada, Y., Fan, M., Bangaru, S. D., Lin, B., and Yang, J. (2010) The beta subunit of voltage-gated Ca^{2+} channels interacts with and regulates the activity of a novel isoform of Pax6. *J Biol Chem* **285**, 2527-2536

158. Ronjat, M., Kiyonaka, S., Barbado, M., De Waard, M., and Mori, Y. (2013) Nuclear life of the voltage-gated Cacnb4 subunit and its role in gene transcription regulation. *Channels (Austin)* **7**, 119-125

159. Etemad, S., Obermair, G. J., Bindreither, D., Benedetti, A., Stanika, R., Di Biase, V., Burtscher, V., Koschak, A., Kofler, R., Geley, S., Wille, A., Lusser, A., Flockerzi, V., and Flucher, B. E. (2014) Differential neuronal targeting of a new and two known calcium channel beta4 subunit splice variants correlates with their regulation of gene expression. *J Neurosci* **34**, 1446-1461

CHAPTER 2

Mammalian Ca^{2+} channel β4c subunit interacts with heterochromatin protein 1 via a PXVXL binding motif

Introduction

The Ca^{2+} channel β4 subunit is a multifunctional protein that acts primarily as a Ca^{2+} channel regulatory subunit but also performs Ca^{2+} channel independent functions (1-3). The latter emerging role of the Ca^{2+} channel β4 subunit began with the cloning of various alternatively spliced isoforms of the β4 subunit (4). In 2003, Hibono et al. identified a chicken β4 subunit (cβ4c-212aa) isoform resulting from a splicing induced frame shift and a subsequent early stop codon. The cβ4c was shown to interact with the heterochromatin protein 1 γ (HP1γ) and both proteins are co-localized in the nuclei of cochlear hair cells. The authors also showed that cβ4c attenuates the gene silencing activity of HP1γ *in vitro* (5).

Heterochromtin protein 1 (HP1) is a non-histone chromosomal protein playing versatile roles not only in heterochromatin formation and gene silencing, but also in telomere stability and positive regulation of gene expression (6-8). HP1 proteins consist of an N-terminal chromo domain (CD), a flexible hinge region, and a highly conserved C-terminal chromo shadow domain (CSD) (9). The CD of HP1 is directly responsible for binding to methylated lysine 9 of histone H3 (H3K9me3), an epigenetic mark for gene silencing according to the histone code. In contrast, the CSD is involved in the homo-or hetero-dimerization of HP1 isotypes and interaction with other proteins (10). Heterochromatin serves as a self-assembling frame work to recruit effector proteins, which in turn regulate various chromosomal processes (11,12).

* This chapter is part of the published paper, *J Biol Chem* 286, 9677-9687 (2011).

After identification of cβ4c, there was no further study on the existence and role of β4c, specifically in mammals. Here, we identified and cloned a truncated splice variant of Ca^{2+} channel β subunit from human brain. Both human and cβ4c contain the β4a N-terminus, the SH3 domain and HOOK sequence, a truncated GK domain, and additional C-terminal sequence resulting from the frame shift. Western blot and immunohistochemistry experiments revealed that β4c was located specifically in the deep cerebellar nuclei and the medial vestibular nucleus (MVN) in the mouse brain. We also determined that β4c interacted with the chromo shadow domains (CSD) dimers of HP1 primarily through its C-terminal PXVXL consensus sequence, and that β4c has no electrophysiological effects on the Ca^{2+} channels.

Results

Molecular cloning of a splice variant of the Ca^{2+} channel β4 subunit (β4c) from human pons

The cβ4c, a truncated splice variant of the Ca^{2+} channel β4 subunit was shown to be highly expressed in the chicken cochlea (5). Previously, our lab reported that alternative splicing of human β4 N-terminal exons made two different subtypes of full-length β4 subunits, β4a and β4b (13). The chicken short isoform contained the human β4a N-terminal sequence, therefore we hypothesized that mammalian β4c has the β4a subtype N-terminus. We identified the truncated spliced variant of Ca^{2+} channel β4 subunit by PCR from human cerebellum and pons, and were subsequently able to clone it (14). Figure 2.1 shows that the Cacnb4 gene codes for full-length β4a containing a SH3-HOOK-GK core and C-terminus. By contrast, β4c is a truncated form that results from exon 9 skipping, and therefore lacks the GK domain.

Figure 2.1 Identification of a truncated splice variant of the human Ca^{2+} channel β4 subunit.

(A) A diagram of exon structure of Cacnb4 and corresponding protein domains of the full-length human β4a subunit (486 amino acids), and truncated β4c subunit (207 amino acids) resulted from alternative splicing (skipping) of exon 9.

(B) Sequence alignment of human and chicken β4c proteins. *, identifies divergent amino acids; ▼, identifies exon translation boundaries. PXVXL, consensus site for binding to HP1γ.

A

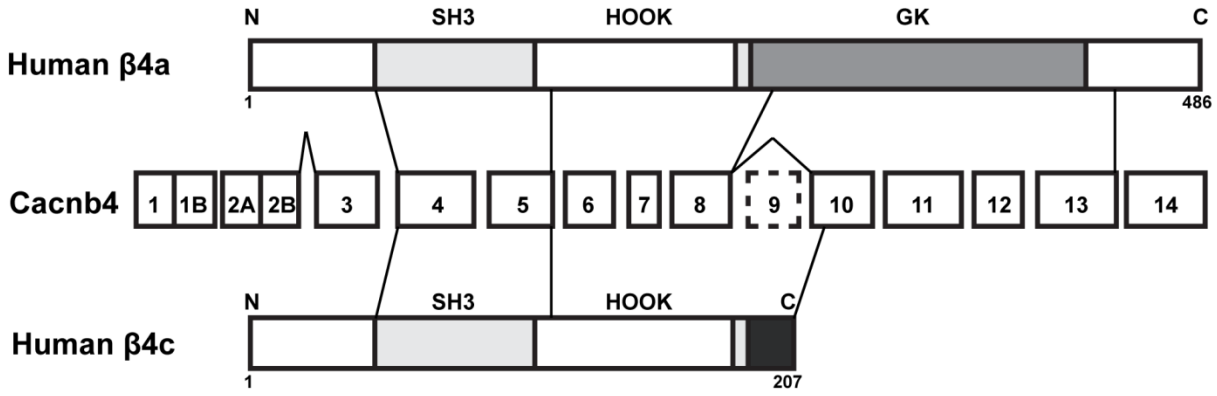

B

```
hβ4c  MYDNLYLHGIEDSEAGSADSYTSRPSDSDVSLEEDREAIRQEREQQAAIQLERAKSKPVA  60
cβ4c  MYDNLYLHGFEDSEAGSADSYTSRPSDSDVSLEEDREAIRQEREQQAAIQLERAKSKPVA  60
                *

hβ4c  FAVKTNVSYCGALDEDVPVPSTAISFDAKDFLHIKEKYNNDWWIGRLVKEGCEIGFIPSP 120
cβ4c  FAVKTNVSYCGALDEDVPVPSTAISFDAKDFLHIKEKYNNDWWIGRLVKEGCEIGFIPSP 120

hβ4c  LRLENIRIQQEQKRGRFHGGKSSGNSSSSLGEMVSGTFRATPTSTAKQKQKVTEHIPPYD 180
cβ4c  LRLENIRIQQEQKRGRFHGGKSSGNSSSSLGEMVSGTFRATPTSTAKQKQKVTEHVPPYD 180
                                                          *
          PXVXL
hβ4c  VVPSMRPVVLVGPSLKGYEDFNNESDS-----  207
cβ4c  VVPSMRPVVLVGPSLKGYEDINNPSDSRHSFC  212
                          *  *   *****
```

This alternative splicing event results in a frame shift and addition of eight amino acids (DFNNESDS) before the newly created stop codon. Sequence alignment of human and chicken β4c shows that these two proteins are nearly identical except for their C-termini (Figure 2.1B).

Identification of mammalian β4c in mice brain

To examine the expression of mammalian β4c in mice, we used a well-characterized β4a/c antibody recognizing its N-terminus (15). In the previous study with chicken, cβ4c was shown to be expressed in brain, spinal cord, eye and heart along with full-length β4 protein. However, cβ4c was found to be the exclusive isoform in the cochlea (5). Our previous immunocytochemistry study revealed that β4c is expressed in cochlea, vestibular, and deep cerebellar nuclei of the mouse brain (14). This specific localization of β4c in the mouse brain suggests that β4c may have a regulatory role in these specific neurons.

β4c interacts with HP1γ via a PXVXL motif

A previous yeast two-hybrid study (5) revealed that the 170-199 sequence of β4c contains critical residues for the interaction with chromo shadow domain (CSD) of HP1γ. Heterochromatin protein 1 (HP1) proteins are characterized by two conserved domains: the chromo domain (CD) at the N-terminus, and the chromo shadow domain (CSD) at the C-terminus.

The CD was shown to directly bind to chromatin, while the CSD is implicated in various protein interactions (16). The CSD binding proteins are classified into four groups according to their binding profiles and the majority of HP1 binding proteins have a consensus PXVXL motif (17). The CSD is responsible for HP1 dimerization, which creates a hydrophobic surface that

binds to the PXVXL motif of HP1-binding proteins (18,19). Further examination of the β4c sequence lead us to the idea that PVVLV, located at residues 187-191 might be a candidate CSD binding motif. To determine whether the binding between β4c and HP1γ was through its PVVLV motif, we turned to isothermal titration calorimetry (ITC). First, we created two constructs: β4cΔ199 that includes the PVVLV motif, and β4cΔ184 that lacks the PVVLV motif. Figure 2.3, top panel, shows the raw data for titration of β4cΔ199 against soluble CSD dimer and indicates that the interaction is exothermic. Figure 2.3, bottom panel, shows that the binding stoichiometry between β4cΔ199 and the CSD is 1:1 (n = 1.04), and the binding affinity is 0.7 μM under our experimental conditions. The flat line for β4cΔ184 (open square) indicates that there is no detectable interaction between β4cΔ184 and the CSD dimer. These ITC results confirm that the fifteen residues between 184 and 199 contain the specific CSD interaction determinants. To further identify the critical residues involved in the β4c-CSD interaction, we made two constructs with mutations in the PVVLV motif: one with the single mutation V189A, and the other with the double mutation P187A/V189A. Our experiments indicate that the single mutation V189A reduces the binding affinity of β4cΔ199 for CSD five-fold to 3.9 μM and the double mutation abolishes the interaction with CSD altogether (Figure 2.4). This result confirms that β4c interacts with CSD through its PVVLV motif and that proline at position 1, and valine at position 3, are critical residues.

Figure 2.2 The chromo shadow domain of HP1γ interacts with β4Δ199.

Isothermal titration calorimetry. Top panel, raw data after base-line correction shows saturating exothermic binding of CSD dimer when titrated into β4Δ199 solution. Bottom panel, integrated data corrected for the heat of dilution of the CSD dimer. Open and filled square represent β4Δ184 and β4Δ199 data, respectively. The solid line represents the best fit to a one-site binding model of the interaction between the CSD dimer and β4Δ199.

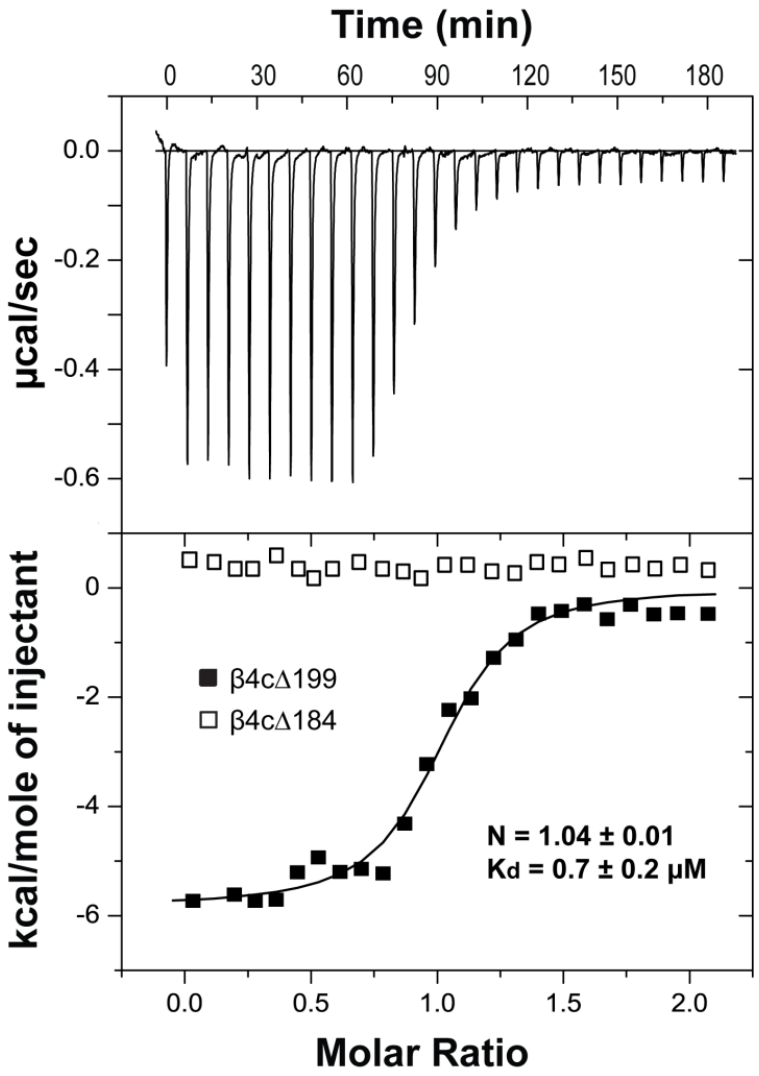

Figure 2.3 Mutations in the PXVXL motif abolish interaction between β4Δ199 and HP1γ chromo shadow domain dimer.

Isothermal titration calorimetry. Top panel, raw data after base-line correction shows saturating exothermic binding of CSD dimer when titrated into β4Δ199/V189A solution. Bottom panel, integrated data corrected for the heat of dilution of the CSD dimer. Open and filled squares represent β4Δ199/P187A/V189A and β4Δ199/V189A data, respectively. The solid line represents the best fit to a one-site binding model of the interaction between the CSD dimer and β4Δ199/V189A.

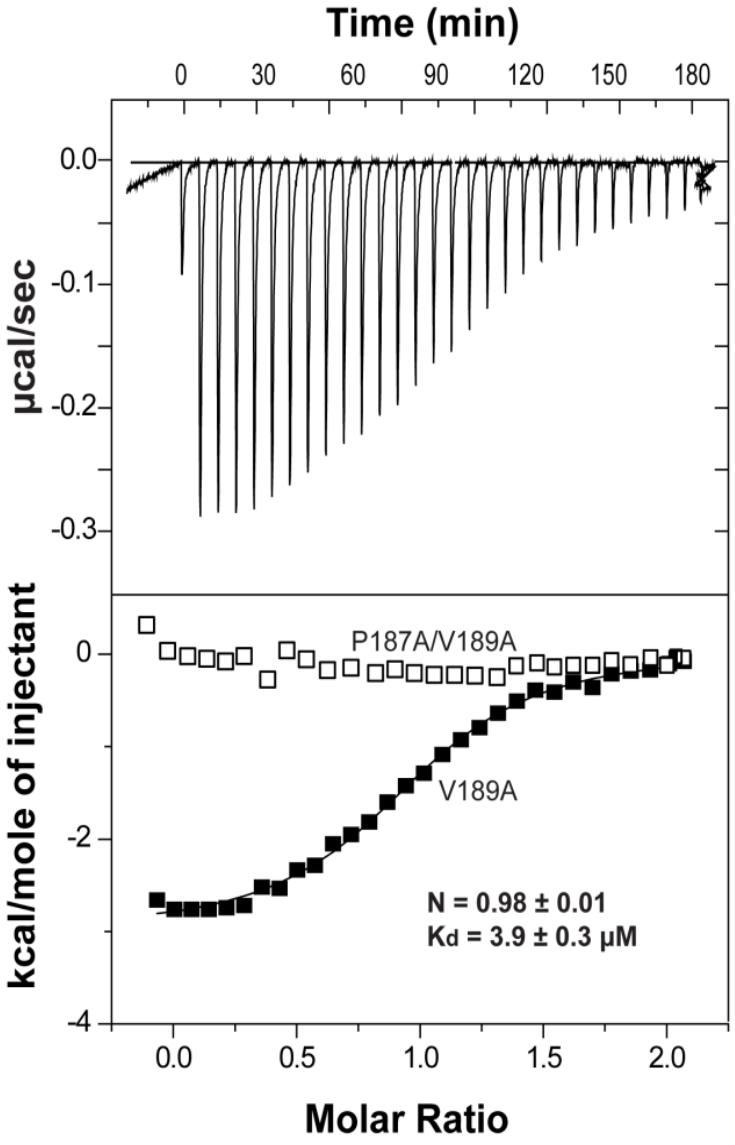

Physiological effects of β4c on Ca^{2+} channels

Considering that β4c lacks more than 90% of the GK domain that interacts with the α1 subunit AID to exert its regulatory function on Ca^{2+} channels (1,3), there is little possibility that β4c directly affects Ca^{2+} channel function. To investigate the physiological effects of β4c on the Ca^{2+} channel, we compared the Ca^{2+} currents in *Xenopus* oocytes expressing α1 and α2δ subunits in the presence or absence of either β4c or β4a. Since β subunit activity is concentration dependent (15), we tested β4c with a ten-fold higher molar concentration of β4a. Figure 2.5 shows that coexpression of β4c had no effect on the rate of expression of $Ca_v2.1$ current, voltage-dependence of activation, or voltage-dependence of inactivation. By contrast, coexpression of β4a dramatically increased the current expression rate and caused a ~10-15 mV hyperpolarizing shift in the voltage-dependence of activation and inactivation, respectively (Table 2.1). These results indicate that β4c does not have physiological effects on trafficking or gating of Ca^{2+} channels.

Discussion

Alternative splicing of the Ca^{2+} channel β subunit

Alternative pre-mRNA splicing gives cells the capacity to modify and selectively re-balance their existing pool of transcripts with a limited number of genes (20). It is essential for normal neuronal development, neuronal excitability, axon targeting, and neuronal circuit formation. Alternative splicing is particularly prevalent in the mammalian brain, consistent with having evolved in parallel with biological complexities (21,22). Mammalian Ca^{2+} channel β subunits are encoded by only four genes; however, multiple isoforms are expressed in different cells.

Figure 2.4 Electrophysiological effects of β4c on Ca^{2+} channels.

(A) $Ca_v2.1$ current size as a function of time after injection of α1:α2δ cRNA mixtures (1:1 molar ratio) containing 0 β cRNA (1:1:0, *squares*), equimolar β4a cRNA (1:1:1, *diamonds*), or 10X molar β4c cRNA (1:1:10, *circles*).

(B) Normalized current traces of voltage-dependent activation of $Ca_v2.1$ channels. Plots were derived from averaged *I–V* data for each cRNA combination. Data points represent the means of the normalized data at a given membrane potential for over ten different recordings.

(C) Normalized current traces of voltage-dependent inactivation of $Ca_v2.1$ channels. Plots were derived from averaged *I–V* data for each cRNA combination. Data points represent the means of the normalized data at a given membrane potential for over eight different recordings.

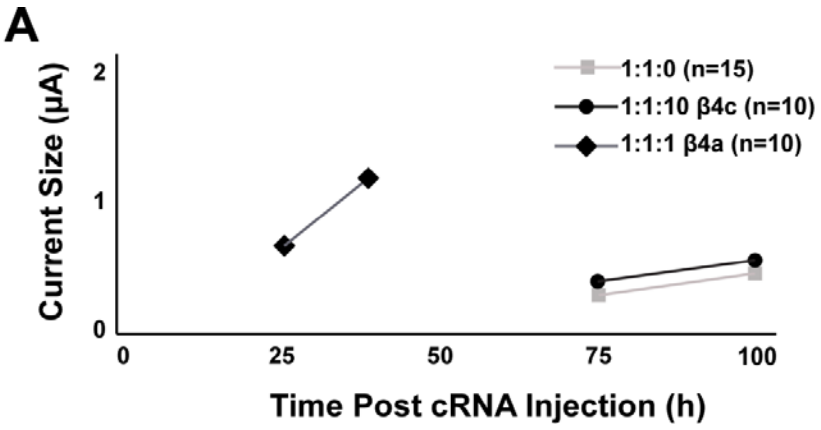
A
Current Size (μA)
2
1
0
0
25
50
75
100
Time Post cRNA Injection (h)
1:1:0 (n=15)
1:1:10 β4c (n=10)
1:1:1 β4a (n=10)

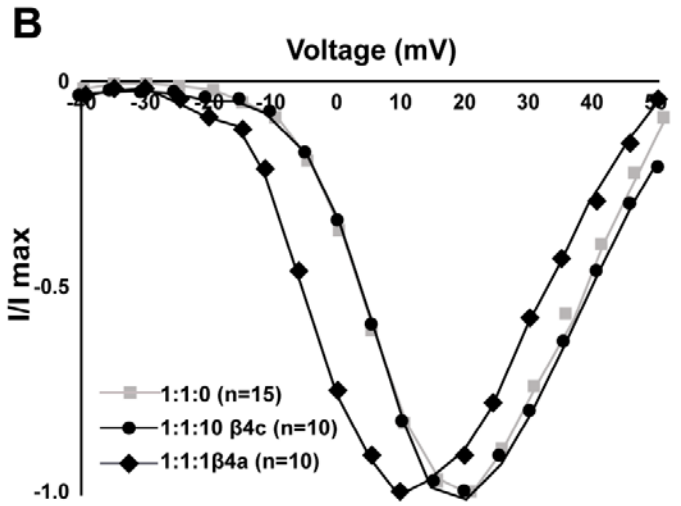
B
Voltage (mV)
0
-30
-10
0
10
20
30
40
I/I max
-0.5
-1.0
1:1:0 (n=15)
1:1:10 β4c (n=10)
1:1:1β4a (n=10)

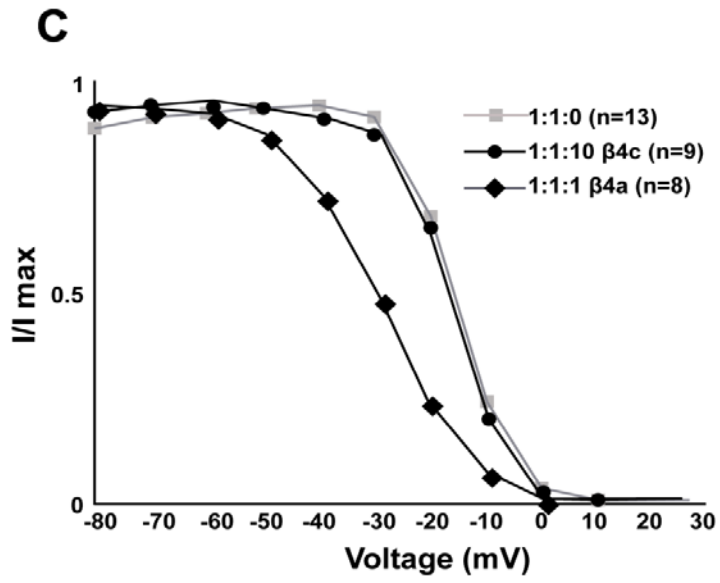
C
1
0.5
0
I/I max
-80
-70
-60
-50
-40
-30
-20
-10
0
10
20
30
Voltage (mV)
1:1:0 (n=13)
1:1:10 β4c (n=9)
1:1:1 β4a (n=8)

Table 2.1 β4c does not affect voltage-dependent gating parameters and expression rate of α1A:α2δ Ca^{2+} channel complexes in *Xenopus* oocytes.

Voltage-dependent gating properties					Ca^{2+} current expression rate		
α1:α2δ:β	n	$V_{1/2}$ Activation (mV)	n	$V_{1/2}$ Inactivation (mV)	α1:α2δ:β	n	Time to 0.5 μA (h)
1:1:0	15	1.29 ± 0.58	13	-14.91 ± 0.87	1:1:0	5	90 ± 3.56
1:1:10 (β4c)	10	1.33 ± 0.63	9	-15.27 ± 0.93	1:1:10 (β4c)	6	89 ± 2.54
1:1:1 (β4a)*	10	-8.00 ± 0.82	8	-33.47 ± 0.86	1:1:1 (β4a)*	5	24.5 ± 1.45

Data presented as mean ± S.E.M. *t*-test, * vs 1:1:0 or 1:1:10 (β4c), $p < 0.001$

Alternative splicing provides heterogeneity in β subunit structure, subcellular localization, and electrophysiological properties of Ca^{2+} channels, and this ultimately results in an increase in the molecular diversity and functionality of HVA Ca^{2+} channels (23). In most cases, alternative splicing occurs in variable domains, namely, the N- and C-termini and the HOOK regions (24). Our lab reported previously that alternative splicing of the N-terminal domain created two functionally distinct proteins, β4a and β4b, and that they distinctively regulate Ca^{2+} channel gating (13). Recent studies showed that alternative splicing can happen in the highly conserved GK domain of the β4 subunit (5,25). Splicing out exon 9 in the GK domain creates a translational frame shift and premature stop codon that generates a short splice variant which cannot bind to the α1 subunit. This type of alternative splicing was first identified in the chicken cochlea, and the newly found short β4 protein, cβ4c, was shown to play a role as a transcriptional regulator through interaction with heterochromatin protein 1γ (HP1γ). Here, we identified mammalian β4c in human brain, and confirmed the existence of β4c in specific nuclei of the mouse brain.

β4c protein interacts with HP1γ via PXVXL motif

HP1 proteins comprise: 1) a chromo domain (CD), which specifically recognizes the methylation sites at di- and tri-methylated H3K9 (26); 2) a flexible interdomain hinge region of variable sequence and length, which contains a putative KRK nuclear localization signal and has been shown to bind DNA (27) ; and 3) a chromo shadow domain (CSD), which mediates dimerization of HP1 and recruitment of a variety of other nuclear chromatin-modifying proteins (10), many of which contain a P*X*V*X*L motif. This consensus pentapeptide is sufficient for specific interaction with the CSD dimer (19). The structural study showed a novel mode of

peptide recognition, where the P*X*V*X*L peptide binds across the dimer interface, sandwiched in a β-sheet between strands from each monomer (18). In examining β4c C-terminal sequence, we found a candidate P*X*V*X*L consensus motif, and hypothesized that it would contain the key residue for binding with HP1γ, although the flanking sequences of PVVLV do not show high homology to other P*X*V*X*L motif containing proteins, such as chromatin assembly factor 1 (CAF1) (28) or transcriptional intermediate factor 1 (TIF1) (19,29). Of residues in the P*X*V*X*L sequence, the first proline and the third valine were found to be the most highly conserved residues, and this is why we mutated these two residues to confirm the role of β4c P*X*V*X*L motif in binding. We confirmed that β4c interacts with the CSD dimer through the P*X*V*X*L motif using the ITC technique.

Effects of β4c on Ca^{2+} channels

In a previous cβ4c report, cβ4c barely affected Ca^{2+} currents in *Xenopus* oocytes expression study, even though it was shown that His-tagged cβ4c interacts with GST fusion protein containing the cytoplasmic I/II loop of the α1D subunit (5). Alternative splicing of exon 9 creates the short variant, which lacks the GK domain responsible for interaction of the β subunit for the regulation of channel activities. As expected, expression of β4c in *Xenopus* oocytes had no effect on trafficking or gating properties of $Ca_v2.1$ channels. Therefore, β4c does not have a direct Ca^{2+} channel regulatory function, but may play an important role as a transcriptional regulator via interaction with HP1γ.

Possible functional implications of β4c-HP1 interaction

Heterochromatin is a higher order assembly that is characterized by a genome-wide distribution, gene-repression, and potential to spread (30). Central to heterochromatin spread is heterochromatin protein 1 (HP1), which recognizes H3K9-methylated chromatin, oligomerizes and forms a versatile platform that participates in diverse nuclear functions, ranging from gene silencing to chromosome segregation (6,7,31,32). HP1 is also required for centromere formation, repression of recombination, sister chromatid cohesion, and maintenance of telomere stability (11). A recent study showed that it is also implicated in DNA repair (33). HP1 exists in mammals as three isoforms (α, β, and γ), which have high sequence homology and similar structures. HP1α is found mostly in cytologically dense heterochromatin, whereas HP1β and HP1γ are also found in euchromatin. The ever-growing list of HP1-interacting protein includes a number of chromatin components, chromatin modifiers, transcriptional regulators, replication and cell cycle-implicated factors, and nuclear structure proteins.

As a transcriptional regulator, β4c binding to HP1 might have several functional effects. β4c interaction with HP1 can promote either transcriptional repression, or transcriptional activation, depending on its chromosomal context and its other interacting partners. Since β4c appears to express in distinctive neurons of brainstem and deep cerebellum, it might be possible that β4c-HP1 interaction has transcriptional regulatory effects on vestibular functions of those neurons such as VOR.

The vestibular neurons play a critical role in encoding self-motion information by detecting the motion of the head in space to stabilize the gaze and control the balance and posture. The role of the vestibular system in ensuring the accuracy of three specific classes of behaviors: 1) the control of gaze to have a clear vision during everyday activities, 2) the

production of the compensatory neck and limb movements required to ensure postural equilibrium during both self-generated and externally applied movements, and 3) more complex voluntary motion tasks such as navigation and reaching (34). The vestibular ocular reflex (VOR), the most thoroughly studies pathway regulated by the cerebellum, functions to stabilize images on the retina during self-motion; its excellent performance throughout life is maintained by robust, experience-dependent learning which relies on the cerebellum (35). Motor learning in the VOR depends on Purkinje cells in the floccular lobe of the cerebellum, and it is revealed that firing responses profoundly change during head and eye movements (36). This firing rate potentiation indicates that plasticity of Purkinje cells synapses contributes to motor learning. Intracellular Ca^{2+} concentration is critical to mediate synaptic plasticity. Ca^{2+} currents at the excitatory synapses in Purkinje cells are largely fine-tuned by full-length β4 subunit (15). The distinctive expression and interaction with HP1 of β4c in vestibular and deep cerebellar neurons might have roles in fine-tuning of Ca^{2+} concentration by regulating expression of genes related to Ca^{2+} homeostasis. Thus, together with full-length β4 subunit, β4c might affect the motor learning in the VOR.

In summary, our experiments have: 1) identified a short splice variant of β4 subunit in human brain, termed β4c; 2) shown that β4c is expressed in vestibular, cochlear and deep cerebellar nuclei in the mouse brain; 3) demonstrated that β4c interacts with CSD dimer of HP1γ via its PXVXL motif; and 4) confirmed that β4c does not affect the trafficking or gating properties of $Ca_v2.1$ channels.

Materials and Methods

Polymerase Chain Reaction, Subcloning, and Mutagenesis

PCR primers designed based on genomic human β4 sequence were used to amplify exon 9 splice variants. The four primers used for PCR reactions were as follows: exon 8 forward (5'-TATCA-TATGGCCACCCCTTACGATGTTGTACCGTCAAT-3'); exon 12 reverse (5'-CTGCTCGAG-CTATTAATCAACCGCTGTAAAAC-3'); β4a forward (5'-TCACATATGATGTATGACAAT-TTGTACCTGCATGG-3'); and β4c reverse (5'-CTGCTCGAGTCAGCTGTCACTCTCGTTA-TTGAAATCCTCG-3'). NdeI and XhoI restriction sequences were added to the 5'-end of primers for ligation into the vector pET-15b. Human brain first-strand cDNA was purchased from Biochain (Hayward, CA), and 10 ng of cDNA was used as templates for PCR amplification. The thermal cycling program was as follows: 1 cycle of 98 °C for 30 s and 35 cycles of 98 °C for 10 s, 58 °C for 25 s, and 72 °C for 30 s. A final step of 72 °C for 5 min was used for the final extension. All PCR products were separated on 1% agarose gel containing ethidium bromide. For protein expression, PCR fragments were excised and purified from the gel, digested with NdeI and XhoI restriction enzymes, and ligated into the similarly digested hexahistidine pET-15b (Novagen) vector. Human β4c 38–184 (β4cΔ184), β4c 38–199 (β4cΔ199), and the CSD of human HP1γ (residues 113–183) were constructed in this manner. Site-directed mutagenesis was performed with the QuikChange (Stratagene) mutagenesis kit according to manufacturer's instructions. All constructs were verified by DNA sequencing.

Protein expression, purification and isothermal titration calorimetry

Proteins used in ITC experiments were expressed in *E. coli* BL21(DE3) (Stratagene) and purified as described previously (14). A single colony of a freshly transformed pET-15b β4c construct

was first inoculated into 25 ml LB pre-culture and grown for overnight before it was scaled up to grow in 1 L of LB medium with 50 μg/ml ampicillin at 37 °C. Protein expression was induced by adding 0.2 mM IPTG to the cell culture once the OD_{600} reached 0.6 AU, and the cells were then grown with shaking at 37 °C for 3 h. Cells were harvested by centrifugation and resuspended in a binding buffer (50 mM Tris-HCl, 0.3 M NaCl, 1 mM DTT, pH 8.0) and lysed by sonication. The lysate was incubated with 50 units of DNase I (Bio-Rad) and 12.5 mM $MgCl_2$ for 30 min and further centrifuged at 17,000 RPM for 30 min, and the supernatant was filtered and collected. The supernatant was then loaded onto a 15-ml Ni^{2+} resin column (Bio-Rad) pre-equilibrated with 100 ml of binding buffer. After washing with eight column volumes of binding buffer, the desired protein was eluted with increasing concentrations of imidazole (up to 300 mM). After the Ni^{2+} column, the His_6 tag was removed by overnight thrombin cleavage (Amersham Biosciences) at 4°C. The His_6 tag-cleaved proteins were further purified by gel filtration using a Superdex 75HR column or a Sephacryl S-200 HR column using an AKTA FPLC (GE healthcare) in 500 mM NaCl, 50 mm sodium phosphate, 1 mM DTT, pH 7.0. Protein purity was analyzed on SDS-polyacrylamide gels, and the protein samples were concentrated via centrifugal filtration. Protein concentrations were determined by UV absorbance at 280 nm using predicted extinction coefficients. Isothermal titration calorimetry (ITC) measurements were carried out at 298 K with a MicroCal (Northampton, MA) VP-ITC microcalorimeter. All proteins were dialyzed against the same buffer (50 mM sodium phosphate, 150 mM NaCl, pH 7.0, 2 mM DTT), and all buffers were degassed before experiments. For measurements, 28 injections of 10 μl of CSD dimer were titrated into 1.4-ml solutions of either β4cΔ199 or β4cΔ184 proteins (or, for base-line correction, buffer alone) to a stoichiometric ratio of 2.1:1. Data were processed and analyzed with MicroCal Origin 7.0.

Ca_v2.1 Channel Expression in X. laevis Oocytes

Complementary RNAs (cRNAs) for each calcium channel subunit [rabbit α1A, rabbit α2δ-1 and human β4a and β4c] were synthesized in vitro with either T3 or T7 using the mMessage mMachine RNA transcription kit (Ambion). Standard methods were used to harvest and prepare *X. laevis* oocytes for cRNA injections. In brief, oocytes were treated with collagenase A (1.3 mg/ml) in OR2 buffer (82.5 mM NaCl, 2.5 mM KCl, 1 mM NaH2PO4, 1 mM MgCl2, and 15 mM HEPES, pH 7.5) for 60 to 90 min to remove the follicular layer. Stage V–VI defolliculated oocytes were sorted and stored primarily in ND96 buffer (96 mM NaCl, 2 mM KCl, 1 mM MgCl2, 1.8 mM CaCl2, and 5 mM HEPES, pH 7.5). In some cases, oocytes were stored in OR3 medium (6.85 g/Leibovitz's L-15 cell culture medium, 10,000 U/ml penicillin G sodium, 10,000 µg/ml streptomycin sulfate, and 5 mM HEPES, pH 7.5) for several days before cRNA injection. Ca_v^{2+} channel α1, α2δ, either β4a and β4c cRNAs in nuclease-free H_2O were injected into oocytes at the molar ratios (1:1:0, 1:1:10 β4a, 1:1:1β4c). Injected oocytes were stored at 16°C.

Electophysiology

Calcium channel currents were recorded 1 to 5 days after injection by standard two-electrode voltage clamp (Warner OC-725C amplifier; Warner Instrument Corp.) Microelectrodes were filled with 3 M KCl, and the resistances of the current and voltage electrodes were 0.5 to 4.0 MΩ. Data were filtered at 2 kHz and sampled at 10 kHz. Currents were recorded in a chloride-free bath containing 5 mM $Ba(OH)_2$, 5 mM HEPES, 85 mM tetraethylammonium hydroxide, and 2 mM KOH, with pH adjusted to 7.4 with methanesulfonic acid. Currents used to generate the data in this study ranged from 0.45 to 2.2 µA. Current levels were measured at 0.5 to 1 h in one or two oocytes until current levels reached 0.5 to 1.5 µA. Single oocytes were then subjected to

both voltage-dependent activation and inactivation protocols. The activation protocol measured peak barium currents elicited by incremental depolarizing steps of 5 mV for 300 ms each from a holding potential of -80 mV (test potentials -40 to 50 mV). The inactivation protocol measured peak barium currents elicited by 300-ms test depolarization to -5, 0, or 5 mV after a 20-s conditioning prepulse to voltages between -80 and 30 mV in 10-mV incremental steps. Leak currents were between 10 and 150 nA. Only recordings with minimal tail currents were used. Data were collected and analyzed using pCLAMP 10 software (Molecular Devices, Sunnyvale) and Microsoft Office Excel 2010 (Microsoft Corp.).

REFERENCES

1. Buraei, Z., and Yang, J. (2013) Structure and function of the beta subunit of voltage-gated Ca^{2+} channels. *Biochim Biophys Acta* **1828**, 1530-1540

2. Dolphin, A. C. (2009) Calcium channel diversity: multiple roles of calcium channel subunits. *Curr Opin Neurobiol* **19**, 237-244

3. Dolphin, A. C. (2012) Calcium channel auxiliary alpha2delta and beta subunits: trafficking and one step beyond. *Nat Rev Neurosci* **13**, 542-555

4. Zhang, Y., Yamada, Y., Fan, M., Bangaru, S. D., Lin, B., and Yang, J. (2010) The beta subunit of voltage-gated Ca^{2+} channels interacts with and regulates the activity of a novel isoform of Pax6. *J Biol Chem* **285**, 2527-2536

5. Hibino, H., Pironkova, R., Onwumere, O., Rousset, M., Charnet, P., Hudspeth, A. J., and Lesage, F. (2003) Direct interaction with a nuclear protein and regulation of gene silencing by a variant of the Ca^{2+} channel beta 4 subunit. *Proc Natl Acad Sci U S A* **100**, 307-312

6. Kwon, S. H., and Workman, J. L. (2011) The changing faces of HP1: From heterochromatin formation and gene silencing to euchromatic gene expression: HP1 acts as a positive regulator of transcription. *Bioessays* **33**, 280-289

7. Fanti, L., and Pimpinelli, S. (2008) HP1: a functionally multifaceted protein. *Curr Opin Genet Dev* **18**, 169-174

8. Kwon, S. H., and Workman, J. L. (2008) The heterochromatin protein 1 (HP1) family: put away a bias toward HP1. *Mol Cells* **26**, 217-227

9. Aasland, R., and Stewart, A. F. (1995) The chromo shadow domain, a second chromo domain in heterochromatin-binding protein 1, HP1. *Nucleic Acids Res* **23**, 3168-3173

10. Lomberk, G., Bensi, D., Fernandez-Zapico, M. E., and Urrutia, R. (2006) Evidence for the existence of an HP1-mediated subcode within the histone code. *Nat Cell Biol* **8**, 407-415

11. Grewal, S. I., and Jia, S. (2007) Heterochromatin revisited. *Nat Rev Genet* **8**, 35-46

12. Canzio, D., Liao, M., Naber, N., Pate, E., Larson, A., Wu, S., Marina, D. B., Garcia, J. F., Madhani, H. D., Cooke, R., Schuck, P., Cheng, Y., and Narlikar, G. J. (2013) A conformational switch in HP1 releases auto-inhibition to drive heterochromatin assembly. *Nature* **496**, 377-381

13. Helton, T. D., and Horne, W. A. (2002) Alternative splicing of the beta4 subunit has alpha1 subunit subtype-specific effects on Ca^{2+} channel gating. *Journal of Neuroscience* **22**, 1573-1582

14. Xu, X., Lee, Y. J., Holm, J. B., Terry, M. D., Oswald, R. E., and Horne, W. A. (2011) The Ca^{2+} channel beta4c subunit interacts with heterochromatin protein 1 via a PXVXL binding motif. *J Biol Chem* **286**, 9677-9687

15. Vendel, A. C., Terry, M. D., Striegel, A. R., Iverson, N. M., Leuranguer, V., Rithner, C. D., Lyons, B. A., Pickard, G. E., Tobet, S. A., and Horne, W. A. (2006) Alternative splicing of the voltage-gated Ca^{2+} channel beta4 subunit creates a uniquely folded N-terminal protein binding domain with cell-specific expression in the cerebellar cortex. *J Neurosci* **26**, 2635-2644

16. Zeng, W., Ball, A. R., Jr., and Yokomori, K. (2010) HP1: heterochromatin binding proteins working the genome. *Epigenetics* **5**, 287-292

17. Nozawa, R. S., Nagao, K., Masuda, H. T., Iwasaki, O., Hirota, T., Nozaki, N., Kimura, H., and Obuse, C. (2010) Human POGZ modulates dissociation of HP1alpha from mitotic chromosome arms through Aurora B activation. *Nat Cell Biol* **12**, 719-727

18. Thiru, A., Nietlispach, D., Mott, H. R., Okuwaki, M., Lyon, D., Nielsen, P. R., Hirshberg, M., Verreault, A., Murzina, N. V., and Laue, E. D. (2004) Structural basis of HP1/PXVXL motif peptide interactions and HP1 localisation to heterochromatin. *EMBO J* **23**, 489-499

19. Smothers, J. F., and Henikoff, S. (2000) The HP1 chromo shadow domain binds a consensus peptide pentamer. *Curr Biol* **10**, 27-30

20. Allen, S. E., Darnell, R. B., and Lipscombe, D. (2010) The neuronal splicing factor Nova controls alternative splicing in N-type and P-type Ca(V)2 calcium channels. *Channels* **4**, 483-489

21. Keren, H., Lev-Maor, G., and Ast, G. (2010) Alternative splicing and evolution: diversification, exon definition and function. *Nat Rev Genet* **11**, 345-355

22. Lipscombe, D., Andrade, A., and Allen, S. E. (2013) Alternative splicing: functional diversity among voltage-gated calcium channels and behavioral consequences. *Biochim Biophys Acta* **1828**, 1522-1529

23. Foell, J. D., Balijepalli, R. C., Delisle, B. P., Yunker, A. M., Robia, S. L., Walker, J. W., McEnery, M. W., January, C. T., and Kamp, T. J. (2004) Molecular heterogeneity of calcium channel beta-subunits in canine and human heart: evidence for differential subcellular localization. *Physiol Genomics* **17**, 183-200

24. Buraei, Z., and Yang, J. (2010) The β subunit of voltage-gated Ca^{2+} channels. *Physiol Rev* **90**, 1461-1506

25. Kobayashi, T., Yamada, Y., Fukao, M., Shiratori, K., Tsutsuura, M., Tanimoto, K., and Tohse, N. (2007) The GK domain of the voltage-dependent calcium channel beta subunit is essential for binding to the alpha subunit. *Biochem Biophys Res Commun* **360**, 679-683

26. Lachner, M., O'Carroll, D., Rea, S., Mechtler, K., and Jenuwein, T. (2001) Methylation of histone H3 lysine 9 creates a binding site for HP1 proteins. *Nature* **410**, 116-120

27. Meehan, R. R., Kao, C. F., and Pennings, S. (2003) HP1 binding to native chromatin in vitro is determined by the hinge region and not by the chromodomain. *EMBO J* **22**, 3164-3174

28. Huang, H., Yu, Z., Zhang, S., Liang, X., Chen, J., Li, C., Ma, J., and Jiao, R. (2010) Drosophila CAF-1 regulates HP1-mediated epigenetic silencing and pericentric heterochromatin stability. *J Cell Sci* **123**, 2853-2861

29. Cammas, F., Oulad-Abdelghani, M., Vonesch, J. L., Huss-Garcia, Y., Chambon, P., and Losson, R. (2002) Cell differentiation induces TIF1beta association with centromeric heterochromatin via an HP1 interaction. *J Cell Sci* **115**, 3439-3448

30. Sharma, R. P., Gavin, D. P., and Chase, K. A. (2012) Heterochromatin as an incubator for pathology and treatment non-response: implication for neuropsychiatric illness. *Pharmacogenomics J* **12**, 361-367

31. Hediger, F., and Gasser, S. M. (2006) Heterochromatin protein 1: don't judge the book by its cover! *Curr Opin Genet Dev* **16**, 143-150

32. Danzer, J. R., and Wallrath, L. L. (2004) Mechanisms of HP1-mediated gene silencing in Drosophila. *Development* **131**, 3571-3580

33. Ayoub, N., Jeyasekharan, A. D., and Venkitaraman, A. R. (2009) Mobilization and recruitment of HP1: a bimodal response to DNA breakage. *Cell Cycle* **8**, 2945-2950

34. Cullen, K. E. (2012) The vestibular system: multimodal integration and encoding of self-motion for motor control. *Trends Neurosci* **35**, 185-196

35. Broussard, D. M., Titley, H. K., Antflick, J., and Hampson, D. R. (2011) Motor learning in the VOR: the cerebellar component. *Exp Brain Res* **210**, 451-463

36. Shin, M., Moghadam, S. H., Sekirnjak, C., Bagnall, M. W., Kolkman, K. E., Jacobs, R., Faulstich, M., and du Lac, S. (2011) Multiple types of cerebellar target neurons and their circuitry in the vestibulo-ocular reflex. *J Neurosci* **31**, 10776-10786

CHAPTER 3

Nuclear targeting of the Ca^{2+} channel β4c subunit and its transcriptional regulation in Neuro2a cells

Introduction

The β subunits of voltage-gated Ca^{2+} channels are best known for their ability to regulate trafficking and gating properties of pore-forming Ca^{2+} channel α1 subunits (1-4). Apart from their classical functions, however, β4 subunits also play crucial roles in a variety of Ca^{2+} channel independent functions by virtue of their translocation to the nucleus. For instance, it has been shown that β4 subunits localize to yolk syncytial layer nuclei early in zebrafish development, and that morpholino knockdown of zebra fish β4 protein impedes initiation of epiboly (5). Recently, several studies have demonstrated that the β4 subunit targets to the nucleus and has a direct effect on gene regulation (6-9). Studies focused on the nuclear localization of the β4b subunit have shown that, in one case, transport to the nucleus occurs via a β4b attachment to a regulatory subunit of protein phosphatase 2 (9), and in another, nuclear targeting was dependent on the presence of two arginines in a conserved β4b N-terminal sequence motif (8). One study showed that the gene regulatory effect of the β4 subunit was dependent on its degree of nuclear targeting ability (10).

The first evidence that the Ca^{2+} channel β4c subunit localized to the nucleus was reported by Hibino et al (7). They showed in a functional assay that β4c entry into the nucleus was dependent on its interaction with heterochromatin protein 1 gamma (HP1γ), and that the result of the interaction was attenuation of HP1γ's transcription repressor function (7). Subsequent to their

publication, we cloned human β4c and determined that it interacts with HP1γ through a consensus PXVXL motif (11). This raised the question of whether the HP1γ interaction was required for nuclear transport of β4c and whether β4c regulates transcriptional activity.

In the present study we show that heterologously expressed human β4c is transported to the nucleus of Neuro2a cells independent of its interaction with HP1γ and identify two specific sequence motifs that are critical for optimal nuclear transport: the first is identical to a classical monopartite nuclear localization sequence (12,13), K(K/R)X(K/R), and the second is a previously unidentified C-terminal sequence that is generated by alternative splicing. Our experiments show that both are required for optimal nuclear localization of ectopically expressed GFP-tagged β4c. Expression profiling of Neuro2a cells expressing β4c demonstrates that the nuclear β4c does not affect expression and function of Ca^{2+} channel subunits, but regulates expression of genes involved in microtubule formation, apoptosis, ion transport, and cell excitability.

Results

Nuclear import of ectopically expressed β4c in Neuro2a cells requires a classical nuclear localization sequence

In our previous study (11), we cloned human β4c, a Ca^{2+} channel β4 subunit splice variant that results from exon 9 skipping in β4a isoform mRNA (Figure 3.1(A), (B)), and showed that it interacts with the nuclear adapter protein, HP1γ via a consensus PXVXL binding motif. Antibody labeling revealed that β4c is highly expressed in the nuclei of specific neurons within the mouse medial vestibular nucleus, as well as in the cochlear nucleus and deep cerebellar nucleus.

Figure 3.1 β4c created by alternative splicing of the human Ca^{2+} channel β4a gene.

(A) Diagram of exon structure and corresponding protein domains of the full-length human β4a subunit (486 amino acids).

(B) Diagram of splice variant mRNA and resulting truncated β4c protein resulting from exon 9 skipping. The deduced domains of the human β4c protein are also shown (207 amino acids).

(C) Sequence alignment of human and chicken β4c proteins. *, identifies divergent amino acids; and v, identifies exon translation boundaries; *"cNLS"*, putative classical nuclear localization signal; *PXVXL*, consensus site for binding to HP1; "o*NLS"*, optimizing nuclear localization sequence

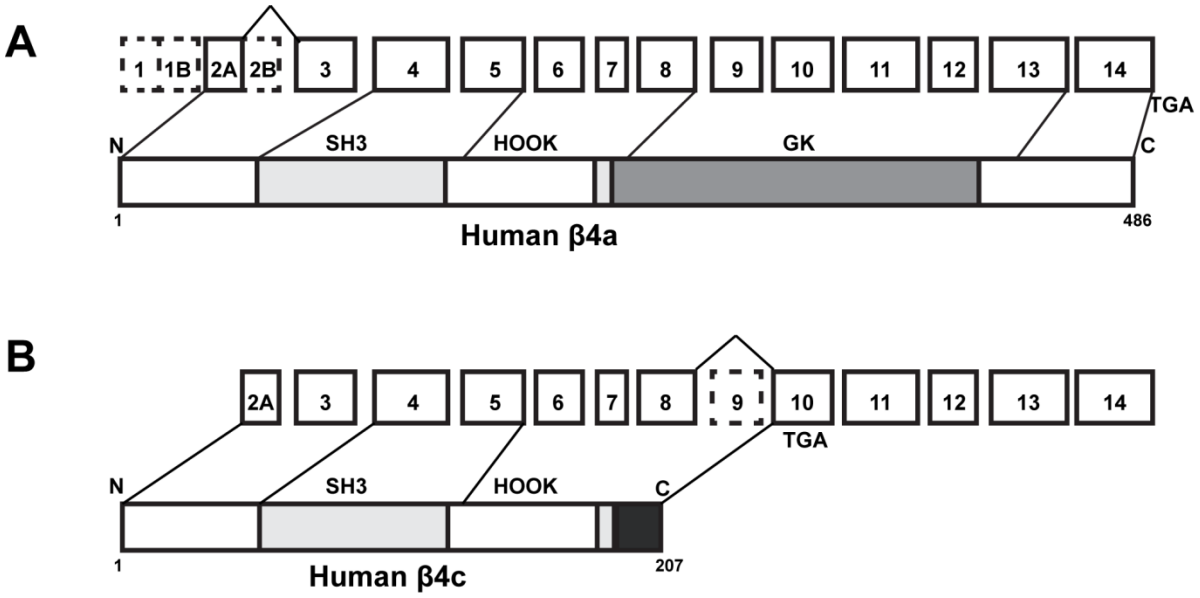

C

```
hβ4c  MYDNLYLHGIEDSEAGSADSYTSRPSDSDVSLEEDREAIRQEREQQAAIQLERAKSKPVA  60
cβ4c  MYDNLYLHGFEDSEAGSADSYTSRPSDSDVSLEEDREAIRQEREQQAAIQLERAKSKPVA  60
                 *

hβ4c  FAVKTNVSYCGALDEDVPVPSTAISFDAKDFLHIKEKYNNDWWIGRLVKEGCEIGFIPSP  120
cβ4c  FAVKTNVSYCGALDEDVPVPSTAISFDAKDFLHIKEKYNNDWWIGRLVKEGCEIGFIPSP  120

                 "cNLS"
hβ4c  LRLENIRIQQEQKRGRFHGGKSSGNSSSSLGEMVSGTFRATPTSTAKQKQKVTEHIPPYD  180
cβ4c  LRLENIRIQQEQKRGRFHGGKSSGNSSSSLGEMVSGTFRATPTSTAKQKQKVTEHVPPYD  180
                                                          *
         PXVXL          "oNLS"
hβ4c  VVPSMRPVVLVGPSLKGYEDFNNESDS- - - - -  207
cβ4c  VVPSMRPVVLVGPSLKGYEDINNPSDSRHSFC  212
                        *  *   *****
```

To study further the molecular determinants of β4c nuclear localization in neuronal cells, we used the mouse neuroblastoma derived Neuro2a cell transient expression system and a number of GFP-tagged β4c constructs. To determine whether β4c was expressed in Neuro2a cells, we performed PCR using cDNA from mock pKH3 vector transfected cells or pKH3-β4c transfected cells as templates. Figure 3.2 (A) shows that the expected 639 bp PCR product was amplified from cDNA extracted from pKH3-β4c transfected cells but not from cDNA from pKH3 vector transfected control cells. For further confirmation that β4c is not expressed in Neuro2a cells, we used an antibody directed toward the N-terminus of β4a (11,14) in Western blot experiments. Figure 3.2 (B) shows that the antibody labels a 29.6 kDa HA-β4c fusion protein in a total protein extract from pKH3-β4c transfected cells but not in the extract from the vector transfected control cells. Next, to confirm that HP1γ is expressed in Neuro2a cells, we performed Western blot experiments. Figure 3.2 (C) shows that anti-HP1γ antibody labels a 21 kDa HP1γ protein in total protein extract from both vector transfected control cells, and β4c transfected cells. Upper bands likely represent the phosphorylated form of HP1γ. Taken together, these results indicate that HP1γ is endogenously expressed in Neuro2a cells but β4c is not expressed at detectable level, and thus point to the suitability of this system for studying the subcellular localization of ectopically expressed β4c.

Next, we sought to determine whether expressed β4c localizes to the nucleus of Neuro2a cells, and whether this occurred under the direction of a putative classic nuclear localization sequence ("cNLS") that we identified in the HOOK region (Figure 3.1(C)). The figure shows that β4c contains an amino acid sequence, ^{133}KRGR^{136}, that fits the description of a monopartite classical nuclear localization signal, K(K/R)*X*(K/R) that could be accessible to importin binding (12,15). To explore this possibility, we prepared DNA constructs that expressed green

fluorescent protein (GFP)-tagged full-length β4a and β4c proteins, and a β4c protein in which we mutated the putative cNLS to ^{133}AAAA^{136} (Figure 3.2(D)). Figure 3.2 (E) compares confocal GFP images (*left column*) with same-cell DAPI stained nuclei (*middle column*), and then shows merged images of a single cell under both experimental conditions (*right column*). Figure 3.2 (E), *top row*, shows that fluorescence intensity from GFP protein alone is diffusely spread throughout the cytoplasm, indicating that GFP does not localize to the nucleus. Likewise, GFP-β4a was almost exclusively localized outside the nucleus, but its fluorescence pattern was strikingly different from GFP alone (Figure 3.2 (E), *second row*). This can be explained by its high-affinity association with voltage-gated Ca^{2+} channels, some of which may be inserted as clusters with other proteins in the plasma membrane (16). By contrast, and consistent with our previous immunohistochemistry experiments (11), the GFP-β4c fusion protein was detected mostly in the nucleus (Figure 3.2 (E), *third row*). The ectopically expressed GFP-^{133}AAAA^{136}-KRGR mutant protein is not present in the nucleus, but rather is diffusely confined to the cytoplasm (Figure 3.2 (E), *bottom row*). These results show clearly that β4c nuclear localization is dependent on the ^{133}KRGR^{136} sequence.

We quantified subcellular expression by calculating the mean nuclear/cytoplasm fluorescence ratio for cells expressing each GFP construct (Figure 3.4). The nuclear/cytoplasm fluorescence intensity (FI) ratio of both β4c and the β4c KRGR mutant is significantly higher ($p<0.001$) than vector alone; however, the FI ratio of the β4c KRGR mutant is significantly lower ($p<0.001$) than β4c. These results indicated that the basic ^{133}KRGR^{136} motif is necessary but not entirely sufficient for proper nuclear localization of β4c, and prompted us to explore what other regions of β4c might be required.

Figure 3.2 Expression and nuclear localization of β4c in Neuro2a cells.

(A) Results of PCR amplification using cDNA from mock transfected or β4c transfected Neuro2a cells as templates. The 639 bp amplified fragment from β4c transfected cells represents full-length β4c.

(B) Western blot showing that an affinity-purified β4a/c antibody labels a 29.6 kDa HA tag fused β4c protein in a total protein extract from β4c transfected cells.

(C) Western blot showing that an anti-HP1γ antibody labels a 21 kDa HP1γ protein in a total protein extract from mock or β4c transfected cells.

(D) Schematic representation of β4c with ^{133}KRGR^{136} sequence mutation.

(E) Ectopically expressed β4c localizes to the nucleus of Neuro2a cells. Representative fluorescent images of Neuro2a cells expressing GFP-vector, GFP- β4a, GFP- β4c, or GFP-β4c cNLS mutant. *Left column*, GFP fluorescence; *middle column*, nuclear DAPI staining; and *right column*, merged images. *Scale bar*, 5 μm.

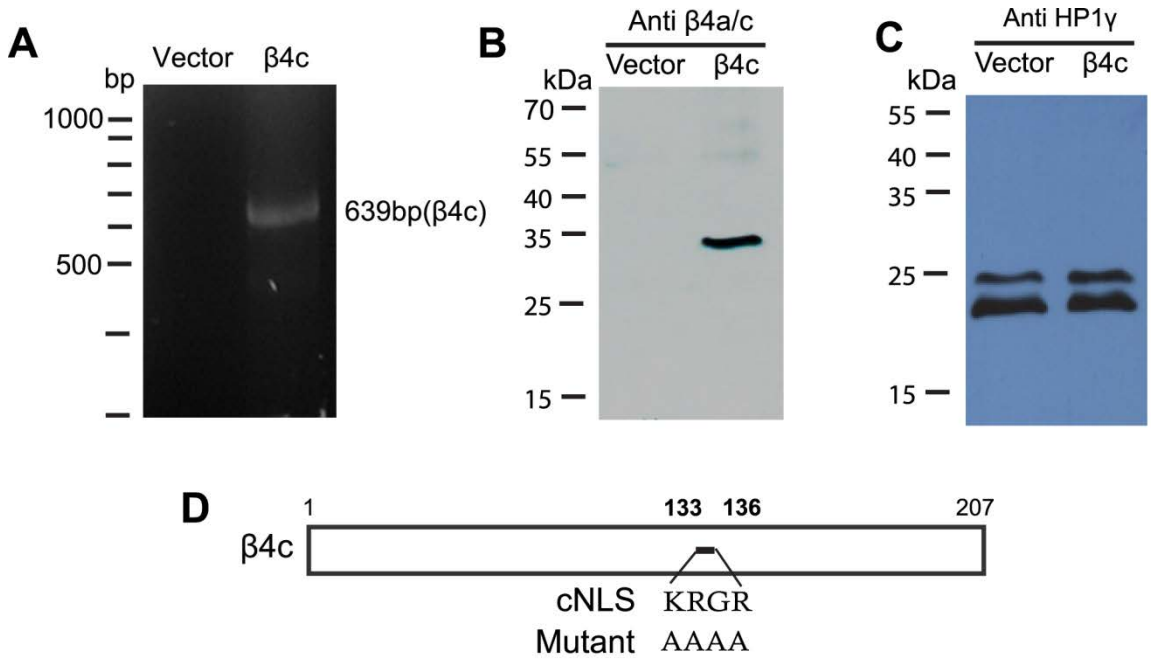
A
Vector
β4c
bp
1000
500
639bp(β4c)
B
Anti β4a/c
Vector
β4c
kDa
70
55
40
35
25
15
C
Anti HP1γ
Vector
β4c
kDa
55
40
35
25
15

D
1
133
136
207
β4c
cNLS
KRGR
Mutant
AAAA

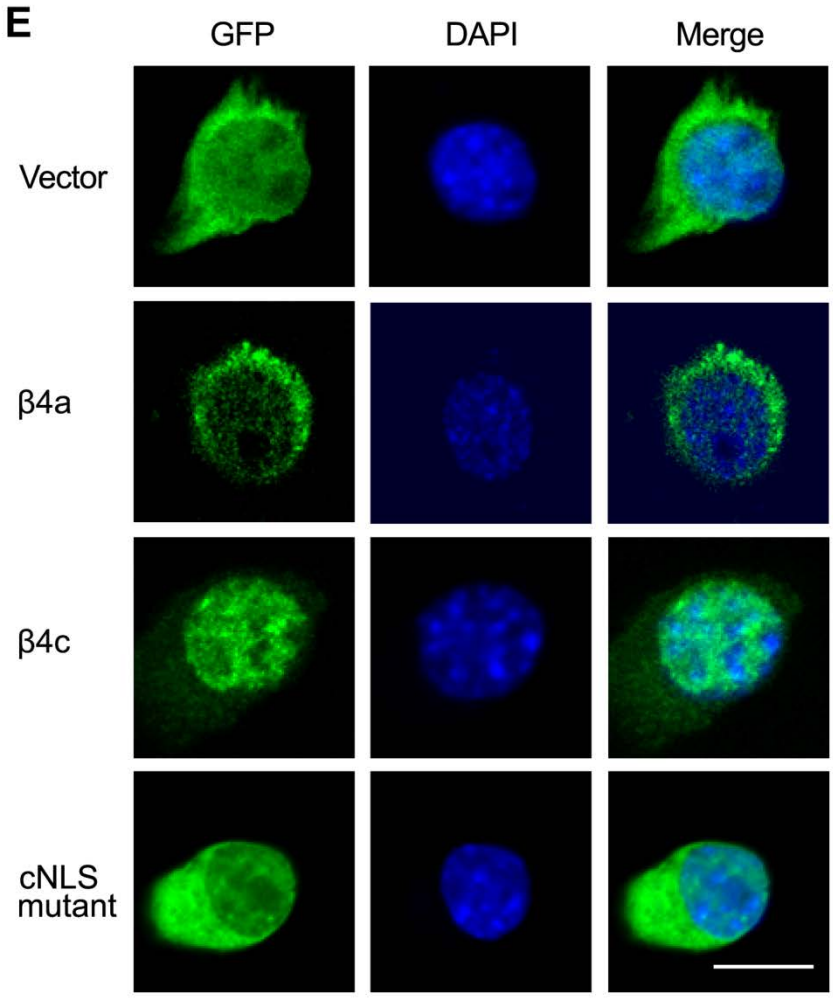
E
GFP
DAPI
Merge
Vector
β4a
β4c
cNLS
mutant

The C-terminus of β4c is critical for nuclear localization in Neuro2a cells, whereas interaction with the HP1γ PXVXL motif is not

The β4c protein was first identified in chicken cochlear and brain cDNA libraries (7). This early report showed that coexpression with HP1γ prompted β4c nuclear translocation in tsA201 cells (human embryonic kidney cell line). We subsequently determined that interaction with the HP1γ chromo shadow domain occurred via a conserved PXVXL motif (shown in Figure 3.1 (C)). To determine whether this interaction with HP1γ is critical for β4c nuclear localization in Neuro2a cells, we created a GFP-β4c construct containing a P187A/V189A double mutation that, based on our previous NMR and isothermal titration calorimetry results (11), does not interact with the chromo shadow domain of HP1γ. We also created two β4c C-terminal truncation constructs: GFP-β4c-199 (ends at residue 199), which contains the HP1γ ^{187}PVVLV^{191} interaction motif; and GFP-β4c-184 (ends at residue 184), which lacks the entire unstructured C-terminus, including the HP1γ interacting motif (Figure 3.3 (A)). Each construct was expressed in Neuro2a cells and, as was done for experiments shown in Figure. 3.2, the nuclear/cytoplasm FI ratios were measured for each cell. Figure 3.3 (B) shows that the GFP-β4c P187A/V189A mutant (Figure 3.3 (B), *second row*) was localized to the nucleus similar to the GFP-β4c protein (Figure 3.3 (B), *top row*). Comparing a large number of cells (n=100 each), there was no significant difference in the nuclear/cytoplasmic FI ratio between GFP-β4c and the GFP-β4c P187A/V189A double mutant (Figure 3.4). This result suggests that, in apparent contrast to chicken β4c in tsA201 cells (7), ectopically expressed human β4c in Neuro2a cells can be imported into the nucleus independent of its interaction with the chromo shadow domain of HP1γ. In contrast, both GFP-β4c-199 and GFP-β4c-184 showed a substantial decrease in nuclear localization (Figure 3.3 (B), *third and fourth rows*, respectively).

Figure 3.3 C-terminal eight residues of β4c are critical for nuclear localization in Neuro2a cells, whereas interaction with HP1γ via its PXVXL motif is not.

(A) Schematic representation of three β4c constructs. *Top*, full length β4c; *Middle*, truncated β4c-199 lacking C-terminal eight residues; *Bottom*, β4c-184 lacking PXVXL motif necessary for binding to HP1γ.

(B) Representative fluorescent images of Neuro2a cells transiently transfected with plasmids encoding various β4c constructs fused with GFP: full length β4c, P187A/V189A, β4c-199, β4c-184 and β4c-199 cNLS mutant. *Left column*, GFP fluorescence; *middle column*, DAPI staining; and *right column*, merged images. *Scale bar*, 5 μm.

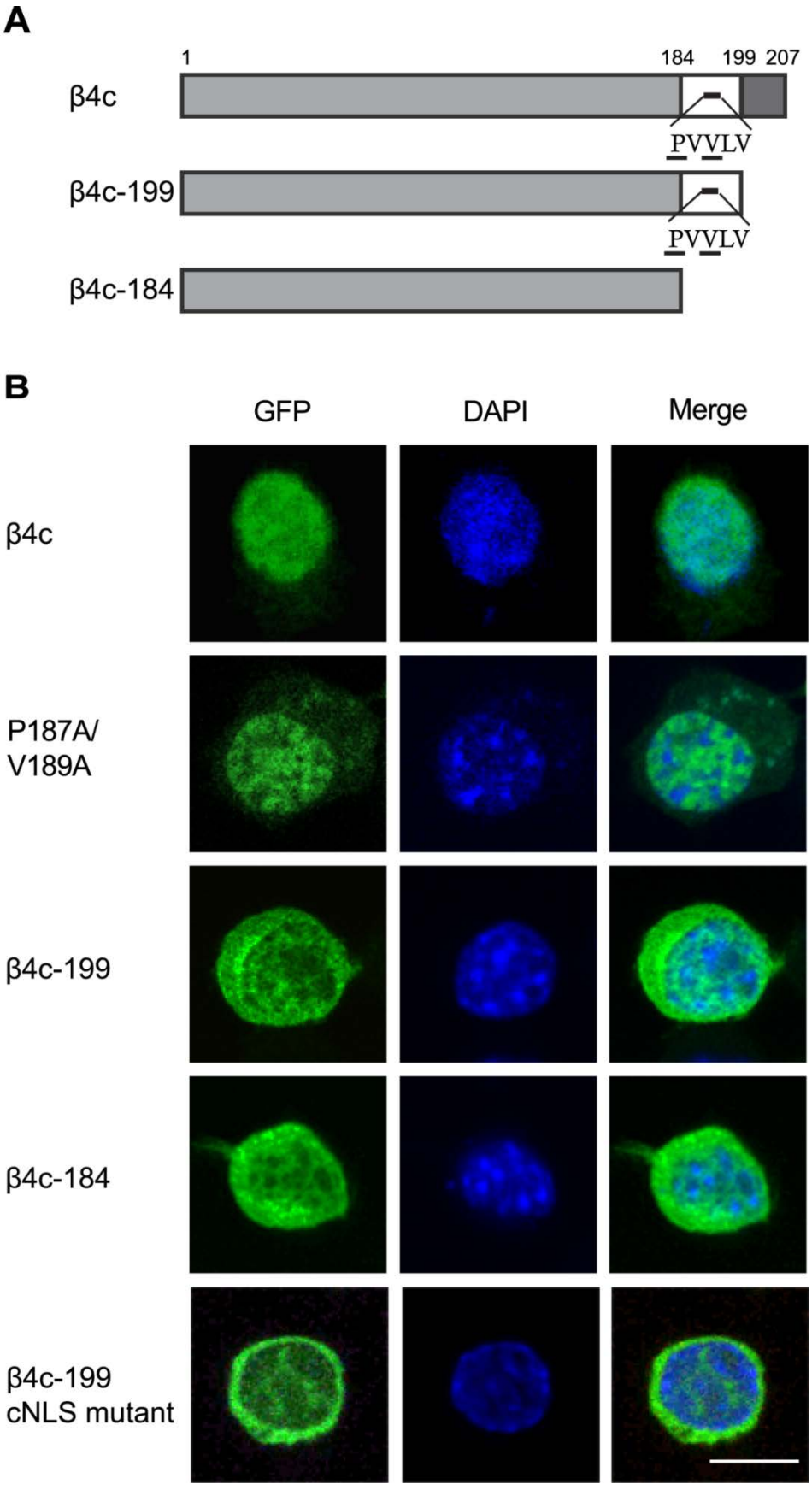
A
1
184
199
207
β4c
PVVLV
β4c-199
PVVLV
β4c-184
B
GFP
DAPI
Merge
β4c
P187A/
V189A
β4c-199
β4c-184
β4c-199
cNLS mutant

Figure 3.4 Nuclear localization of β4c.

Nucleus/cytoplasm fluorescence intensity ratio determined for Neuro2a cells transfected with: vector alone, β4a, full-length β4c; ^{133}AAAA^{136} KRGR motif mutant (cNLS mutant); C-terminal truncation mutant, β4c-199; C-terminal truncation mutant, β4c-184, and β4c-199 containing the ^{133}AAAA^{136} mutation. (means ± SEM; n=100 for all experiments except β4a (n=40), and β4c-199 cNLS (n=80)) *p<0.001 vs vector

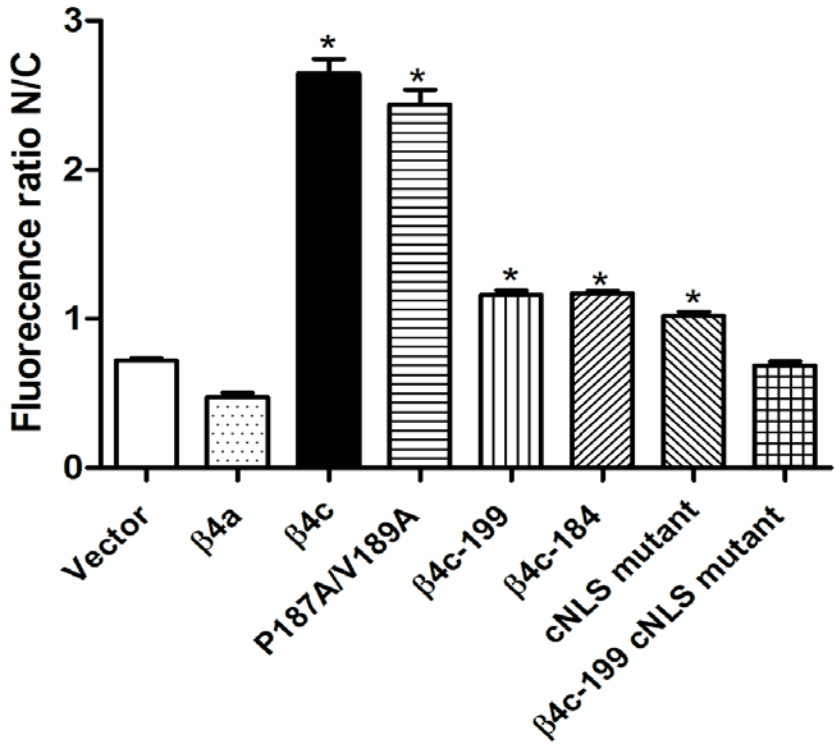

The nuclear/cytoplasm FI ratios of these two constructs were significantly reduced compared to GFP-β4c ($p<0.001$); however, there was no significant difference between GFP-β4c-199 and GFP-β4c-184 (Figure 3.4). This result indicates that amino acids 184-199 of the unstructured C-terminus do not play a role in nuclear localization, and identifies the next highly conserved 8 residues, ^{200}DFNNESDS^{207}, (Figure 3.1 (C)), generated by alternative splicing, as being critically important. One possible explanation for this result is that the C-terminal eight residues contribute to the binding of β4c, along with the ^{187}PVVLV^{191} motif, to the CSD of HP1γ. To test this possibility, we compared the binding affinities of β4c and β4c-199 to the HP1γ CSD using isothermal titration calorimetry. The results show no difference in binding affinity between β4c and β4c-199 (Figure 3.5), which indicates that the C-terminal eight residues do not contribute to β4c binding to HP1γ CSD.

To confirm the combined role of the ^{133}KRGR^{136} motif and the C-terminal eight residues of β4c in nuclear localization, we created a GFP-β4c-199 construct containing the ^{133}AAAA^{136} mutations and expressed it in Neuro2a cells. This protein localizes mostly in the cytoplasm similar to the distribution of GFP alone (Figure 3.3 (B), *bottom row)*, and there is no statistical difference in the mean nuclear/cytoplasm FI ratio of the GFP-β4c-199 KRGR mutant and GFP alone (Figure 3.4). Taken together, these results show that the C-terminal eight residue nuclear localization optimizing sequence ("oNLS") along with the putative "cNLS" motif (putative in that we have not yet shown that β4c interacts with importin) are critical for the proper localization of β4c in nuclei of Neuro2a cells.

Figure 3.5 β4c C-terminal residues do not enhance affinity for HP1γ.

Top panel: Raw isothermal titration calorimetry data after base-line correction shows saturation binding of CSD to β4c-199. *Bottom panel*: Integrated data corrected for the heat of dilution of the CSD dimer. Filled and open squares represent full-length β4c and β4c-199 data, respectively. The solid lines in the bottom panel represent the best fit to a one-site binding model. The affinity represented by dissociation constant (Kd) is around 0.5 μM for full length β4c.

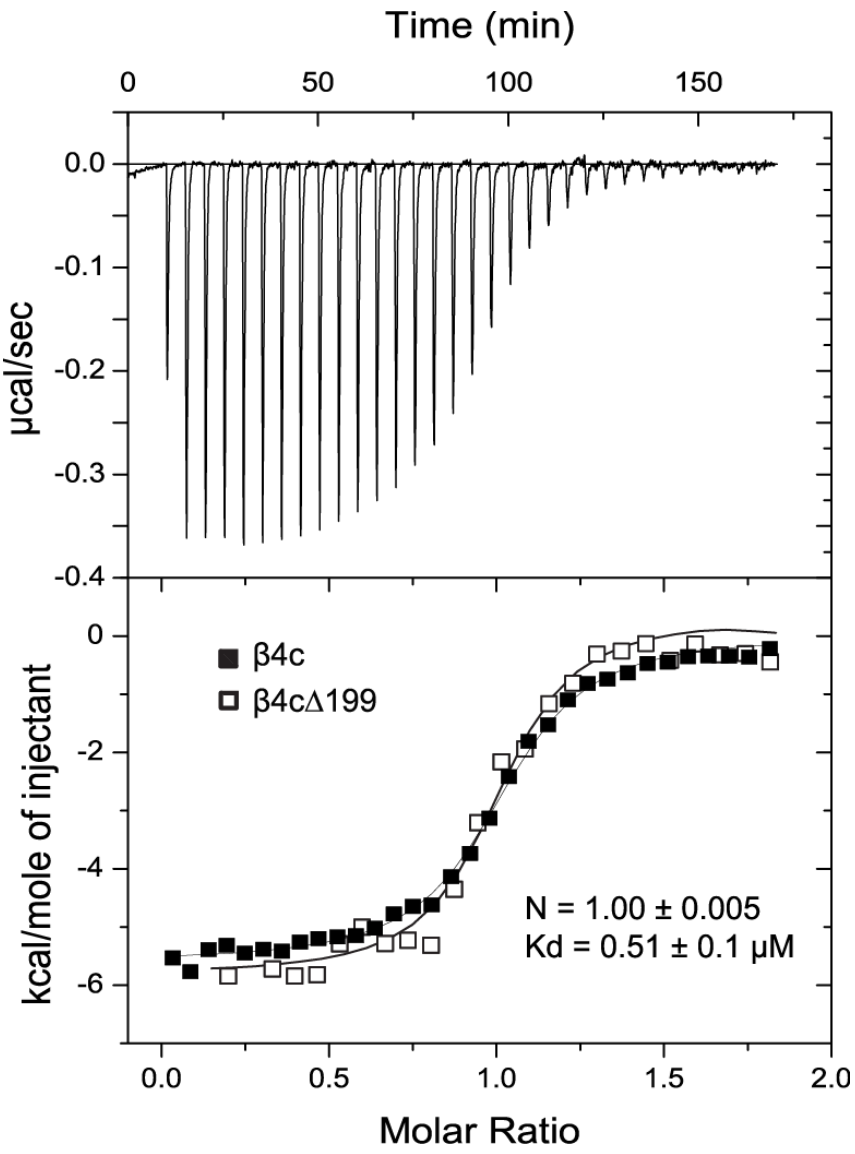

Site-directed mutagenesis identifies key C-terminal residues required for β4c nuclear localization

To examine the specific molecular determinants within the C-terminal eight residues required for β4c nuclear localization in Neuro2a cells, we first made three different constructs with residue type-specific (charged versus neutral-polar) double and triple point mutations (Figure 3.6 (A)). The nuclear localization of the three mutants was nearly the same as the GFP-β4c-199 nuclear localization, showing similar nuclear/cytoplasm fluorescence intensity ratio (Figure 3.6 (B) and (C)). This result supports the idea that each of the C-terminal eight residues is involved in optimal β4c nuclear localization, perhaps by forming a specific ligand sequence.

Next, we generated point mutants of each of the eight C-terminal residues by substitutions with alanine. As shown in Figure 3.7 (A), seven of the eight constructs showed significantly reduced nuclear/cytoplasm fluorescence ratio compared to GFP-β4c (all except GFP-β4c E204A). Among them, the GFP-β4c N202A and N203A mutants showed the most significant decreases. The GFP-β4c N202A mutant is primarily distributed in the cytoplasm compared to the nuclear localization of GFP-β4c (Figure 3.7 (B)). This indicates that the asparagine residues at position 202 and 203 are the most critical C-terminal molecular determinants for optimal localization of β4c into the nucleus of Neuro2a cells.

Functional consequences of ectopic expression β4c

Beyond the observation that chicken β4c attenuates the gene repressor function of HP1γ (7), very little is known about the nuclear function of β4c. To address the matter, we thought it logical to start with the question of whether β4c regulates Ca^{2+} channel gene expression.

Figure 3.6 Residue type-specific double and triple point mutations have similar effects on nuclear localization of β4c in Neuro 2a cells.

(A) Schematic representation of three C-terminal mutant β4c constructs. Cmut 1, alanine substitution of acidic residues; Cmut 2, alanine substitution of two asparagine residues; and Cmut 3, alanine substitution of two serine residues.

(B) Representative fluorescent images of Neuro2a cells expressing different constructs of β4c fused with GFP (from top to bottom): β4c-199, Cmut 1, Cmut 2, and Cmut 3. *Left column*, GFP fluorescence; *middle column*, DAPI staining; and *right column*, merged images. *Scale bar*, 5 µm.

(C) Nucleus/cytoplasm fluorescence intensity ratio determined for Neuro2a cells transfected with: vector alone, full-length β4c, β4c 199, Cmut1, Cmut2, and Cmut3. (means ± SEM; n=100 for vector and full-length β4c, n=85 for three Cmut constructs) *$p<0.001$ vs vector**.**

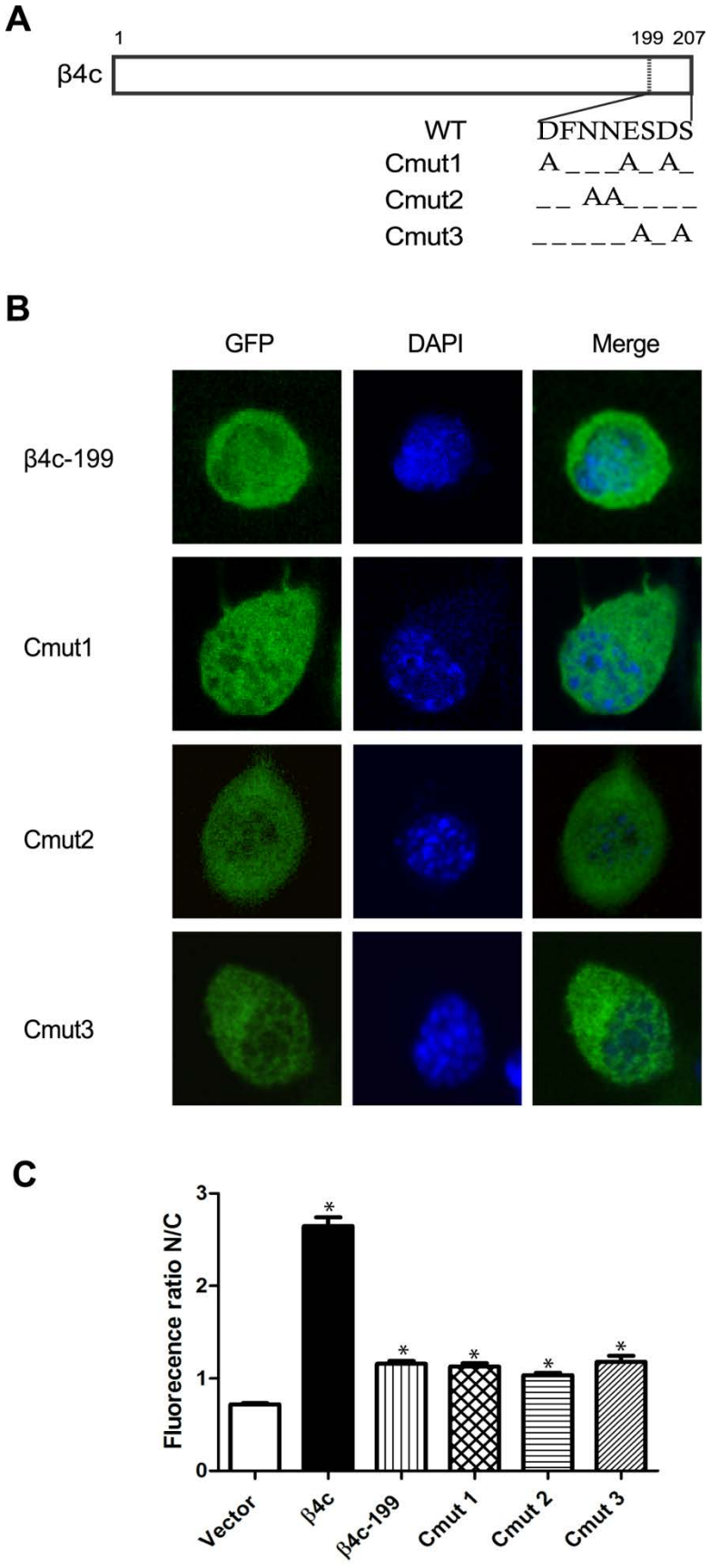
A
1
199 207
β4c
WT DFNNESDS
Cmut1 A _ _ _A_ A_
Cmut2 _ _ AA_ _ _ _
Cmut3 _ _ _ _ _ A_ A
B
GFP
DAPI
Merge
β4c-199
Cmut1
Cmut2
Cmut3
C
Fluorecence ratio N/C
3
2
1
0
*
Vector
β4c
β4c-199
Cmut 1
Cmut 2
Cmut 3

Figure 3.7 Determinants of β4c nuclear localization.

(A) Nucleus/cytoplasm fluorescence intensity ratio determined for Neuro2a cells transfected with eight individual β4c C-terminal constructs containing single alanine point mutations. (means ± SEM, n=100) *p<0.001 vs vector.

(B) Representative fluorescent images of Neuro2a cells expressing GFP- β4c or GFP- β4c N202A mutant. *Left column*, GFP fluorescence; *middle column*, DAPI staining; and *right column*, merged images. *Scale bar*, 5 μm.

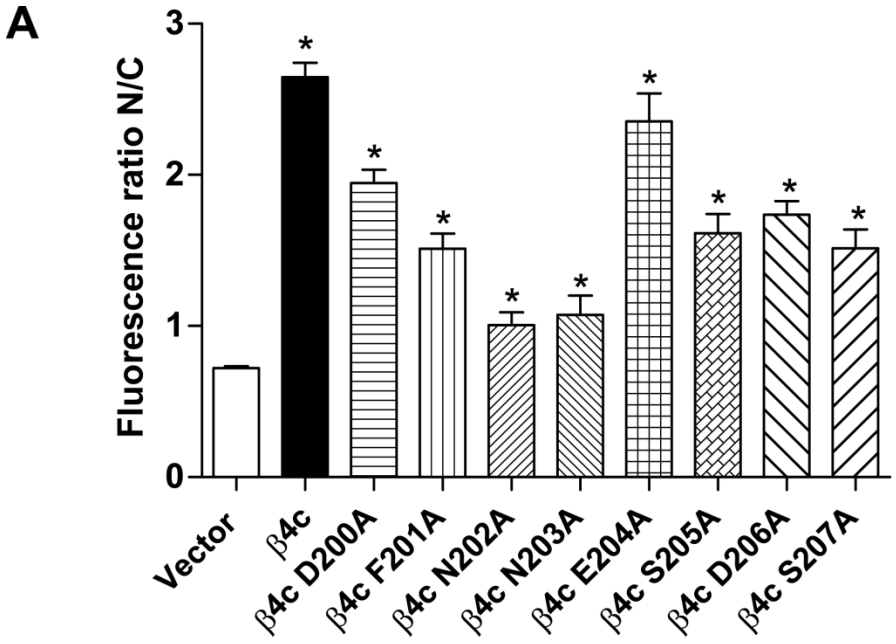
A
Fluorescence ratio N/C
0
1
2
3
*
Vector
β4c
β4c D200A
β4c F201A
β4c N202A
β4c N203A
β4c E204A
β4c S205A
β4c D206A
β4c S207A

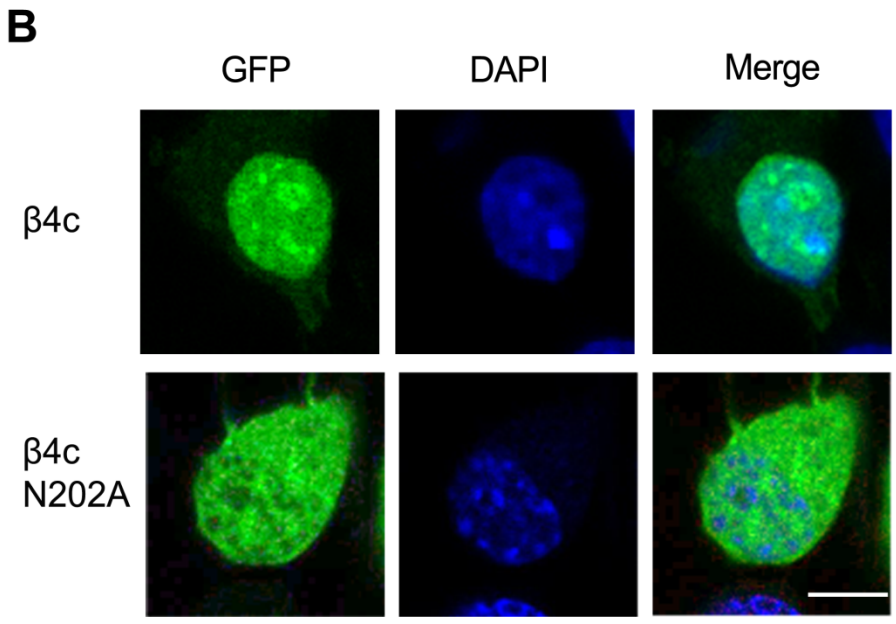
B
GFP
DAPI
Merge
β4c
β4c
N202A

To address the specific question of what role the β4c-HP1γ interaction plays in regulating Ca^{2+} -channel gene expression, we transfected undifferentiated Neuro2a cells with either β4c or the truncated β4c protein, β4c-184, that lacks both the ^{187}PVVLV^{191} motif and the C-terminal residues required for optimal nuclear localization (truncation results in >50% decrease in nuclear localization, Figure 3.4). Using real-time quantitative PCR, we compared the expression of Cacna genes 1a, 1b, 1c, and 1e, Cacna2d1, and Cacnb1- Cacnb4 in both groups of transfectants, and, as shown in Figure 3.8, we found no significant difference in the expression of any of these genes. Taken together with the result that β4c does not affect trafficking or gating properties of α1A: α2δ channel complexes (Figure 2.4), these results indicate that β4c does not have either direct or indirect effects on expression or gating of α1A: α2δ channel complexes.

Next, we performed Affymetrix GeneChip analysis on total RNA extracts from Nuero2a cells transiently transfected with β4c and compared the expression profile with that of β4c-184 transfected cells as a control to determine the functional consequences of β4c nuclear targeting. The microarray analysis was performed in biological duplicates. As a first step in our analysis, we sought to assess the similarities between the arrays in a global fashion. To establish relationships and compare variability between replicate arrays, principal component analysis (PCA) was used. PCA was chosen for its ability to reduce the effective dimensionality of complex gene-expression without significant loss of information (17). We performed PCA mapping with our four arrays (two groups in duplicate). The PCA plot clearly shows that equivalent array duplicates cluster with one another, providing confidence of sample quality in each duplicate (Figure 3.9 (A)). A volcano plot represents the distribution of all probe sets according to expression fold-change and p-value for statistical comparison between β4c and β4c-184 (Figure 3.9 (B)).

Figure 3.8 Nuclear localization of β4c does not regulate Ca^{2+} channel gene expression in Neuro2a cells.

qRT-PCR analysis of endogenous mRNA levels from Neuro2a cells overexpressing β4c-184 (white bar) or β4c (black bar) for *Cacna1a, Cacna1b, Cacna1c, Cacna1e, Cacna2d1, Cacnb1, Cacnb2, Cacnb3,* and *Cacnb4.* Bars represent mean fold changes of β4c relative to β4c-184 using $2^{-\Delta\Delta C_T}$ method. Data are means ± SD of five independent experiments performed in triplicate. Statistical analysis is performed by t-test with significant level $p \leq 0.05$.

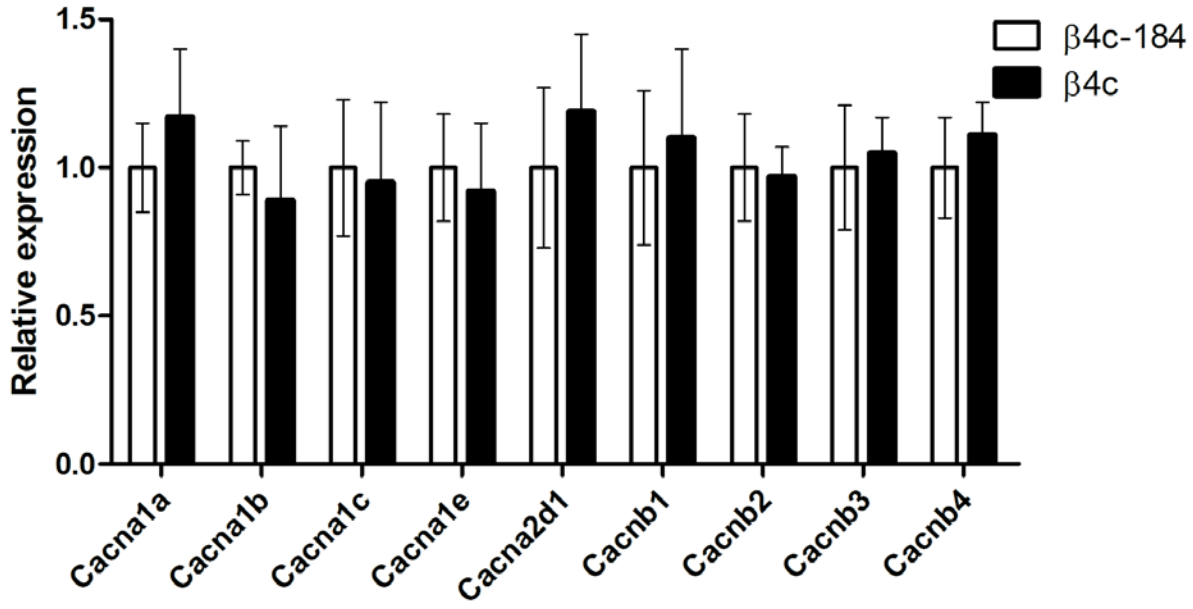

The plot indicates that 135 probe sets are differentially regulated by β4c compared to β4c-184 (p-value <0.1, fold change > ±1.4). A total 43 probes are up-regulated, and 92 probes are down-regulated. Among these probe sets, 91 probe sets have gene names (see appendix 1 and 2). To assess correlations among samples for each identified gene set, we performed hierarchical clustering analysis of differentially expressed probe sets. The heatmap shows that β4c expression leads to distinct expression profiles compared with β4c-184 expression (Figure 3.9 (C)). Some of the representative genes significantly up-regulated and down-regulated respectively in cells transfected with β4c compared with β4c-184 are shown in Figure 3.9 (D). As can be seen in the gene list, the Ca^{2+} channel related genes are not significantly regulated, which is consistent with the qRT-PCR results. Confirmation of the β4c effect was done with four representative genes by qRT-PCR using purified mRNA from Neuro2a cells transfected with β4c or β4c-184. The results of these experiments demonstrate that *Nfyc* and *Scn2a1* were significantly up-regulated, and *Kcnj10* and *Celsr2* were significantly down-regulated. This is consistent with the fold-change observed in microarray experiments (Figure 3.10).

We conducted Gene Ontology (GO) enrichment analysis to explore the possible functional relevance of differentially expressed genes identified in this study (Table 3.1). GO analysis organizes genes into functional categories and can uncover gene regulatory networks on the basis of biological processes and molecular functions (18,19). Enrichment provides a measure of the significance of the function, and as the enrichment increases, the corresponding function is more specific, which helps us to identify GOs with more concrete functional description in the experiment (20).

Figure 3.9 Differential transcriptional activities by expression of β4c compared with β4c-184 in Neuro2a cells.

(A) Principal component analysis of global gene expression profiles from Neuro2a cells expressing β4c (two red squares) or β4c-184 (two blue squares). Each square represents one profile. The percent represents the percentage variation that the particular principal component contributes to the total variation in the data.

(B) Volcano plot analysis of transcript levels in β4c expressed cells compared with β4c-184 expressed cells. Small squares represent the distribution of all probe sets according to fold-change and p-value. The vertical green lines indicate fold change cut-off ±1.4, and the horizontal green line indicate p-value cut-off <0.1. The expression of 135 probes (orange squares) was significantly changed. A total of 43 probes (include 2 unknown genes) are up-regulated and 92 (include 42 unknown genes) are down-regulated.

(C) Heatmap of 135 significantly regulated probe sets in β4c expressed cells compared with β4c-184 expressed cells by hierarchical clustering algorithm. Lane 1, 2, and lane 3, 4 represent two biological replicates of β4c-184, and two biological replicates of β4c, respectively. Probe sets and samples were ordered using Euclidean test and the Ward clustering algorithm. The red and the green colors represent positive and negative expression changes, respectively. The intensity of the color is proportional to the magnitude of the differential expression. Each row on the Y axis represents a single gene probe set and the phylograms represent distinct signaling pathways.

(D) Histogram showing the genes up-regulated (in red) and down-regulated (in green) with fold change >±1.4. Gene names and gene symbols (in the parenthesis) are indicated.

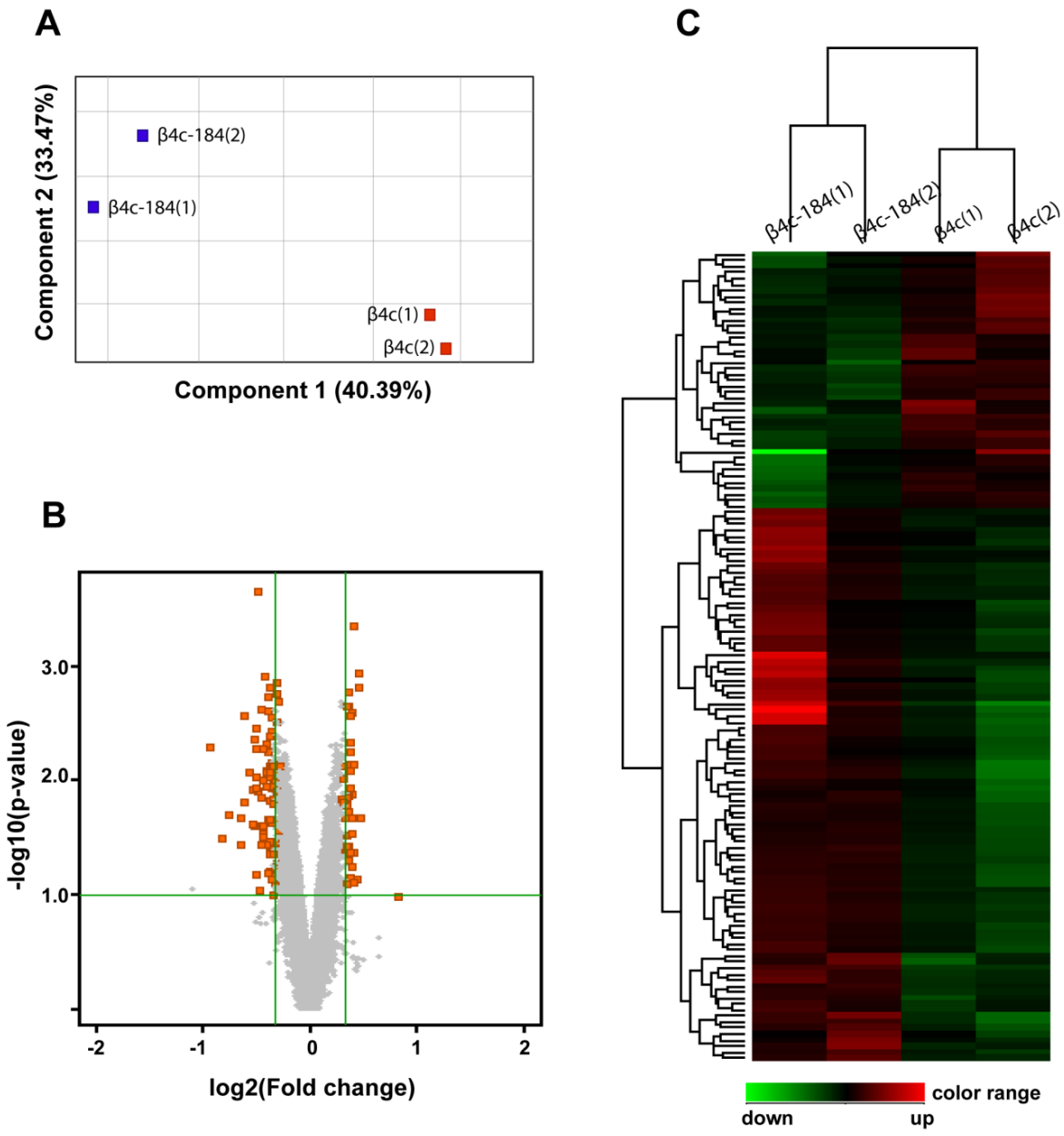
A
β4c-184(2)
β4c-184(1)
β4c(1)
β4c(2)
Component 2 (33.47%)
Component 1 (40.39%)
B
3.0
2.0
1.0
-log10(p-value)
-2
-1
0
1
2
log2(Fold change)
C
β4c-184(1)
β4c-184(2)
β4c(1)
β4c(2)
color range
down
up

D

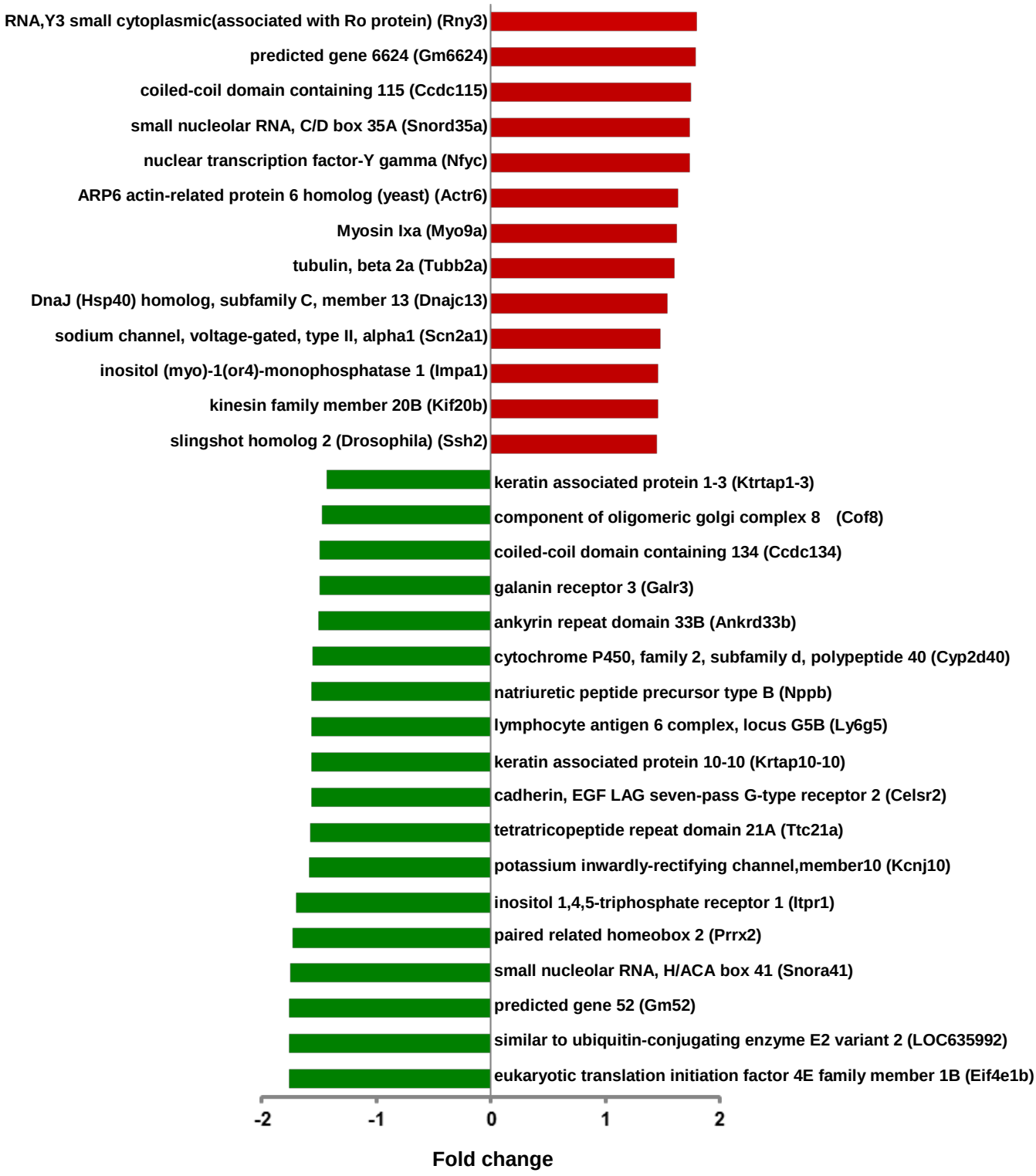
RNA,Y3 small cytoplasmic(associated with Ro protein) (Rny3)
predicted gene 6624 (Gm6624)
coiled-coil domain containing 115 (Ccdc115)
small nucleolar RNA, C/D box 35A (Snord35a)
nuclear transcription factor-Y gamma (Nfyc)
ARP6 actin-related protein 6 homolog (yeast) (Actr6)
Myosin Ixa (Myo9a)
tubulin, beta 2a (Tubb2a)
DnaJ (Hsp40) homolog, subfamily C, member 13 (Dnajc13)
sodium channel, voltage-gated, type II, alpha1 (Scn2a1)
inositol (myo)-1(or4)-monophosphatase 1 (Impa1)
kinesin family member 20B (Kif20b)
slingshot homolog 2 (Drosophila) (Ssh2)
keratin associated protein 1-3 (Ktrtap1-3)
component of oligomeric golgi complex 8 (Cof8)
coiled-coil domain containing 134 (Ccdc134)
galanin receptor 3 (Galr3)
ankyrin repeat domain 33B (Ankrd33b)
cytochrome P450, family 2, subfamily d, polypeptide 40 (Cyp2d40)
natriuretic peptide precursor type B (Nppb)
lymphocyte antigen 6 complex, locus G5B (Ly6g5)
keratin associated protein 10-10 (Krtap10-10)
cadherin, EGF LAG seven-pass G-type receptor 2 (Celsr2)
tetratricopeptide repeat domain 21A (Ttc21a)
potassium inwardly-rectifying channel,member10 (Kcnj10)
inositol 1,4,5-triphosphate receptor 1 (Itpr1)
paired related homeobox 2 (Prrx2)
small nucleolar RNA, H/ACA box 41 (Snora41)
predicted gene 52 (Gm52)
similar to ubiquitin-conjugating enzyme E2 variant 2 (LOC635992)
eukaryotic translation initiation factor 4E family member 1B (Eif4e1b)
-2
-1
0
1
2
Fold change

Figure 3.10 Quantitative real-time RT-PCR validates representative up- and down-regulated genes.

qRT-PCR analysis validates two up-regulated genes; Nfyc, and Scn2a1, and two down-regulated genes, Kcnj10, and Celsr2 in cells expressing β4c. Bars represent mean expression intensity fold change relative to β4c 184 expression using $2^{-\Delta\Delta C_T}$ method. Data are means ± SD of three independent experiments performed in triplicate. Statistical analysis is performed by ANOVA with significance level at $p \leq 0.05$.

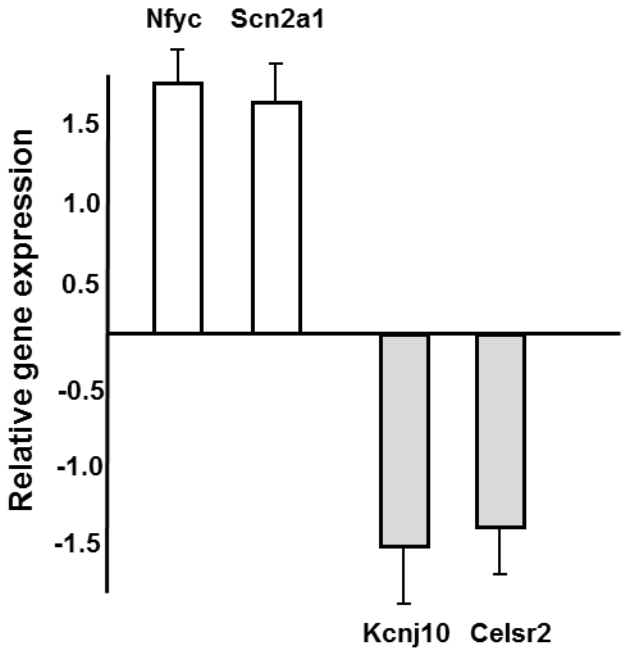

Table 3.1 GO analysis of differentially regulated genes by expression of β4c in Neuro2a cells. GO enrichment corrected p-value < 0.1 by Benjamini-Yekutieli method

GO Term	corrected p-value	Count in Selection	% Count in Selection
intermediate filament	0.013	6	9.84
cytoskeletal part	0.013	11	18.03
glycine C-acetyltransferase activity	0.014	2	3.28
calcineurin complex	0.055	2	3.28
C-acetyltransferase activity	0.055	2	3.28
cation channel activity	0.065	6	9.84
inositol phosphate-mediated signaling	0.069	2	3.28
voltage-gated sodium channel complex	0.089	2	3.28
ion gated channel activity	0.093	6	9.84
endoplasmic reticulum calcium ion homeostasis	0.093	2	3.28
ligand-gated ion channel activity	0.096	4	6.56
nuclear inner membrane	0.096	2	3.28

The regulated genes are related with 21 GO terms (see Appendix 3), and Table 3.1 shows the representative GOs. Interestingly, the most enriched GOs were associated with intermediate filament (GO:0005882), and cytoskeletal part (GO:0044430). These GOs are associated with genes that are involved in microtubule and actin filament formation (*Tubb2a*) (21,22), neuronal polarization (*Kif20b*) (23,24), spine morphology (*Itpr1*) (25), chromatin structure (*Actr6*) (26), and actin cytoskeleton (*Actr6*) (27). In addition, there are GOs related to the ion channel activity including voltage-gated sodium channel (*Scn2a1*), and ion gated channel activity (*Kcnj10*).

Discussion

This study had two main objectives: 1) identify the key amino acids required for nuclear localization of β4c subunit, and 2) determine which genes are under the control of β4c in Nuero2a cells. Several studies have revealed that Ca^{2+} channel independent activities of the β4 subunit are driven by its nuclear localization (6-10,28). The story is complicated by the existence of several splice variants of the Cacnb4 gene that code for β4a, β4b, β4e, and β4c proteins (7,10,11,29). The N-terminal β4 splice variants (β4a, β4b and β4e) are full-length, meaning that they contain a complete SH3-GK core and identical C-termini, and can therefore regulate voltage-gated Ca^{2+} channels by interactions with the α1 subunit (10,29). By contrast, the β4c splice variant is a truncated, GK-lacking, form of β4a that results from exon 9 skipping (Figure 3.1). This splicing event in mammals results in the addition of intron sequence that codes for eight amino acids (DFNNESDS) before reaching a stop codon (11). Interestingly, the splicing mechanism has been conserved in birds (7); however, the avian sequence has two amino acid substitutions and is four residues longer (DINNPSDSHSFC). Importantly, only the β4b and β4c splice variants have been shown to localize to the nucleus: β4b in heart (6), skeletal muscle cells

and neurons (8,9); and β4c in neurons (7,11). In marked contrast, β4a is excluded from the nucleus under conditions in which β4b and β4c are readily translocated (7, 9, this study). There is one study that shows that β4a can enter the nucleus of reconstituted young hippocampal neurons, but the degree of nuclear targeting is significantly less than that of β4b (10). There are two major differences in the mechanisms by which β4b and β4c enter the nucleus. In contrast to β4c, nuclear entry of β4b appears to be dependent on N-terminal amino acids 28-38 (8), rather than using the "cNLS" ^{133}KRGR^{136} sequence in the HOOK region. This sequence (T/SRRSRLKRSDGSTT) has been very highly conserved throughout the evolution of teleosts and tetrapods (30), and may serve as a non-canonical nuclear localization sequence. The newly identified β4e subunit, which lacks the variable N-terminus, shows poor nuclear targeting properties (10). Together with our findings, the results from these very recent studies point to the possibility that mechanisms of β4 mRNA splicing have evolved to provide cell-type and condition-specific regulation of gene transcription.

Alternative splicing results in unmasking of a classical nuclear localization sequence in β4c.

Classical nuclear localization sequences (cNLS) usually consist of one (monopartite) or more (i.e. bipartite) short sequences of positively charged lysines (K) or arginines (R) (15,31). The monopartite cNLS typically contains the consensus sequence, K(K/R)X(K/R), which binds to importin α (Impα) with nanomolar affinity (15,31,32). We identified in this study a putative "cNLS" (^{133}KRGR^{136}) at the 5' end of the HOOK domain found in all β subunit isoforms. (We consider it putative until we have determined that β4c binds to Impα. Mutation of this sequence significantly decreased β4c nuclear targeting. Though the positively charged ^{133}KRGR^{136} motif is also present in full-length β4a, heterologously expressed β4a, as shown above, showed little or

no nuclear accumulation. This is surprising given that the ^{133}KRGR^{136} sequences are relatively exposed in both β4a and β4c. The explanation for the inability of Impα to transport β4a likely lies in the location of the Impα KRGR binding pocket. Impα is an elongated, kidney bean shaped, protein composed of 10 tandem arranged armadillo (ARM) motifs (33,34). The major cNLS binding site is located on the surface of the concave groove formed by ARM repeats 1- 4 (31,34). Given this location, it is very likely that the presence of the GK domain in β4a causes steric hindrance and prevents access to the Impα KRGR binding pocket (Figure 3.11). Further binding and structural studies are required to explore this possibility in more detail.

Binding to HP1γ via PXVXL motif is not required for nuclear localization of β4c in Neuro2a cells

The role of the β4c subunit in regulating transcription was first revealed by the work of Hibino et al. showing that chicken β4c interacts directly with the chromo shadow domain of HP1γ and attenuates its gene silencing activity (7). However, when expressed alone in tsA201 (modified human embryonic kidney) cells, chicken β4c was mostly cytosolic and showed only modest labeling of nuclei. It was only when co-expressed with HP1 proteins that β4c was able to enter the nucleus. We took a different approach in determining whether HP1γ was required for nuclear localization of mammalian β4c in Neuro2a cells. In a previous report, we identified a consensus PXVXL site (^{187}PVVLV^{191}) in β4c that was required for HP1γ binding, and found that mutating the site to ^{187}AVAVV^{191} completely prevented the HP1γ interaction (11). In the present study, we found that the P187A/V189A β4c mutant was readily transported to the nucleus in a manner indistinguishable from wild-type β4c.

Figure 3.11 Steric hindrance by GK domain may prevents β4a interaction with importin α. Manual docking model aligning β4 ^{133}KRGR^{136} to the major cNLS binding site of importin α. *A*, The model predicts likely steric hindrance imposed by the β4a GK domain (indicated by *oval*), while *B*, shows minimal interference once the GK domain has been removed by alternative splicing to form β4c.

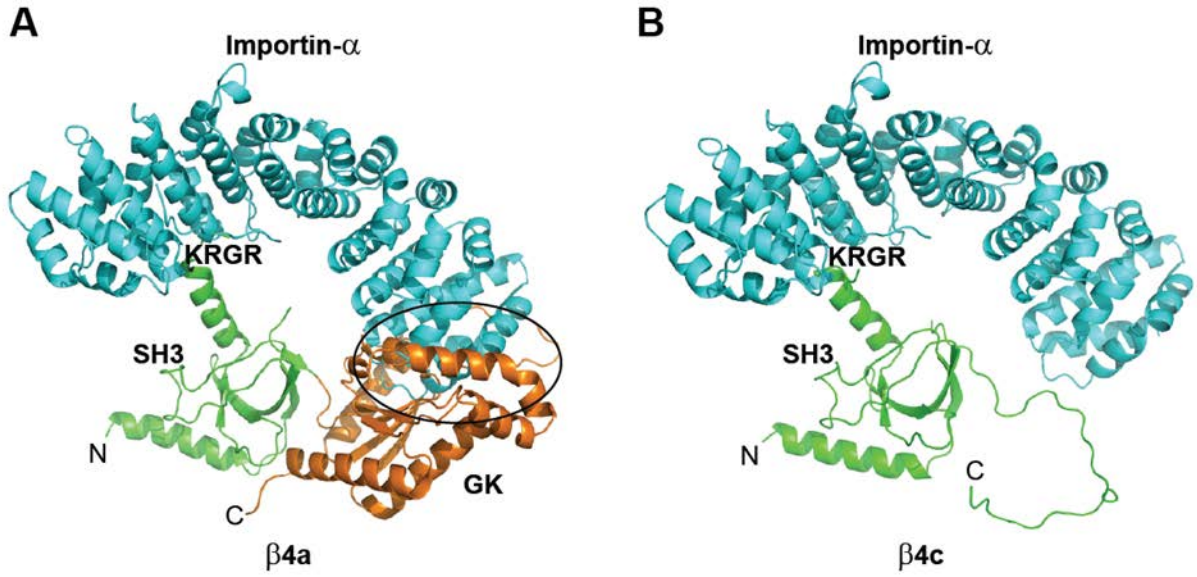

This suggests that β4c nuclear transport mechanisms may vary in different species and/or cell types, or that HP1γ may play a role in nuclear transport that is independent of its direct interaction with β4c.

Requirement of β4c C-terminal residues for optimal nuclear localization

In the course of studying the role of HP1γ in nuclear localization of β4c, it became apparent that although the ^{133}KRGR^{136} cNLS was necessary for β4c transport, it was not sufficient. A C-terminal truncation mutant (β4c199) containing the ^{133}KRGR^{136} sequence but lacks the C-terminal 8 amino acids, displayed significantly reduced nuclear localization compared to full-length β4c. Further site-directed mutagenesis studies identified Asp202 and Asp203 as the key residues involved in the localization mechanism. This result raises the question of whether the C-terminus might also interact with Impα, perhaps at the minor NLS binding site formed by ARM repeats 6-8 (13,35). Though we did not test this directly, the possibility is likely ruled out by studies showing that, as with the major site, basic residues are also required for binding (31). This leaves open the possibility that the β4c C-terminus binds to a previously unidentified site on Impα, or to another protein that is involved in optimization of its nuclear transport. It is also possible that the C-terminal sequence does not optimize transport, but rather serves to enhance retention of β4c in the nucleus. Our future studies will address these questions in more detiail.

Functional consequences of ectopic expression of β4c

Our previous study showed that β4c binds to HP1γ in vitro and that its distribution pattern resembles that of HP1γ in vivo (11). When transfected into tsA201 cells (7), chicken β4c

inhibits the gene silencing activity of HP1γ, but as of yet, we have no knowledge of what genes might be regulated. Our preliminary survey of Ca^{2+} channel genes indicates that ectopic expression of human full-length β4c in Neuro2a cells has no effect on their expression when compared to a disabled β4c-184 that cannot bind HP1γ. Likewise, we showed that expression of β4c in *Xenopus* oocytes had no effect on trafficking or gating of α1A subunits (Figure 2.5). These results suggest that nuclear localization of β4c does not function as part of a signaling feedback mechanism that directly regulates the number and properties of plasma membrane Ca^{2+} channels. This result is consistent with our global gene expression data showing that Ca^{2+} channel subunit genes are not regulated by overexpression of β4c, and with Ronjat et al. (28) who showed that changes in Ca^{2+} channel subunit gene expression were not readily apparent following nuclear localization of β4b in NG108-15 cells. Interestingly however, the β4 subunit, most notably β4b was shown to down-regulate expression of $Ca_v2.1$ gene in reconstituted lethargic mouse cerebellar granule cells (CGCs) (10).

The results from our microarray experiments reveal an interesting complementarity between genes that are up and down regulated in Neuro2a cells in response to transfection with full-length β4c. Those genes that are turned on are involved in microtubule and actin filament formation (tubulin beta 2A (see (21) for review), kinesin family member 20b (24), and slingshot homolog 2 (36)), have anti-apoptotic effects (Nfyc (37) and Ccdc 115 (38)), play a role in endosomal trafficking (Dnajc13, (39)), and enhance membrane excitability (Scn2a1(40)); while those genes that are turned off regulate contact-mediated cell-cell communication (Celsr2 (41)), have pro-apoptotic effects (Ccdc134 (42)), regulate glycosylation (Cog8 (43)), and dampen membrane excitability (Kcnj10 (44)). This suggests the intriguing possibility that the β4c C-terminus regulates gene expression in a way that primes the cell for branching neurite outgrowth.

Neurite outgrowth is supported by microtubule formation and endosomal trafficking (45), and has long been associated with up-regulation of sodium channels (46). In contrast, protein glycosylation and growth factor induced apoptosis have been shown to have inhibitory effects on neurite outgrowth (47,48). Of note is the fact that neurite outgrowth does not occur with transfection of β4c alone, suggesting that a transforming stimulus is required to initiate the process. This will be the focus of our future studies. Also of interest is the fact that mutations in several of the genes regulated by β4c have been linked with human neurological disorders: Tmem126a with degeneration of retinal ganglion cells and atrophy of the optic nerve (49); Dnajc13 with Parkinson disease (50); Scn2a and Kcnj10 with various forms of epilepsy (51,52); and Itpr1 with congenital spinocerebellar ataxia (53).

In summary, our experiments have: 1) identified two important sequence motifs that are required for optimal nuclear localization of β4c; 2) shown that β4c binding to HP1γ via its PXVXL binding motif is not necessary for nuclear translocation; 3) confirmed in a neuronal cell-type that, in contrast to its alternatively spliced truncated variant, β4c, full-length β4a does not enter the nucleus; 4) revealed that ectopic expression of β4c does not affect the expression or function of Ca^{2+} channel subunits; and 5) determined that β4c regulates expression of genes involved in microtubule formation, apoptosis, endosomal trafficking, and cell excitability. Taken together, our results suggest that the C-terminus of β4c does not regulate Ca^{2+} channel expression, but instead plays a role in preparing the cell for neurite growth.

Materials and Methods

Plasmid construction

The cDNA constructs coding for GFP-tagged β4c fragments were generated by PCR amplification using pET-15b-β4c plasmid as the template. Amplicons were subcloned into the XhoI and EcoRI sites of the Vitality® phrGFP II-N mammalian expression vector (Strategene). Mutants GFP-P187A/V189A, GFP- Cmut 1, GFP- Cmut 2, GFP- Cmut 3, GFP-^{133}KRGR^{136}/^{133}AAAA^{136} and eight GFP C-terminal point mutant constructs were generated by PCR based site-directed mutagenesis of the GFP-β4c construct using appropriate oligonucleotide primers. For qRT-PCR transfection, β4c and β4c- 184 were subcloned into the BamHI and EcoRI sites of the pKH3 vector (Addgene) using primers forward β4c and β4c-184 (5'-TATGGATCCATGTATGCAATTTGTACCTG-3'), reverse β4c (5'-TATGAATTCCTACTAG-CTGTCACTCTCGTTATTGA-3'), and reverse β4c-184 (5'- CTGGAATTCCTATGACGGTAC-AACATCGTA-3'). All constructs were verified by DNA sequencing.

Polymerase Chain Reaction

Total RNA was extracted from Neuro2a cells transfected with pKH3 vector alone or pKH3-β4c using the RNAeasy kit (Qiagen). Single strand cDNAs for PCR were synthesized using a High-Capacity cDNA Reverse Transcription Kit (Applied Biosystems). PCR primers for detecting β4c in Neuro2a cells were: forward (5'-TCACATATGATGTCTGACAATTTGTACCTGCATGG-3'), and reverse (5'-CTGCTCGAGTCAGCTGTCACTCTCGTTATTGAAATCCTCG-3') (11). The thermal cycling program was as follows: 1 cycle of 98°C for 30s, 35 cycles of 98°C for 10, 58°C for 20s, and 72°C for 30s and final extension of 72°C for 30s.

Western blot analysis

Proteins were extracted from mock transfected or pKH3-β4c transfected Neuro2a cells using M-PER® mammalian protein extraction reagent (Thermo Scientific) 48 hours after transfection according to the manufacturer's instructions. Proteins were separated by SDS-PAGE and transferred at 90 V for one hour to PVDF membrane (Thermo Scientific). Membranes were blocked with 5% milk/TBST and incubated with rabbit polyclonal primary antibody (anti-β4a/c; 1:5000) for β4c detection, and mouse monoclonal antibody (anti HP1γ; 1:5000, Abcam) for HP1γ detection overnight at 4 ^{o}C. Membranes were washed three times with TBST and then incubated with HRP-conjugated goat anti-rabbit IgG (1:5000, Bio-Rad), and HRP-conjugated goat anti-mouse IgG (1:5000, Bio-Rad) respectively for one hour at room temperature. Membranes were washed five times with TBST prior to development with peroxide and luminol enhancer solution (Thermo Scientific) according to the manufacturer's instructions.

Cell culture and Transfection

Mouse neuro-blastoma Neuro2a cells were maintained in Dulbecco's Minimal Essential Media (Invitrogen) supplemented with 10% fetal bovine serum. Cell cultures were incubated at 37^{o}C under 5% CO_2 and subcultivated at a ratio of 1:5 every 2-3 days. Neuro2a cells were transfected at a confluence of 40-50%. Transfections were performed using Lipofectamine™ LTX reagent (Invitrogen) according to the manufacturer's instructions.

Protein expression, purification and isothermal titration calorimetry

Proteins used in ITC experiments were expressed in *E. coli* BL21(DE3) (Stratagene) and purified as described previously (11). A single colony of freshly transformed pET-15b β4c construct was

first inoculated into 25 ml LB pre-culture and grown for overnight before it was scaled up to grow in 1 L of LB medium with 50 μg/ml ampicillin at 37 °C. Protein expression was induced by adding 0.2 mM IPTG to the cell culture once the OD_{600} reached 0.6 AU, and the cells were then grown with shaking at 37 °C for 3 h. Cells were harvested by centrifugation and resuspended in a binding buffer (50 mM Tris-HCl, 0.3 M NaCl, 1 mM DTT, pH 8.0) and lysed by sonication. The lysate was incubated with 50 units of DNase I (Bio-Rad) and 12.5 mM $MgCl_2$ for 30 min and further centrifuged at 17,000 RPM for 30 min, and the supernatant was filtered and collected. The supernatant was then loaded onto a 15-ml Ni^{2+} resin column (Bio-Rad) pre-equilibrated with 100 ml of binding buffer. After washing with eight column volumes of binding buffer, the desired protein was eluted with increasing concentrations of imidazole (up to 300 mM). After the Ni^{2+} column, the His_6 tag was removed by overnight thrombin cleavage (Amersham Biosciences) at 4°C. The His_6 tag-cleaved proteins were further purified by gel filtration using a Superdex 75HR column or a Sephacryl S-200 HR column using an AKTA FPLC (GE healthcare) in 500 mM NaCl, 50 mm sodium phosphate, 1 mM DTT, pH 7.0. Protein purity was analyzed on SDS-polyacrylamide gels, and the protein samples were concentrated via centrifugal filtration. Protein concentrations were determined by UV absorbance at 280 nm using predicted extinction coefficients. Isothermal titration calorimetry (ITC) measurements were carried out at 298 K with a MicroCal (Northampton, MA) VP-ITC microcalorimeter. All proteins were dialyzed against the same buffer (50 mM sodium phosphate, 150 mM NaCl, pH 7.0, 2 mM DTT), and all buffers were degassed before experiments. For measurements, 28 injections of 10 μl of CSD dimer were titrated into 1.4-ml solutions of either β4cΔ199 or β4c proteins (or, for base-line correction, buffer alone) to a stoichiometric ratio of 2.1:1. Data were processed and analyzed with MicroCal Origin 7.0.

Imaging and analysis

Forty-eight hours after transfection, cells were fixed with 4% paraformaldehyde for 10 min and washed with phosphate-buffered saline. Following fixation, cells were mounted on glass slides with ProLong® Gold Antifade reagent (with DAPI) (Invitrogen). The cell slides were imaged with an LSM 510 Meta confocal microsope (Zeiss) using a 63X oil immersion lens. Analysis of digitized LSM images was performed using ImageJ software (v1.44p) as described previously (54), to determine the ratio of nuclear to cytoplasmic fluorescence for single cells. The mean fluorescence ratio was calculated for 65-100 cells for each construct and statistical analysis (1-way ANOVA test) was performed using GraphPad Prism software.

Microarray experiment and statistical analysis

The microarray experiments were performed and processed by Cornell Weill microarray core facility, using the Affymetrix GeneChip® Mouse Gene 1.0 ST arrays. Approximately 5µg of total RNA extracted from transfected Neuro2a cells were used for each array. Preparation of biotin-labeled cRNA was performed according to the protocols of the manufacturer (Affymetrix). The cRNA were chemically fragmented to 35 to 200 base fragments before hybridization overnight on Affymetrix Mouse Gene 1.0 ST Array. After sixteen hours of hybridization, washes and streptavidin-phycoerythrin (SAPE) staining procedures were performed using Affymetrix Fluidics Station 450 and arrays were scanned into Affymetrix GeneChip Scanner 3000. Raw gene expression data were analyzed using the GeneSpringGx 12.6 software (Agilent® Technologies). All samples were normalized and summarized by Robust Multichip Analysis (RMA) normalization method, which includes background correction, normalization and

calculation of expression values (55) . Baseline was set to median for all samples, where median of the log-transformed value of each probe from all samples was calculated and this value was subtracted from all samples. Probes were filtered and eliminated on expression level as part of quality control (QC) and probes with expression values <20% were excluded. Differentially expressed genes between β4c transfected cells and β4c-184 transfected cells were selected with a with a p-value cutoff of <0.1 based on Moderated *t*-test and a fold-change cutoff of >±1.4. The p-values were adjusted using Benjamini and Hochberg procedure to control false discovery rate (FDR) (56). PCA analysis was performed on conditions using GeneSpring PCA analysis tool. Hierarchical cluster analysis was performed on a gene list of filtered probe sets using Euclidean clustering and average linkage statistical methods. To assess the functional repertoire of differentially expressed genes GO term enrichment analysis was performed using GeneSpringGx 12.0 software (Agilent® Technologies) with Benjamini-Yekutieli corrected p-value cutoff<0.1

Quantitative real-time RT-PCR

Total RNA was extracted from transfected Neuro2a cells using RNAeasy kit (Qiagen) 72 hours after transfection. Single strand cDNAs were synthesized from 1μg total RNA using the High-Capacity cDNA Reverse Transcription Kit (Applied Biosystems). Real-time PCR was performed using *power* SYBR® green PCR master mix (Applied Biosystems) and the 7500 Fast Real-Time PCR System (Applied Biosystems). Each PCR experiment was done in triplicate, and the cycling protocol was as follows: initial activation at 95°C for 2 min and 40 cycles of denaturation at 95°C for 30 s and annealing and extension at 53°C for 45 s. Fluorescence intensities were analyzed using the manufacturer's software. The calculated threshold cycle (C_t) value for each gene was normalized to the C_t of the house keeping gene, β-actin. The fold induction of gene

expression in β4c versus β4c-184 transfected cells was obtained using the $2^{-\Delta\Delta Ct}$ method (57). For each gene, five independent real-time PCRs were performed. For Ca^{2+} channel transcript analysis, cDNAs from two independent transfections were used. Sequences for real-time primers were as follows: β-actin forward (5'-CATCCTCTTCCTCCCTGGAGAAGA-3') and β-actin reverse (5'-ACAGGATTCCATACCCAAGAAGGAAGG3'); Cacna1a forward (5'-AGGCTGG-AATTAAGATCGTGG-3') and Cacna1a reverse (5'-CTCAGTGTCCGTAGGTCAAAC-3'); Cacna1b forward (5'-GTTTCCCTGTTCCACCCTC-3') and Cacna1b reverse (5'-TCCTTGAT-GCCACTTTCCTG-3'); Cacna1c forward (5'-CAAGAAACGGAAAGAGCAAGG-3') and Cacna1c reverse (5'- GCAAGTCACAGGATATAGCCC-3'); Cacna1e forward (5'-TCGTTGT-CTTTGCTCTCCTG-3') and Cacna1e reverse (5'-CATCACCTCATTCCAGTCTTCC-3'); Cacna2d forward (5'-AGTTAATCCTGGGTGTCATGG-3') and Cacna2d reverse (5'-GGGCTT-GAGATTGGGATGTAG-3'); Cacnb1 forward (5'-AAGTACAGCAAGAGGAAAGGG-3') and Cacnb1 reverse (5'-CTCCAGAGACACATCAGAGTC-3'); Cacnb2 forward (5'-GCAAAACAC-CTCAATGTCCAG-3') and Cacnb2 reverse (5'-TCCAGTATGCCTCCAGATAGTC-3'); Cacnb3 forward (5'-GAGGCCAAAGATTTTCTGCAC-3') and Cacnb3 reverse (5'-TCTGTTCC-TGTTTGAGCCG-3'); Cacnb4 forward (5'-TCACCATATCCCACAGCAATC-3') and Cacnb4 reverse (5'-TTTCATCCGAGGTCATTAGGC-3'); Scn2a1 forward (5'- CTCCGAACATTAAG-AGCACTGAGG-3') and Scn2a1 reverse (5'-AGGAGAGCGTTTACAACAACCC-3'); Kcnj10 forward (5'- TTCTCAGCAAAGCCGGTTCTCTCT-3') and Kcnj10 reverse (5'- CAGGAAAG-GTGGCTGCTTGTGTTT-3'); Nfyc forward (5'-TGTATCAGGCACCCAAGTTGTCC-3') and Nfyc reverse (5'- ACCTCTGTCTGTGTGATCTGTTGG-3'); Celsr2 forward (5'- ACCATCGT-CACACCCAACATTGTC-3') and Celsr2 reverse (5'- AGCTTGGTCCCAGCAAAGTTCC-3').

REFERENCES

1. Arikkath, J., and Campbell, K. P. (2003) Auxiliary subunits: essential components of the voltage-gated calcium channel complex. *Curr Opin Neurobiol* **13**, 298-307

2. Buraei, Z., and Yang, J. (2010) The β subunit of voltage-gated Ca^{2+} channels. *Physiol Rev* **90**, 1461-1506

3. Buraei, Z., and Yang, J. (2013) Structure and function of the beta subunit of voltage-gated Ca^{2+} channels. *Biochim Biophys Acta* **1828**, 1530-1540

4. Dolphin, A. C. (2012) Calcium channel auxiliary alpha2delta and beta subunits: trafficking and one step beyond. *Nat Rev Neurosci* **13**, 542-555

5. Ebert, A. M., McAnelly, C. A., Srinivasan, A., Linker, J. L., Horne, W. A., and Garrity, D. M. (2008) Ca^{2+} channel-independent requirement for MAGUK family CACNB4 genes in initiation of zebrafish epiboly. *Proc Natl Acad Sci U S A* **105**, 198-203

6. Colecraft, H. M., Alseikhan, B., Takahashi, S. X., Chaudhuri, D., Mittman, S., Yegnasubramanian, V., Alvania, R. S., Johns, D. C., Marban, E., and Yue, D. T. (2002) Novel functional properties of Ca^{2+} channel beta subunits revealed by their expression in adult rat heart cells. *Journal of Physiology-London* **541**, 435-452

7. Hibino, H., Pironkova, R., Onwumere, O., Rousset, M., Charnet, P., Hudspeth, A. J., and Lesage, F. (2003) Direct interaction with a nuclear protein and regulation of gene silencing by a variant of the Ca^{2+} channel beta 4 subunit. *Proc Natl Acad Sci U S A* **100**, 307-312

8. Subramanyam, P., Obermair, G. J., Baumgartner, S., Gebhart, M., Striessnig, J., Kaufmann, W. A., Geley, S., and Flucher, B. E. (2009) Activity and calcium regulate nuclear targeting of the calcium channel beta4b subunit in nerve and muscle cells. *Channels* **3**, 343-355

9. Tadmouri, A., Kiyonaka, S., Barbado, M., Rousset, M., Fablet, K., Sawamura, S., Bahembera, E., Pernet-Gallay, K., Arnoult, C., Miki, T., Sadoul, K., Gory-Faure, S., Lambrecht, C., Lesage, F., Akiyama, S., Khochbin, S., Baulande, S., Janssens, V., Andrieux, A., Dolmetsch, R., Ronjat, M., Mori, Y., and De Waard, M. (2012) Cacnb4 directly couples electrical activity to gene expression, a process defective in juvenile epilepsy. *EMBO J* **31**, 3730-3744

10. Etemad, S., Obermair, G. J., Bindreither, D., Benedetti, A., Stanika, R., Di Biase, V., Burtscher, V., Koschak, A., Kofler, R., Geley, S., Wille, A., Lusser, A., Flockerzi, V., and Flucher, B. E. (2014) Differential neuronal targeting of a new and two known calcium channel beta4 subunit splice variants correlates with their regulation of gene expression. *J Neurosci* **34**, 1446-1461

11. Xu, X., Lee, Y. J., Holm, J. B., Terry, M. D., Oswald, R. E., and Horne, W. A. (2011) The Ca^{2+} channel beta4c subunit interacts with heterochromatin protein 1 via a PXVXL binding motif. *J Biol Chem* **286**, 9677-9687

12. Lange, A., Mills, R. E., Lange, C. J., Stewart, M., Devine, S. E., and Corbett, A. H. (2007) Classical nuclear localization signals: definition, function, and interaction with importin alpha. *J Biol Chem* **282**, 5101-5105

13. Xu, D., Farmer, A., and Chook, Y. M. (2010) Recognition of nuclear targeting signals by Karyopherin-beta proteins. *Curr Opin Struct Biol* **20**, 782-790

14. Vendel, A. C., Terry, M. D., Striegel, A. R., Iverson, N. M., Leuranguer, V., Rithner, C. D., Lyons, B. A., Pickard, G. E., Tobet, S. A., and Horne, W. A. (2006) Alternative splicing of the voltage-gated Ca^{2+} channel beta4 subunit creates a uniquely folded N-terminal protein binding domain with cell-specific expression in the cerebellar cortex. *J Neurosci* **26**, 2635-2644

15. Kosugi, S., Hasebe, M., Matsumura, N., Takashima, H., Miyamoto-Sato, E., Tomita, M., and Yanagawa, H. (2009) Six classes of nuclear localization signals specific to different binding grooves of importin alpha. *J Biol Chem* **284**, 478-485

16. Turner, R. W., Anderson, D., and Zamponi, G. W. (2011) Signaling complexes of voltage-gated calcium channels. *Channels (Austin)* **5**, 440-448

17. Quackenbush, J. (2001) Computational analysis of microarray data. *Nat Rev Genet* **2**, 418-427

18. Gene Ontology, C. (2006) The Gene Ontology (GO) project in 2006. *Nucleic Acids Res* **34**, D322-326

19. Ashburner, M., Ball, C. A., Blake, J. A., Botstein, D., Butler, H., Cherry, J. M., Davis, A. P., Dolinski, K., Dwight, S. S., Eppig, J. T., Harris, M. A., Hill, D. P., Issel-Tarver, L., Kasarskis, A., Lewis, S., Matese, J. C., Richardson, J. E., Ringwald, M., Rubin, G. M., and Sherlock, G. (2000) Gene ontology: tool for the unification of biology. The Gene Ontology Consortium. *Nat Genet* **25**, 25-29

20. Schlitt, T., Palin, K., Rung, J., Dietmann, S., Lappe, M., Ukkonen, E., and Brazma, A. (2003) From gene networks to gene function. *Genome Res* **13**, 2568-2576

21. Conde, C., and Caceres, A. (2009) Microtubule assembly, organization and dynamics in axons and dendrites. *Nat Rev Neurosci* **10**, 319-332

22. Niwa, S., Takahashi, H., and Hirokawa, N. (2013) Beta-tubulin mutations that cause severe neuropathies disrupt axonal transport. *EMBO J* **32**, 1352-1364

23. Janisch, K. M., Vock, V. M., Fleming, M. S., Shrestha, A., Grimsley-Myers, C. M., Rasoul, B. A., Neale, S. A., Cupp, T. D., Kinchen, J. M., Liem, K. F., Jr., and Dwyer, N. D. (2013) The vertebrate-specific Kinesin-6, Kif20b, is required for normal cytokinesis of polarized cortical stem cells and cerebral cortex size. *Development* **140**, 4672-4682

24. Sapir, T., Levy, T., Sakakibara, A., Rabinkov, A., Miyata, T., and Reiner, O. (2013) Shootin1 acts in concert with KIF20B to promote polarization of migrating neurons. *J Neurosci* **33**, 11932-11948

25. Sugawara, T., Hisatsune, C., Le, T. D., Hashikawa, T., Hirono, M., Hattori, M., Nagao, S., and Mikoshiba, K. (2013) Type 1 inositol trisphosphate receptor regulates cerebellar circuits by maintaining the spine morphology of purkinje cells in adult mice. *J Neurosci* **33**, 12186-12196

26. Ohfuchi, E., Kato, M., Sasaki, M., Sugimoto, K., Oma, Y., and Harata, M. (2006) Vertebrate Arp6, a novel nuclear actin-related protein, interacts with heterochromatin protein 1. *Eur J Cell Biol* **85**, 411-421

27. Abouhamed, M., Grobe, K., San, I. V., Thelen, S., Honnert, U., Balda, M. S., Matter, K., and Bahler, M. (2009) Myosin IXa regulates epithelial differentiation and its deficiency results in hydrocephalus. *Mol Biol Cell* **20**, 5074-5085

28. Ronjat, M., Kiyonaka, S., Barbado, M., De Waard, M., and Mori, Y. (2013) Nuclear life of the voltage-gated Cacnb4 subunit and its role in gene transcription regulation. *Channels (Austin)* **7**, 119-125

29. Helton, T. D., and Horne, W. A. (2002) Alternative splicing of the beta4 subunit has alpha1 subunit subtype-specific effects on Ca^{2+} channel gating. *Journal of Neuroscience* **22**, 1573-1582

30. Ebert, A. M., McAnelly, C. A., Handschy, A. V., Mueller, R. L., Horne, W. A., and Garrity, D. M. (2008) Genomic organization, expression, and phylogenetic analysis of Ca^{2+} channel beta4 genes in 13 vertebrate species. *Physiol Genomics* **35**, 133-144

31. Marfori, M., Mynott, A., Ellis, J. J., Mehdi, A. M., Saunders, N. F., Curmi, P. M., Forwood, J. K., Boden, M., and Kobe, B. (2011) Molecular basis for specificity of nuclear import and prediction of nuclear localization. *Biochim Biophys Acta* **1813**, 1562-1577

32. Freitas, N., and Cunha, C. (2009) Mechanisms and signals for the nuclear import of proteins. *Curr Genomics* **10**, 550-557

33. Teh, T., Tiganis, T., and Kobe, B. (1999) Crystallization of importin alpha, the nuclear-import receptor. *Acta Crystallogr D Biol Crystallogr* **55**, 561-563

34. Chook, Y. M., and Suel, K. E. (2011) Nuclear import by karyopherin-betas: recognition and inhibition. *Biochim Biophys Acta* **1813**, 1593-1606

35. Fontes, M. R., Teh, T., Jans, D., Brinkworth, R. I., and Kobe, B. (2003) Structural basis for the specificity of bipartite nuclear localization sequence binding by importin-alpha. *J Biol Chem* **278**, 27981-27987

36. Endo, M., Ohashi, K., and Mizuno, K. (2007) LIM kinase and slingshot are critical for neurite extension. *J Biol Chem* **282**, 13692-13702

37. Cha-Molstad, H., Xu, G., Chen, J., Jing, G., Young, M. E., Chatham, J. C., and Shalev, A. (2012) Calcium channel blockers act through nuclear factor Y to control transcription of key cardiac genes. *Mol Pharmacol* **82**, 541-549

38. Francesca Pellicano, R. E. T., Gareth J Inman, and Tomoko Iwata (2010) Regulation of cell proliferation and apoptosis in neuroblastoma cells by ccp1, a FGF2 downstream gene. . *BMC Cancer* **10**, 657

39. Girard, M., Poupon, V., Blondeau, F., and McPherson, P. S. (2005) The DnaJ-domain protein RME-8 functions in endosomal trafficking. *J Biol Chem* **280**, 40135-40143

40. Ballas, N., Battaglioli, E., Atouf, F., Andres, M. E., Chenoweth, J., Anderson, M. E., Burger, C., Moniwa, M., Davie, J. R., Bowers, W. J., Federoff, H. J., Rose, D. W., Rosenfeld, M. G., Brehm, P., and Mandel, G. (2001) Regulation of neuronal traits by a novel transcriptional complex. *Neuron* **31**, 353-365

41. Boutin, C., Goffinet, A. M., and Tissir, F. (2012) Celsr1-3 Cadherins in PCP and Brain Development. in *Planar Cell Polarity During Development* (Yang, Y. ed.). pp 161-183

42. Huang, J., Zhang, L., Liu, W., Liao, Q., Shi, T., Xiao, L., Hu, F., and Qiu, X. (2012) CCDC134 interacts with hADA2a and functions as a regulator of hADA2a in acetyltransferase activity, DNA damage-induced apoptosis and cell cycle arrest. *Histochem Cell Biol* **138**, 41-55

43. Pokrovskaya, I. D., Willett, R., Smith, R. D., Morelle, W., Kudlyk, T., and Lupashin, V. V. (2011) Conserved oligomeric Golgi complex specifically regulates the maintenance of Golgi glycosylation machinery. *Glycobiology* **21**, 1554-1569

44. Zschuentzsch, J., Schuetze, S., Huelsmann, S., Dibaj, P., and Neusch, C. (2013) Heterologous expression of a glial Kir channel (KCNJ10) in a neuroblastoma spinal cord (NSC-34) cell line. *Physiological Research* **62**, 95-105

45. Sann, S., Wang, Z., Brown, H., and Jin, Y. (2009) Roles of endosomal trafficking in neurite outgrowth and guidance. *Trends Cell Biol* **19**, 317-324

46. Pollock, J. D., Krempin, M., and Rudy, B. (1990) Differential effects of NGF, FGF, EGF, cAMP and dexamethasone on neurite outgrowth and sodium channel expression in PC12 cells. *Journal of Neuroscience* **10**, 2626-2637

47. Ji, S., Kang, J. G., Park, S. Y., Lee, J., Oh, Y. J., and Cho, J. W. (2011) O-GlcNAcylation of tubulin inhibits its polymerization. *Amino Acids* **40**, 809-818

48. Dekkers, M. P., Nikoletopoulou, V., and Barde, Y. A. (2013) Cell biology in neuroscience: Death of developing neurons: new insights and implications for connectivity. *J Cell Biol* **203**, 385-393

49. Desir, J., Coppieters, F., Van Regemorter, N., De Baere, E., Abramowicz, M., and Cordonnier, M. (2012) TMEM126A mutation in a Moroccan family with autosomal recessive optic atrophy. *Mol Vis* **18**, 1849-1857

50. Foo, J. N., Liany, H., Tan, L. C., Au, W. L., Prakash, K. M., Liu, J., and Tan, E. K. (2014) DNAJ mutations are rare in Chinese Parkinson's disease patients and controls. *Neurobiol Aging* **35**, 935 e931-932

51. Matalon D, G. E., Medne L, Marsh ED (2014) Confirming an expanded spectrum of SCN2A mutations: a case series. *Epileptic Disord* **Mar 21**, Epub ahead of print

52. Heuser, K., Eid, T., Lauritzen, F., Thoren, A. E., Vindedal, G. F., Tauboll, E., Gjerstad, L., Spencer, D. D., Ottersen, O. P., Nagelhus, E. A., and de Lanerolle, N. C. (2012) Loss of perivascular Kir4.1 potassium channels in the sclerotic hippocampus of patients with mesial temporal lobe epilepsy. *J Neuropathol Exp Neurol* **71**, 814-825

53. Huang, L., Chardon, J. W., Carter, M. T., Friend, K. L., Dudding, T. E., Schwartzentruber, J., Zou, R., Schofield, P. W., Douglas, S., Bulman, D. E., and Boycott, K. M. (2012) Missense mutations in ITPR1 cause autosomal dominant congenital nonprogressive spinocerebellar ataxia. *Orphanet J Rare Dis* **7**, 67

54. Boehm, C., Seibel, N. M., Henkel, B., Steiner, H., Haass, C., and Hampe, W. (2006) SorLA signaling by regulated intramembrane proteolysis. *Journal of Biological Chemistry* **281**, 14547-14553

55. Irizarry RA, H. B., Collin F, Beazer-Barclay YD, Antonellis KJ, Scherf U, Speed TP. (2003) Exploration, normalization, and summaries of high density oligonucleotide array probe level data. *Biostatistics* **4**, 249–264

56. Benjamini Y, H. Y. (1995) Controlling the false discovery rate: a practical and powerful approach to multiple testing. *J Royal Stat Soc B Met* **57**, 289-300

57. Livak, K. J., and Schmittgen, T. D. (2001) Analysis of relative gene expression data using real-time quantitative PCR and the 2(-Delta Delta C(T)) Method. *Methods* **25**, 402-408

CHAPTER 4

Conclusions and future directions

The β subunits of voltage-gated Ca^{2+} channels are thought to be engaged in the regulation of trafficking and gating of the channels (1-5). Apart from this traditional Ca^{2+} channel dependent function; a stream of recent studies focus on Ca^{2+} channel independent functions. In particular, it has been discovered that some isoforms of the β4 subunit are targeted into the nucleus where they act as transcriptional regulators. Our results add to this growing story of a newly discovered role for β4 subunits in the nuclei of excitable cells. In this thesis, I set out to expand upon our understanding of how the β4c subunit enters the nucleus and to determine the functional consequences of this newly discovered phenomenon.

In the first study presented in Chapter 2, we identified and cloned the mammalian β4c subunit from human brain. We also showed that β4c is expressed in vestibular, cochlear and deep cerebellar nuclei in the mouse brain. The β4c subunit consists of the β4a N-terminus, the SH3 domain and HOOK sequence, a truncated GK domain, and additional C-terminal sequence (DFNNESDS) resulting from the frame shift. This splicing mechanism has been conserved in birds (6); however, the avian sequence has two amino acid substitutions and is four residues longer (DINNPSDSHSFC).

Alternative splicing of pre-mRNAs in higher eukaryotes is one major source of protein diversity. Usually, the following major subtypes of alternative splicing are distinguished: exon skipping, intron retention, and alternative 3' and 5' splice sites. Among these, β4c is generated by an exon skipping event (7,8). Amplification of molecular diversity by alternative splicing is critical for normal neuronal development, neuronal excitability, axon targeting, and neuronal

circuit formation (9,10). Mammalian Ca^{2+} channel β subunits are encoded by only four genes; however, multiple isoforms are expressed in different cells. Alternative splicing results in heterogeneity in β subunit structure, subcellular localization, and changes in the electrophysiological properties of voltage-gated Ca^{2+} channels. The overall result is an increase in the molecular diversity and functionality of HVA Ca^{2+} channels. In the case of the β4 subunit, our lab previously determined that β4a and β4b were expressed differentially in adult mouse cerebellum (11). We have expanded on this to show that β4c is expressed in specific nuclei. Moreover, β4 expression varies with the development stage of the brain (12). Unfortunately, there is no information on spatial and temporal expression of individual β4 splice variants (β4a, β4b and β4c) in the developing and adult brain. Determining the spatiotemporal profile of the β4 subunits is important to fully understand the specific role of each isoform in the neuron. We developed an antibody which recognizes the N-terminus of β4 subunit, and thus can differentiate β4a and β4b (11); however, we need to generate an antibody that can specifically recognize the C-terminal sequence of endogenous β4c to immunohistochemically differentiate β4a and β4c in the brain.

After cloning of human β4c, we demonstrated that β4c interacts with the chromo shadow domain (CSD) dimer of HP1γ via its C-terminal PVVLV motif, located at residues 187-191. Double mutant, β4c P187A/V189A does not bind to CSD *in vitro*, therefore position 1, proline, and position 3, valine are critical for β4c binding to HP1γ. However, it needs to be verified whether the β4c double mutant interacts with HP1γ or not in vivo by performing co-immunoprecipitation experiment. We also confirmed that β4c does not promote the trafficking or affect the gating properties of $Ca_v2.1$ channels. Considering that the β4c lacks more than 90% of the GK domain that interacts with the α1 subunit (2,4,13-15), it is not surprising that there is

little evidence that β4c directly affects Ca^{2+} channel function.

In the subsequent study, we characterized the molecular determinants of β4c nuclear targeting in Neuro2a cells. Optimal nuclear targeting of β4c is dependent on two specific sequence motifs. The first is identical to a classical monopartite nuclear localization sequence (16,17), K(K/R)X(K/R), and the second is a previously unidentified C-terminal sequence that is generated by alternative splicing. In the traditional nuclear protein import pathway, a classical nuclear localization sequence (cNLS) (18) is first recognized by the adaptor protein importin α (Impα), which in turn binds importin β through an N-terminal importin β binding (IBB) domain (19). Impα is built by a repeated helical motif, known as Armadillo (ARM), which consists of three α-helices. ARMs stack together to form a helical core (20), which harbors two binding sites for NLSs, a major site, between ARM repeats 1-4, and a minor site, between ARM 7-8. Classical monopartite NLSs primarily bind the major site, although a partially occupied NLS peptide is also seen at the minor binding site (18,21). As pointed out in Chapter 3, the ^{133}KRGR^{136} motif exists in both β4a and β4c, therefore we hypothesize that the GK domain in the β4a might impede the binding of Impα to β4a. To examine this possibility and to determine the role of ^{133}KRGR^{136} motif in detail, further binding and structural studies are needed. Moreover, many questions still remain to be answered about how the C-terminal sequence contributes to nuclear targeting. We suspect that β4c C-terminus binds to another protein that is involved in its nuclear targeting, or to previously unidentified site on Impα. Also, the C-terminus might intensify the retention of β4c in the nucleus instead of playing a role in transport of β4c to the nucleus.

Recently, several groups investigated nuclear localization of full-length β4 subunits. Interestingly, the nuclear entry of full-length β4b is regulated by electric activity of the neuronal cells. However, there is controversy whether electrical activity is required for β4b nuclear

targeting or not. Tadmouri el al. claimed that electric activity prompted β4b nuclear transport, so β4b nuclear translocalization increases with more days in vitro (DIV) of hippocampal neuronal cell culture (22). On the other hand, one report claimed that spontaneous electrical activity and calcium influx negatively regulated β4b nuclear localization by an export protein mediated nuclear export mechanism (23). Another report also showed that β4b nuclear targeting was limited to young and electrically silent hippocampal cultures (24).

Considering that β4c lacks the GK domain responsible for coupling the β subunit to voltage-dependent channel activity, it is expected that β4c can enter the nucleus without being induced by electrical activity. However, there is still the possibility that differentiation of the cells might influence nuclear targeting of β4c. In the future, we need to examine the nuclear localization of β4c in differentiated Neuro2a cells and compare this result with the nuclear localization in undifferentiated cells to verify this hypothesis.

In accordance with the several studies demonstrating that nuclear targeting of β4 subunit having a direct function in gene regulation (6,22,24,25), ectopically expressed β4c was shown to regulate gene expression in Neuro2a cells. Our transcriptome profile confirms that β4c does not regulate Ca^{2+} channel related genes, which we confirmed in the qRT-PCR study. Combining the electrophysiological study in Chapter 2, this result demonstrates that β4c serves exclusively in gene regulation, which is Ca^{2+} channel independent, whereas β4b plays a dual role in Ca^{2+} channel modulation and gene regulation (22,24,25). Interestingly, two ion channel genes are regulated by nuclear β4c subunit: *Scn2a1*, encoding a voltage-gated sodium channel Na(v)1.2, and *Kcnj10*, encoding a inwardly rectifying potassium channel Kir4.1. Mutations in these genes have been linked to ataxia and epilepsy in mice and human (26,27). Na(v)1.2 is responsible for sodium current in brain; therefore, mutations in the gene cause hyperexcitability

of the cells and lead to the development of epilepsy (28-31). One study reports that a patient with neonatal-onset seizure and late-onset myoclonia, ataxia, and pain carries a missense mutation in SCN2A gene (32). Another report demonstrated that a mutation in Scn2a gene results in hyperexitability in hippocampal neurons (33). Alterations of the Kir4.1 channel have been linked to seizure susceptibility in both mice (34) and humans (35). The Kir4.1 channel controls the resting membrane potential of astrocytes, and is believed to maintain the extracellular ionic environment. A detailed electrophysiology study is required to determine that β4c gene regulation affects cell excitability.

Based on the GO analysis, the regulated genes by β4c overexpression is significantly related to intermediate filament and cytoskeleton formation. Consistent with these functions, there are up-regulated genes that are involved in microtubule and actin filament formation (*Tubb2a*) (36,37), and neuronal polarization (*Kif20b*) (38,39). And also, genes that are involved in anti-apoptotic effects (*Nfyc* (40) and *Ccdc 115* (41)) and endosomal trafficking (Dnajc13, (42)) are up-regulated. On the other hand, down-regulated genes are involved in contact-mediated cell-cell communication (*Celsr2* (43)), pro-apoptotic effects (Ccdc134 (44)), maintenance of Golgi glycosylation (Cog8 (45)). Microtubule formation and endosomal trafficking have shown to support neurite outgrowth (46), however protein glycosylation and growth factor induced apoptosis have been shown to have inhibitory effects on neurite outgrowth (47,48). Taken together, the functional analysis implies that the β4c C-terminus might regulate gene expression for the cells to prepare for neurite outgrowth. Neurite outgrowth is a key process during neuronal migration and differentiation. Complex intracellular signaling is involved in the initiation of neurite protrusion and subsequent elongation (49). Many signaling molecules have been identified to be involved in neurite outgrowth, from membrane receptors to cytoskeleton

constituents (50). Therefore, some neurotrophic factors are needed to initiate the neurite outgrowth in Neuro2a cells. Expression profiling study using differentiated Neuro2a cells could provide more information about the effect of β4c on the neurite outgrowth.

Neurite outgrowth is an important step in the sequential stages of neural development (51). Among the four β subunits, β4 protein shows the most dramatic increase in expression during newborn to adult, in which extensive neuronal development occurs (52). Still, there is no information on β4c expression level change according to different stages of development. It is only known that β4c is specifically expressed in medial vestibular nuclei in a mouse brain (53). It might possible that β4c nuclear function potentially involving neurite outgrowth regulates the neuronal development in vestibular neurons. This regulation might affect several vestibular functions including vestibular-ocular reflex and long term vestibular ocular memory.

As mentioned in Chapter1, mutated β4 was reported in *lethargic* mice, which have a neurological pheynotype characterized by ataxia, seizure, and epilepsy (54,55). The underlying mechanism of how a dysfunctional β4 subunit causes these phenotypes still remains unknown. Recent β4 subunit nuclear gene regulation studies try to explain this. One group suggested a signaling pathway related to β4b and thyrosine hydroxylase (TH) gene (22), whereas others claimed that the lethargic phenotype might result from altered Ca^{2+} channel function rather than from nuclear function of β4b (24,56,57). Even though β4c does not mediate Ca^{2+} channel dependent function, there is still the possibility that the abnormal nuclear function of β4c may contribute to the lethargic phenotype. Expression profiling experiments using primary cerebellar granular cells from *lethargic* mice reconstituted with β4c could give us more information about β4c nuclear function.

In conclusion, a number of recent studies have greatly expanded our understanding of the

biochemical, structural, and functional activities of the Ca^{2+} channel β subunit which was mostly recognized for its Ca^{2+} channel dependent activity. With our latest results, β4 subunit is now appreciated as a nuclear protein that is involved in transcriptional regulation. During the course of this thesis work, I characterized a short splice variant of the β4 subunit from human pons, and uncovered the molecular determinants of its nuclear targeting. Hopefully, these insights will open up new areas of research involving the Ca^{2+} channel β subunit, and enhance our understanding of the specific nuclear role of the β4c subunit in regulating neuronal growth. .

REFERENCES

1. Buraei, Z., and Yang, J. (2010) The β subunit of voltage-gated Ca^{2+} channels. *Physiol Rev* **90**, 1461-1506

2. Buraei, Z., and Yang, J. (2013) Structure and function of the beta subunit of voltage-gated Ca^{2+} channels. *Biochim Biophys Acta* **1828**, 1530-1540

3. Dolphin, A. C. (2003) Beta subunits of voltage-gated calcium channels. *J Bioenerg Biomembr* **35**, 599-620

4. Dolphin, A. C. (2012) Calcium channel auxiliary alpha2delta and beta subunits: trafficking and one step beyond. *Nat Rev Neurosci* **13**, 542-555

5. Catterall, W. A. (2011) Voltage-gated calcium channels. *Cold Spring Harb Perspect Biol* **3**, a003947

6. Hibino, H., Pironkova, R., Onwumere, O., Rousset, M., Charnet, P., Hudspeth, A. J., and Lesage, F. (2003) Direct interaction with a nuclear protein and regulation of gene silencing by a variant of the Ca^{2+} channel beta 4 subunit. *Proc Natl Acad Sci U S A* **100**, 307-312

7. Allen, S. E., Darnell, R. B., and Lipscombe, D. (2010) The neuronal splicing factor Nova controls alternative splicing in N-type and P-type Ca(V)2 calcium channels. *Channels* **4**, 483-489

8. Zheng, S., and Black, D. L. (2013) Alternative pre-mRNA splicing in neurons: growing up and extending its reach. *Trends Genet* **29**, 442-448

9. Keren, H., Lev-Maor, G., and Ast, G. (2010) Alternative splicing and evolution: diversification, exon definition and function. *Nat Rev Genet* **11**, 345-355

10. Lipscombe, D., Andrade, A., and Allen, S. E. (2013) Alternative splicing: functional diversity among voltage-gated calcium channels and behavioral consequences. *Biochim Biophys Acta* **1828**, 1522-1529

11. Vendel, A. C., Terry, M. D., Striegel, A. R., Iverson, N. M., Leuranguer, V., Rithner, C. D., Lyons, B. A., Pickard, G. E., Tobet, S. A., and Horne, W. A. (2006) Alternative splicing of the voltage-gated Ca^{2+} channel beta4 subunit creates a uniquely folded N-terminal protein binding domain with cell-specific expression in the cerebellar cortex. *J Neurosci* **26**, 2635-2644

12. Ferrandiz-Huertas, C., Gil-Minguez, M., and Lujan, R. (2012) Regional expression and subcellular localization of the voltage-gated calcium channel beta subunits in the developing mouse brain. *J Neurochem* **122**, 1095-1107

13. Chen, Y. H., Li, M. H., Zhang, Y., He, L. L., Yamada, Y., Fitzmaurice, A., Shen, Y., Zhang, H., Tong, L., and Yang, J. (2004) Structural basis of the alpha1-beta subunit interaction of voltage-gated Ca^{2+} channels. *Nature* **429**, 675-680

14. Opatowsky, Y., Chen, C. C., Campbell, K. P., and Hirsch, J. A. (2004) Structural analysis of the voltage-dependent calcium channel beta subunit functional core and its complex with the alpha 1 interaction domain. *Neuron* **42**, 387-399

15. Van Petegem, F., Clark, K. A., Chatelain, F. C., and Minor, D. L., Jr. (2004) Structure of a complex between a voltage-gated calcium channel beta-subunit and an alpha-subunit domain. *Nature* **429**, 671-675

16. Lange, A., Mills, R. E., Lange, C. J., Stewart, M., Devine, S. E., and Corbett, A. H. (2007) Classical nuclear localization signals: definition, function, and interaction with importin alpha. *J Biol Chem* **282**, 5101-5105

17. Xu, D., Farmer, A., and Chook, Y. M. (2010) Recognition of nuclear targeting signals by Karyopherin-beta proteins. *Curr Opin Struct Biol* **20**, 782-790

18. Marfori, M., Mynott, A., Ellis, J. J., Mehdi, A. M., Saunders, N. F., Curmi, P. M., Forwood, J. K., Boden, M., and Kobe, B. (2011) Molecular basis for specificity of nuclear import and prediction of nuclear localization. *Biochim Biophys Acta* **1813**, 1562-1577

19. Lott, K., and Cingolani, G. (2011) The importin beta binding domain as a master regulator of nucleocytoplasmic transport. *Biochimica et Biophysica Acta* **1813**, 1578-1592

20. Lott, K., Bhardwaj, A., Sims, P. J., and Cingolani, G. (2011) A minimal nuclear localization signal (NLS) in human phospholipid scramblase 4 that binds only the minor NLS-binding site of importin alpha1. *J Biol Chem* **286**, 28160-28169

21. Freitas, N., and Cunha, C. (2009) Mechanisms and signals for the nuclear import of proteins. *Curr Genomics* **10**, 550-557

22. Tadmouri, A., Kiyonaka, S., Barbado, M., Rousset, M., Fablet, K., Sawamura, S., Bahembera, E., Pernet-Gallay, K., Arnoult, C., Miki, T., Sadoul, K., Gory-Faure, S., Lambrecht, C., Lesage, F., Akiyama, S., Khochbin, S., Baulande, S., Janssens, V., Andrieux, A., Dolmetsch, R., Ronjat, M., Mori, Y., and De Waard, M. (2012) Cacnb4 directly couples electrical activity to gene expression, a process defective in juvenile epilepsy. *EMBO J* **31**, 3730-3744

23. Subramanyam, P., Obermair, G. J., Baumgartner, S., Gebhart, M., Striessnig, J., Kaufmann, W. A., Geley, S., and Flucher, B. E. (2009) Activity and calcium regulate nuclear targeting of the calcium channel beta4b subunit in nerve and muscle cells. *Channels* **3**, 343-355

24. Etemad, S., Obermair, G. J., Bindreither, D., Benedetti, A., Stanika, R., Di Biase, V., Burtscher, V., Koschak, A., Kofler, R., Geley, S., Wille, A., Lusser, A., Flockerzi, V., and Flucher, B. E. (2014) Differential neuronal targeting of a new and two known calcium channel beta4 subunit splice variants correlates with their regulation of gene expression. *J Neurosci* **34**, 1446-1461

25. Ronjat, M., Kiyonaka, S., Barbado, M., De Waard, M., and Mori, Y. (2013) Nuclear life of the voltage-gated Cacnb4 subunit and its role in gene transcription regulation. *Channels (Austin)* **7**, 119-125

26. Meisler, M. H., and Kearney, J. A. (2005) Sodium channel mutations in epilepsy and other neurological disorders. *J Clin Invest* **115**, 2010-2017

27. Hawkins, N. A., Martin, M. S., Frankel, W. N., Kearney, J. A., and Escayg, A. (2011) Neuronal voltage-gated ion channels are genetic modifiers of generalized epilepsy with febrile seizures plus. *Neurobiol Dis* **41**, 655-660

28. Catterall, W. A., Goldin, A. L., and Waxman, S. G. (2005) International Union of Pharmacology. XLVII. Nomenclature and structure-function relationships of voltage-gated sodium channels. *Pharmacol Rev* **57**, 397-409

29. Eijkelkamp, N., Linley, J. E., Baker, M. D., Minett, M. S., Cregg, R., Werdehausen, R., Rugiero, F., and Wood, J. N. (2012) Neurological perspectives on voltage-gated sodium channels. *Brain* **135**, 2585-2612

30. Bay, V., and Butt, A. M. (2012) Relationship between glial potassium regulation and axon excitability: a role for glial Kir4.1 channels. *Glia* **60**, 651-660

31. Udagawa, T., Tatsumi, N., Tachibana, T., Negishi, Y., Saijo, H., Kobayashi, T., Yaguchi, Y., Kojima, H., Moriyama, H., and Okabe, M. (2012) Inwardly rectifying potassium channel Kir4.1 is localized at the calyx endings of vestibular afferents. *Neuroscience* **215**, 209-216

32. Liao, Y., Anttonen, A. K., Liukkonen, E., Gaily, E., Maljevic, S., Schubert, S., Bellan-Koch, A., Petrou, S., Ahonen, V. E., Lerche, H., and Lehesjoki, A. E. (2010) SCN2A mutation associated with neonatal epilepsy, late-onset episodic ataxia, myoclonus, and pain. *Neurology* **75**, 1454-1458

33. Kile, K. B., Tian, N., and Durand, D. M. (2008) Scn2a sodium channel mutation results in hyperexcitability in the hippocampus in vitro. *Epilepsia* **49**, 488-499

34. Ferraro, T. N., Golden, G. T., Smith, G. G., Martin, J. F., Lohoff, F. W., Gieringer, T. A., Zamboni, D., Schwebel, C. L., Press, D. M., Kratzer, S. O., Zhao, H. Y., Berrettini, W. H., and Buono, R. J. (2004) Fine mapping of a seizure susceptibility locus on mouse Chromosome 1: nomination of Kcnj10 as a causative gene. *Mammalian Genome* **15**, 239-251

35. Buono, R. J., Lohoff, F. W., Sander, T., Sperling, M. R., O'Connor, M. J., Dlugos, D. J., Ryan, S. G., Golden, G. T., Zhao, H., Scattergood, T. M., Berrettini, W. H., and Ferraro, T. N. (2004) Association between variation in the human KCNJ10 potassium ion channel gene and seizure susceptibility. *Epilepsy Research* **58**, 175-183

36. Conde, C., and Caceres, A. (2009) Microtubule assembly, organization and dynamics in axons and dendrites. *Nat Rev Neurosci* **10**, 319-332

37. Niwa, S., Takahashi, H., and Hirokawa, N. (2013) Beta-tubulin mutations that cause severe neuropathies disrupt axonal transport. *EMBO J* **32**, 1352-1364

38. Janisch, K. M., Vock, V. M., Fleming, M. S., Shrestha, A., Grimsley-Myers, C. M., Rasoul, B. A., Neale, S. A., Cupp, T. D., Kinchen, J. M., Liem, K. F., Jr., and Dwyer, N. D. (2013) The vertebrate-specific Kinesin-6, Kif20b, is required for normal cytokinesis of polarized cortical stem cells and cerebral cortex size. *Development* **140**, 4672-4682

39. Sapir, T., Levy, T., Sakakibara, A., Rabinkov, A., Miyata, T., and Reiner, O. (2013) Shootin1 acts in concert with KIF20B to promote polarization of migrating neurons. *J Neurosci* **33**, 11932-11948

40. Cha-Molstad, H., Xu, G., Chen, J., Jing, G., Young, M. E., Chatham, J. C., and Shalev, A. (2012) Calcium channel blockers act through nuclear factor Y to control transcription of key cardiac genes. *Mol Pharmacol* **82**, 541-549

41. Francesca Pellicano, R. E. T., Gareth J Inman, and Tomoko Iwata (2010) Regulation of cell proliferation and apoptosis in neuroblastoma cells by ccp1, a FGF2 downstream gene. . *BMC Cancer* **10**, 657

42. Girard, M., Poupon, V., Blondeau, F., and McPherson, P. S. (2005) The DnaJ-domain protein RME-8 functions in endosomal trafficking. *J Biol Chem* **280**, 40135-40143

43. Boutin, C., Goffinet, A. M., and Tissir, F. (2012) Celsr1-3 Cadherins in PCP and Brain Development. in *Planar Cell Polarity During Development* (Yang, Y. ed.). pp 161-183

44. Huang, J., Zhang, L., Liu, W., Liao, Q., Shi, T., Xiao, L., Hu, F., and Qiu, X. (2012) CCDC134 interacts with hADA2a and functions as a regulator of hADA2a in acetyltransferase activity, DNA damage-induced apoptosis and cell cycle arrest. *Histochem Cell Biol* **138**, 41-55

45. Pokrovskaya, I. D., Willett, R., Smith, R. D., Morelle, W., Kudlyk, T., and Lupashin, V. V. (2011) Conserved oligomeric Golgi complex specifically regulates the maintenance of Golgi glycosylation machinery. *Glycobiology* **21**, 1554-1569

46. Sann, S., Wang, Z., Brown, H., and Jin, Y. (2009) Roles of endosomal trafficking in neurite outgrowth and guidance. *Trends Cell Biol* **19**, 317-324

47. Ji, S., Kang, J. G., Park, S. Y., Lee, J., Oh, Y. J., and Cho, J. W. (2011) O-GlcNAcylation of tubulin inhibits its polymerization. *Amino Acids* **40**, 809-818

48. Dekkers, M. P., Nikoletopoulou, V., and Barde, Y. A. (2013) Cell biology in neuroscience: Death of developing neurons: new insights and implications for connectivity. *J Cell Biol* **203**, 385-393

49. Khodosevich, K., and Monyer, H. (2010) Signaling involved in neurite outgrowth of postnatally born subventricular zone neurons in vitro. *BMC Neurosci* **11**, 18

50. Mattila, P. K., and Lappalainen, P. (2008) Filopodia: molecular architecture and cellular functions. *Nat Rev Mol Cell Biol* **9**, 446-454

51. Valtorta, F., Pozzi, D., Benfenati, F., and Fornasiero, E. F. (2011) The synapsins: multitask modulators of neuronal development. *Semin Cell Dev Biol* **22**, 378-386

52. Vance, C. L., Begg, C. M., Lee, W. L., Haase, H., Copeland, T. D., and McEnery, M. W. (1998) Differential expression and association of calcium channel alpha(1B) and beta subunits during rat brain ontogeny. *Journal of Biological Chemistry* **273**, 14495-14502

53. Xu, X., Lee, Y. J., Holm, J. B., Terry, M. D., Oswald, R. E., and Horne, W. A. (2011) The Ca^{2+} channel beta4c subunit interacts with heterochromatin protein 1 via a PXVXL binding motif. *J Biol Chem* **286**, 9677-9687

54. Burgess, D. L., Jones, J. M., Meisler, M. H., and Noebels, J. L. (1997) Mutation of the Ca^{2+} channel β subunit gene cchb4 is associated with ataxia and seizures in the lethargic (lh) mouse. *Cell* **88**, 385-392

55. Hosford, D. A., Lin, F. H., Wang, Y., Caddick, S. J., Rees, M., Parkinson, N. J., Barclay, J., Cox, R. D., Gardiner, R. M., Hosford, D. A., Denton, P., Wang, Y., Seldin, M. F., and Chen, B. (1999) Studies of the lethargic (lh/lh) mouse model of absence seizures: regulatory mechanisms and identification of the lh gene. *Adv Neurol* **79**, 239-252

56. McEnery, M. W., Copeland, T. D., and Vance, C. L. (1998) Altered expression and assembly of N-type calcium channel alpha1B and beta subunits in epileptic lethargic (lh/lh) mouse. *J Biol Chem* **273**, 21435-21438

57. McEnery, M. W., Vance, C. L., Begg, C. M., Lee, W. L., Choi, Y., and Dubel, S. J. (1998) Differential expression and association of calcium channel subunits in development and disease. *J Bioenerg Biomembr* **30**, 409-418

APPENDIX 1

List of genes up-regulated by expression of β4c (p-value <0.1, fold change >1.4)

Transcripts Cluster Id	p	Fold Change	Gene description	Gene symbol	Refseq
10537909	0.09	1.80	RNA, Y3 small cytoplasmic (associated with Ro protein)	Rny3	NR_024202
10423503	0.02	1.79	predicted gene 6624	Gm6624	XM_890363
10353783	0.00	1.74	coiled-coil domain containing 115	Ccdc115	NM_027159
10563108	0.08	1.74	small nucleolar RNA, C/D box 35A	Snord35a	NR_000003
10515974	0.00	1.74	nuclear transcription factor-Y gamma	Nfyc	NM_008692 |NM_001048168
10490061	0.00	1.64	breast carcinoma amplified sequence 1	Bcas1	NM_029815
10371830	0.01	1.64	ARP6 actin-related protein 6 homolog (yeast)	Actr6	NM_025914
10585976	0.02	1.62	myosin IXa	Myo9a	NM_173018
10414576	0.01	1.61	predicted gene 5622	Gm5622	NM_001013816
10595909	0.01	1.61			
10408610	0.00	1.60	tubulin, beta 2A	Tubb2a	NM_009450
10565570	0.05	1.59	RIKEN cDNA 4632434I11 gene	4632434I11Rik	XM_006508245
10552433	0.00	1.57	zinc finger protein 658	Zfp658	NM_001008549
10596279	0.00	1.55	DnaJ (Hsp40) homolog, subfamily C, member 13	Dnajc13	NM_001163026
10526120	0.05	1.53	protein-tyrosine sulfotransferase 1	Tpst1	NM_001130476|NM_013837
10472372	0.04	1.48	sodium channel, voltage-gated, type II, alpha 1	Scn2a1	NM_001099298
10410362	0.07	1.48	RIKEN cDNA 6720487G11 gene | zinc finger protein 712	6720487G11Rik|Zfp712	NM_001008549
10499130	0.06	1.48	U73B small nuclear RNA	Rnu73b	NR_004418
10565570	0.00	1.48	RIKEN cDNA 4632434I11 gene	4632434I11Rik	NM_001080995
10362428	0.00	1.48	triadin	Trdn	NM_029726
10376320	0.03	1.48	mitochondrial ribosomal protein L22	Mrpl22	NM_175001
10456717	0.04	1.48	small nucleolar RNA, C/D box	Snord58b	NR_028552.

			58B		1
10606376	0.01	1.47	RIKEN cDNA 2610002M06 gene	2610002 M06Rik	NM_025921
10494369	0.02	1.47	splicing factor 3b, subunit 4	Sf3b4	NM_153053
10461909	0.08	1.47		BC016495	
10599673	0.01	1.47	RIKEN cDNA 4930527E24 gene	4930527E 24Rik	NM_029181 .1
10518366	0.01	1.47	RIKEN cDNA 2810408P10 gene	2810408P 10Rik	NM_198619
10565519	0.07	1.47	transmembrane protein 126B	Tmem126 b	NM_026734
10497285	0.02	1.46	inositol (myo)-1(or 4)-monophosphatase 1	Impa1	NM_018864
10462632	0.00	1.46	kinesin family member 20B	kif20b	NM_183046
10491952	0.01	1.46	microsomal glutathione S-transferase 2	Mgst2	NM_174995
10408870	0.03	1.45	TBC1 domain family, member 7	Tbc1d7	NM_025935
10378855	0.01	1.45	slingshot homolog 2 (Drosophila)	Ssh2	NM_001291 190.1
10514219	0.00	1.45	small Cajal body-specific RNA 8	Scarna8	NC_000070. 6
10560043	0.01	1.44	zinc finger protein 329	Zfp329	NM_026046
10445147	0.00	1.44	olfactory receptor 119	Olfr119	NM_001011 830
10557231	0.04	1.44	predicted gene 6905	Gm6905	XR_034502
10439881	0.05	1.44	RIKEN cDNA 5330426P16 gene	5330426P 16Rik	NR_028300. 1
10384483	0.01	1.44			
10406270	0.02	1.42	glutaredoxin	Glrx	NM_053108
10565514	0.01	1.42	transmembrane protein 126A	Tmem126 a	NM_025460
10489041	0.04	1.41	programmed cell death 10	Pdcd10	NM_019745
10545210	0.03	1.41	predicted gene 1524	Gm1524	NC_000072. 6

APPENDIX 2

List of genes down-regulated by expression of β4c (p-value <0.1, fold change >-1.4)

Transcripts Cluster Id	p	Fold Change	Gene description	Gene symbol	refseq
10369479	0.02	-1.41	leucine rich repeat containing 20 | RIKEN cDNA D830039M14 gene	Lrrc20| D830039M14Rik	NR_028300.1
10514791	0.02	-1.43	proprotein convertase subtilisin/kexin type 9	Pcsk9	NM_153565
10558653	0.01	-1.44	olfactory receptor 538 | olfactory receptor 46 | olfactory receptor GA_x5J8B7TT63N-1148-873	Olfr538| Olfr46|GA_x5J8B7TT63N-1148-873	NM_001011867|NM_146934|NM_146954
10390907	0.01	-1.44	keratin associated protein 1-3	Krtap1-3	NM_001085526
10398100	0.01	-1.44	T-cell leukemia/lymphoma 1B, 5 | similar to T-cell leukemia protein Tcl1b5	Tcl1b5| LOC100041466	NM_013776.1
10572271	0.03	-1.44	transmembrane 6 superfamily member 2	Tm6sf2	NM_181540
10480649	0.01	-1.45	RIKEN cDNA 2310002J15 gene	2310002J15Rik	NM_026415.3
10534428	0.00	-1.45	FK506 binding protein 6	Fkbp6	NM_001277891.1
10569356	0.01	-1.45	microRNA 483	Mir483	NR_030251.1
10575142	0.01	-1.48	component of oligomeric golgi complex 8 | predicted gene 10627	Cog8|Gm10627	NM_139229
10575976	0.00	-1.49	cysteine-rich secretory protein LCCL domain containing 2	Crispld2	NM_030209
10425686	0.00	-1.49	coiled-coil domain containing 134	Ccdc134	NM_172428
10474269	0.02	-1.50	predicted gene 6306	Gm6306	XM_006500499.1
10425223	0.01	-1.50	galanin receptor 3 | glycine C-acetyltransferase (2-amino-3-ketobutyrate-coenzyme A ligase)	Galr3|Gcat	NM_015738|NM_001161712
10428002	0.01	-1.50	ankyrin repeat domain 33B	Ankrd33b	NM_001164441.1
10469081	0.00	-1.51	predicted gene 10859	Gm10859	
10453602	0.07	-1.52	predicted gene 2889 | hypothetical	Gm2889	XR_032134|

			protein LOC100047557 | hypothetical protein LOC100045342 | hypothetical protein LOC100044384 | hypothetical protein LOC100044795	|LOC100047557|LOC100045342|LOC100044384|LOC100044795	XM_001478429|XR_030763|XR_030628|XM_001473515|XR_034671
10521811	0.01	-1.52			
10408249	0.03	-1.53			
10578042	0.00	-1.53	predicted gene 5117	Gm5117	XM_282816
10450772	0.01	-1.54	histocompatibility 2, M region locus 10.3	H2-M10.3	NM_201608
10598216	0.06	-1.54			
10538352	0.01	-1.54			
10536052	0.04	-1.54	predicted gene 7682 | similar to D5Ertd577e protein	Gm7682|LOC624931	
10490852	0.08	-1.54			
10427742	0.07	-1.55	glyceraldehyde-3-phosphate dehydrogenase pseudogene	Gm8174	XR_001896
10484733	0.07	-1.55	olfactory receptor 1174	Olfr1174	XM_621554
10402606	0.06	-1.55	retrotransposon-like 1 | RIKEN cDNA 6430411K18 gene	Rtl1|6430411K18Rik	NM_184109|NR_002848
10430899	0.05	-1.56	cytochrome P450, family 2, subfamily d, polypeptide 40	Cyp2d40	NM_023623
10510260	0.01	-1.57	natriuretic peptide precursor type B	Nppb	NM_008726
10450431	0.05	-1.57	lymphocyte antigen 6 complex, locus G5B	Ly6g5b	NM_148939
10501319	0.00	-1.57	cadherin, EGF LAG seven-pass G-type receptor 2 (flamingo homolog, Drosophila)	Celsr2	NM_017392|NM_001004177
10590212	0.00	-1.57	tetratricopeptide repeat domain 21A	Ttc21a	NM_028735
10526229	0.01	-1.57	predicted gene 10369	Gm10369	
10427468	0.09	-1.57			
10603005	0.05	-1.58	similar to thyroid hormone receptor associated protein 3	LOC676160	XR_033102
10496862	0.04	-1.58			
10348713	0.01	-1.58	RIKEN cDNA E030010N08 gene	E030010N08Rik	XM_001474855
10602722	0.01	-1.58	spindlin family, member 2	Spin2	NM_001005370

10603247	0.07	-1.58			XR_032134|XR_030763
10364328	0.03	-1.58	predicted gene 10318 | keratin associated protein 10-10 | keratin associated protein 10-4 | predicted gene 3285 | predicted gene 3238 | similar to A030009A09Rik protein	Gm10318|Krtap10-10|Krtap10-4|Gm3285|Gm3238|LOC100046352	NM_001162944|NM_001024709|NM_001135991|NM_001101631|NM_001101630|XM_001477350
10440134	0.05	-1.58	olfactory receptor 172	Olfr172	NM_147001
10507473	0.01	-1.58			
10351781	0.00	-1.59	potassium inwardly-rectifying channel, subfamily J, member 10	Kcnj10	NM_001039484
10464110	0.01	-1.59	RIKEN cDNA D730002M21 gene	D730002M21Rik	
10426081	0.00	-1.69	family with sequence similarity 19, member A5	Fam19a5	NM_134096
10473584	0.00	-1.69			
10598073	0.02	-1.69			NC_005089
10598075	0.02	-1.69			NC_005089
10562649	0.01	-1.70			
10511014	0.01	-1.70			
10472042	0.07	-1.70	predicted gene 13498	Gm13498	XR_034671|XR_032134|XR_030628|XM_001473515|
10411609	0.03	-1.70			
10546803	0.00	-1.70	inositol 1,4,5-triphosphate receptor 1 | predicted gene 10429	Itpr1|Gm10429	NM_010585
10572461	0.00	-1.71	RIKEN cDNA 2410018E23 gene	2410018E23Rik	XM_912668
10545099	0.02	-1.71			
10414920	0.01	-1.71	T-cell receptor alpha variable region 7D-2	Trav7d-2	
10578681	0.04	-1.71			
10396440	0.00	-1.71	predicted gene 5068	Gm5068	XM_204772
10562592	0.01	-1.71	predicted gene 5114	Gm5114	NM_177890
10460146	0.01	-1.72			
10360185	0.01	-1.73			
10471067	0.01	-1.73	paired related homeobox 2	Prrx2	NM_009116
10417068	0.04	-1.73			
10386756	0.00	-1.75			

10423570	0.08	-1.76			
10431635	0.01	-1.76			
10473107	0.00	-1.76			
10582899	0.03	-1.76			
10399657	0.01	-1.76			
10394938	0.01	-1.76			
10346876	0.03	-1.76	small nucleolar RNA, H/ACA box 41	Snora41	
10424381	0.03	-1.76			
10598169	0.03	-1.76	RIKEN cDNA 4930449I24 gene | predicted gene 3402 | predicted gene 3415 | predicted gene 3409 | predicted gene 6370 | predicted gene 6408 | hypothetical protein LOC674338	4930449I24Rik|Gm3402|Gm3415|Gm3409|Gm6370|Gm6408|LOC674338	NM_026136|XM_001476794|XM_973848
10576556	0.01	-1.76			
10534301	0.00	-1.76	predicted gene 52	Gm52	NM_001013751
10569303	0.03	-1.76			
10398396	0.00	-1.76			
10400708	0.01	-1.76			
10434283	0.01	-1.76	similar to ubiquitin-conjugating enzyme E2 variant 2	LOC635992	
10367475	0.01	-1.76			
10356170	0.00	-1.76			
10405334	0.01	-1.77	eukaryotic translation initiation factor 4E family member 1B	Eif4e1b	NM_001033269|NM_001039683
10474102	0.07	-1.77			
10582882	0.02	-1.77			
10412657	0.02	-1.77			
10582884	0.02	-1.78			
10548752	0.00	-1.78			
10582890	0.03	-1.81			
10582888	0.03	-1.85			
10582916	0.02	-1.87			
10582896	0.01	-1.88			

APPENDIX 3

List of GO analysis **(**GO enrichment corrected p-value < 0.1 by Benjamini-Yekutieli method)

GO ACCESSION	GO Term	corrected p-value	Count in Selection	% Count in Selection	Count in Total	% Count in Total
GO:0005882	intermediate filament	0.01	6	9.84	140	0.76
GO:0045111	intermediate filament cytoskeleton	0.01	6	9.84	143	0.78
GO:0044430	cytoskeletal part	0.01	11	18.03	623	3.39
GO:0008890	glycine C-acetyltransferase activity	0.01	2	3.28	2	0.01
GO:0050882	voluntary musculoskeletal movement	0.05	2	3.28	4	0.02
GO:0005856	cytoskeleton	0.05	12	19.67	974	5.30
GO:0005220| GO:0008095	inositol 1,4,5-trisphosphate-sensitive calcium-release channel activity	0.05	2	3.28	4	0.02
GO:0015278	calcium-release channel activity	0.06	2	3.28	5	0.03
GO:0005955	calcineurin complex	0.06	2	3.28	5	0.03
GO:0016453	C-acetyltransferase activity	0.06	2	3.28	5	0.03
GO:0005261| GO:0015281| GO:0015338	cation channel activity	0.06	6	9.84	239	1.30
GO:0048016	inositol phosphate-mediated signaling	0.07	2	3.28	6	0.03
GO:0001518	voltage-gated sodium channel complex	0.09	2	3.28	7	0.04
GO:0022839	ion gated channel activity	0.09	6	9.84	277	1.51
GO:0022836	gated channel activity	0.09	6	9.84	277	1.51
GO:0005217	intracellular ligand-gated ion channel activity	0.09	2	3.28	8	0.04

GO:0032469	endoplasmic reticulum calcium ion homeostasis	0.09	2	3.28	8	0.04
GO:0015276	ligand-gated ion channel activity	0.10	4	6.56	104	0.57
GO:0022834	ligand-gated channel activity	0.10	4	6.56	104	0.57
GO:0005248	voltage-gated sodium channel activity	0.10	2	3.28	9	0.05
GO:0005637	nuclear inner membrane	0.10	2	3.28	9	0.05